

Aus dem Institut für Agrar- und Ernährungswissenschaften
(Geschäftsführender Direktor: Herr Prof. Dr. Olaf Christen)

der Naturwissenschaftlichen Fakultät III
(Dekan: Herr Prof. Dr. Peter Wycisk)

der Martin-Luther-Universität Halle-Wittenberg

Fachgebiet: Pflanzenzüchtung

Characterization of NIMA-like kinases in *Arabidopsis thaliana*

Dissertation
zur Erlangung des akademischen Grades
doctor agriculturarum (Dr. agr.)

von

Herr Francesco Agueci
geb. am: 07/03/1979 in: Pescina, Italien

verteidigt am

21.06.2010

begutachtet von

Herr Prof. Dr. Klaus Pillen [Halle]
Herr Dr. habil. Andreas Houben [Gatersleben]
Herr Dr. habil. Helmut Bäumlein [Gatersleben]

Halle/Saale 2010

ACKNOWLEDGEMENTS

This work was performed from January 2006 till June 2009 at the Leibniz Institute of Plant Genetics and Crop Plant Research (IPK), Gatersleben.

Since October 2004 till July 2005 it was funded by the Land Saxony-Anhalt, afterwards the financial support from IPK made possible the accomplishment of the research.

First of all I would like to express my gratitude to my supervisor Dr. Andreas Houben, the head of the “Chromosome Structure and Function” workin group, for giving me the opportunity to work in his team, for continuous support and guidance, inspiration and permanent encouragement.

Many thanks to Dr. Dmitri Demidov for providing support and useful comments as well as for sharing his experience during the entire period of the research

I'm very thankful to Dr. Twan Rutten for his assistance with the microscopy analysis of the AtNIMA mutants and fluorescence constructs, and to Dr. Frank Blattner for his help during the phylogenetic anaylsis of the AtNIMA family.

I wish to thank my mentor Dr. Helmut Bäumlein, for his helpful suggestions and fruitful discussions.

I am also obliged to the technicians from our group Margit Hantschmann, Katrin Kumke and Oda Weiss for their perfect technical assistance withouth whom this entire work would not have been possible, and all the members of the CSF group for their professional and personal support during all this time.

Finally I would like to thank all my friends and colleagues at the IPK-Gatersleben for making the experience here unique from every point of view and Karo, for supporting me during all the critical moments.

Content

1.	Introduction.....	7
1.1	Cell -cycle dependent histone H3 phosphorylation.....	7
1.2	Histone H3 is phosphorylated by different kinases.....	9
1.3	Role of NIMA kinases in the regulation of mitosis.....	11
1.4	NIMA-like kinases in plants.....	15
2.	Aims of the work.....	18
3.	Material and methods.....	20
3.1	Plant material and growth conditions.....	20
3.1.1	Seed sterilization and plating conditions.....	21
3.2	Sequence processing and primer design.....	21
3.3	Extraction of plant genomic DNA.....	23
3.4	Extraction of plant total RNA.....	24
3.4.1	Determination of the concentration of RNA and DNA.....	24
3.4.2	DNase treatment and cDNA synthesis.....	24
3.4.3	Verification of the T-DNA insertion position via genomic PCR.....	25
3.4.4	Reverse transcription-PCR (RT-PCR).....	25
3.5	Cloning procedures of constructs.....	26
3.5.1	Full length cDNA isolation.....	26
3.5.2	Isolation of putative AtNIMA 2 and AtNIMA 3 promoter regions.....	26
3.5.3	DNA extraction from agarose gel and ethanol precipitation.....	26
3.5.4	Preparation of competent bacteria cells.....	27
3.5.5	Cloning of AtNIMAs and transformation of E. coli bacteria via electroporation.....	27
3.5.6	Plasmid DNA extraction and sequencing.....	28
3.5.7	pENTR plasmid digestion.....	28
3.5.8	Recombination of AtNIMA sequences into destination vectors.....	29
3.5.9	Analysis of the destination vector constructs.....	29
3.6	Stable transformation of <i>A. thaliana</i> via floral dip.....	32
3.7	RNAi-based knockdown of AtNIMA genes.....	32
3.7.1	Design of the constructs.....	32

3.7.2	Transformation of bacteria with AtNIMA RNAi constructs.....	33
3.7.3	Validation of recombinant pAgrikola vectors used for plant transformation.....	33
3.7.4	Selection and validation of AtNIMA RNAi plants.....	33
3.7.5	Analysis of RNAi-based down regulation of AtNIMA genes.....	34
3.7.6	Analysis of the phenotype of RNAi-based down regulated AtNIMA Plants.....	34
3.8	Southern hybridization of genomic DNA.....	34
3.9	Indirect immunostaining and Western blotting.....	35
3.9.1	Generation of putative AtNIMA-specific polyclonal antibodies.....	35
3.9.2.	Preparation of squashed mitotic cells	35
3.9.3	Preparation of chromosomes suspension from <i>Vicia faba</i>	36
3.9.4	Indirect immunostaining of cells and seedlings	37
3.9.5	Anti-tubuline staining of leaf cells.....	37
3.9.6	Extraction of proteins.....	38
3.9.7	Western Blotting.....	38
3.10	Quantification of seed settings.....	38
3.11	Alexander staining of pollen.....	39
3.12	Transient expression of AtNIMA::YFP constructs in <i>Nicotiana benthamiana</i> leaves.....	39
3.12.1	Preparation of AtNIMA::YFP constructs and plant infiltration.....	39
3.12.2	Analysis of transiently expressed AtNIMA::YFP proteins in <i>N.benthamiana</i>	40
3.12.3	Treatment of leaf cells with tubuline inhibitors	40
3.13	GUS histochemical staining.....	40
4.	Results.....	42
4.1	Identification of AtNIMA genes in <i>A. thaliana</i>	42
4.2	Phylogenetic relationship of AtNIMAs with NIMA related kinases from other plants.....	43
4.3	Organ specific expression of AtNIMA 2, 3 and 5.....	47
4.4	Inactivation of AtNIMA 2, 3 and 5 via T-DNA insertions.....	51

4.4.1	Characterization of AtNIMA 5 T-DNA plants.....	54
4.4.1.1	AtNIMA 5 knock out mutant plants does not show major differences in the phenotype.....	54
4.4.1.2	Inactivation of AtNIMA 5 does not influence the cell cycle dependent phosphorylation of histone H3 at position serine 10.....	56
4.4.2	Characterization of AtNIMA 2 T-DNA plants.....	57
4.4.2.1	Reduced seed setting of AtNIMA 2 T-DNA heterozygous plants.....	57
4.4.2.2	Sequence analysis of Salk_093269 confirms T-DNA position in the AtNIMA 2 gene.....	59
4.4.2.3	Salk_093269 line could contain two tandemly oriented T-DNA copies inserted in AtNIMA 2.....	60
4.5	Down regulation of AtNIMA 2 gene using an RNAi construct.....	62
4.5.1	AtNIMA 2 RNAi mutants are delayed in plant development.....	64
4.5.2	Histological analysis of AtNIMA 2 RNAi mutants.....	68
4.5.3	The vascularization process of cotyledons is affected in AtNIMA 2 RNAi mutants.....	72
4.5.4	RNAi down regulation of AtNIMA 2 does not influence the cell cycle dependent phosphorylation of histone H3S10.....	74
4.6	Cloning of the full length AtNIMA 2 cDNA.....	75
4.7	Characterization of putative AtNIMA 2 and 3 specific antibodies.....	75
4.8	Analysis of <i>A. thaliana</i> plants transformed with 35S::AtNIMA 2 and 35S::YFP::AtNIMA 2.....	81
4.9	Analysis of 35S::YFP::AtNIMA 2-specific signals in transiently transformed leaves on <i>N. benthamiana</i>	82
4.9.1	Disruption of the AtNIMA 2::YFP-fluorescence decorated filamentous system by oryzalin and colchicine.....	86
4.9.2	Immunostaining signal from anti-tubuline antibody seems to overlap with 35S::YFP::AtNIMA 2 fluorescence.....	88
4.10	Determination of AtNIMA 2 promoter expression pattern using GUS histochemical staining.....	89

5.	Discussion.....	94
5.1	The catalytic domain of AtNIMA kinases is highly conserved.....	94
5.1.1	The NIMA-like kinase family in plants has an early evolutionary origin..	95
5.1.2	The transcription profiles of AtNIMA 2, 3 and 5 are similar in an organ specific way and are not associated with the mitotic cell cycle.....	96
5.2	AtNIMA 5 does not play a major role in plant development and histone H3 phosphorylation.....	97
5.3	AtNIMA 2 is a gene fundamental for the plant development.....	98
5.3.1	Complete inactivation of <i>AtNIMA 2</i> has a lethal effect.....	98
5.3.2	Down-regulation of <i>AtNIMA 2</i> influences the correct plant development.....	99
5.3.3	<i>AtNIMA 2</i> seems to be involved in the control of cell morphogenesis..	100
5.3.4	Organization of vascular bundles in cotyledons is altered by <i>AtNIMA 2</i> down-regulation.....	101
5.3.5	AtNIMA 2 kinase is not involved in the process of cell cycle- dependent histone H3 phosphorylation.....	102
5.4	Overexpression of <i>AtNIMA 2</i> has a lethal effect on plants.....	102
5.5	AtNIMA 2 co-distributes with microtubules.....	103
5.5.1	The fluorescence signal of 35S::YFP::AtNIMA 2 decorates filamentous structures in <i>N. benthamiana</i> cells.....	103
5.5.2	Drug treatments proofs that AtNIMA 2 is interacting with the microtubular cytoskeleton.....	104
6.	Outlook.....	106
7.	Summary.....	108
8.	Zusammenfassug.....	111
9.	Literature.....	113
	Publications in connection with the submitted thesis.....	124
	Supplementar material.....	125
	Eidesstattliche Erklärung.....	126
	Curriculum Vitae.....	127

Abbreviations

bp	<u>b</u> ase <u>p</u> air	NaOH	sodium hydroxide
BSA	<u>b</u> ovine <u>s</u> erum <u>a</u> lbumin	NPT	neomycin phosphotransferase
CLSM	confocal laser scanning microscopy	nt	nucleotide
cm	centimeter	ON	overnight
CTP	<u>c</u> ytidine 5'- <u>t</u> ri <u>p</u> hosphate	P	probability
Cy3	cyanine 3	PBS	<u>p</u> hosphate- <u>b</u> uffered <u>s</u> aline
DAPI	4',6- <u>d</u> i <u>a</u> midino-2- <u>p</u> henyl <u>i</u> ndole	PCR	<u>p</u> olymerase <u>c</u> hain <u>r</u> eaction
DEPC	<u>d</u> iethylpyro <u>c</u> arbonate	ph	phosphorylated
DMSO	<u>d</u> imethyl <u>s</u> ulfoxide	PPT	phosphinotricin
DNA	<u>d</u> eoxyribo <u>n</u> ucleic <u>a</u> cid	RNA	<u>r</u> ibo <u>n</u> ucleic <u>a</u> cid
dNTP	<u>d</u> eoxyribo <u>n</u> ucleotide <u>t</u> riphosphate	RNAi	<u>r</u> ibo <u>n</u> ucleic <u>a</u> cid interference
EDTA	<u>e</u> thylenediaminetetra- <u>a</u> cetic acid	RP	right genomic primer
GFP	green fluorescent protein	RT	room temperature
GST	<u>g</u> ene-specific <u>s</u> equence <u>t</u> ag	RT PCR	<u>r</u> everse <u>t</u> ranscription <u>p</u> olymerase <u>c</u> hain <u>r</u> eaction
GUS	beta-glucoronidase	s	seconds
h	hours	S10	Serine 10
H2B	Histone H2B	SDS	<u>s</u> odium <u>d</u> odecyl <u>s</u> ulfate
H3	Histone H3	SSC	<u>s</u> odium <u>c</u> hloride <u>s</u> odium <u>c</u> itrate
HCl	hydrochloric acid	T-DNA	<u>t</u> ransfer <u>d</u> eoxyribo <u>n</u> ucleic <u>a</u> cid
HM	homozygous	Tm	melting temperature
HZ	heterozygous	Tris	tris-(hydroxymethyl)-aminomethane
kDa	<u>k</u> ilo Dalton	U	units
kp	<u>k</u> ilo <u>b</u> ase	WT	wild-type
LB	left T-DNA border primer	YFP	yellow fluorescent protein
LP	left genomic primer	µg	micrograms
mg	milligrams	µl	microliters
min	minutes	µm	micrometer
ml	milliliters	µM	micromole
mm	millimeter	%	percent
mM	millimole		
mRNA	<u>m</u> essenger <u>r</u> ibo <u>n</u> ucleic <u>a</u> cid		
MS	Murashige and Skoog		
NaCl	sodium chloride		

1. Introduction

1.1 - Cell-cycle dependent histone H3 phosphorylation

The cell cycle-dependent condensation of chromatin is a crucial step for any eukaryotic organism. The enormous length of their genomes requires it to be packaged into a stable structure that can be safely replicated during mitosis while being still malleable enough to enable access to genetic information. So it is not surprising that the general mechanisms that control the passage between decondensed interphase chromatin and condensed metaphase chromatin are highly conserved through the eukaryotic kingdom. Those regulatory pathways are based on the modulation of the chemical properties of histones and DNA-binding proteins that control the level of chromatin condensation. Post-translational modifications of the N-terminal tail of histone molecules during cell cycle are linked either to regulate chromatin dynamics or to control the transcription level of different genes; such modification includes acetylation, methylation, phosphorylation, ubiquitination and ADP-ribosylation (Nowak and Corces 2004; Johansen and Johansen 2006; Ito 2007). One of the most prominent histone modifications is the phosphorylation of histone H3. Early results were obtained using cells from Chinese hamster: by using suspension cultures in a synchronized state it was demonstrated that the phosphorylation level of histone H3 is low in interphase but greatly increases during mitosis (Gurley et al. 1975; Hohmann et al. 1976) and localized mostly at serine 10 (Paulson and Taylor 1982). The correlation between histone H3 phosphorylation and chromatin condensation was confirmed by the utilization of an antibody specific for histone H3 phosphorylated at serine 10 (Hendzel et al. 1997). Several studies also demonstrated that this modification and its fundamental role in mitosis and meiosis are evolutionarily conserved in eukaryotes (Wei et al. 1998). Mutant strain of *Tetrahymena thermophyla* lacking serine 10 (H3Ser10Ala) exhibits an abnormal chromosome condensation and segregation (Wei et al. 1999; De Souza et al. 2000). There are also evidences that histone H3 phosphorylation at serine 10 is linked with the transcriptional activation of

immediate early genes (Thomson et al. 1999) and the induction of oncogenes (Chadee et al. 1999).

Although the process of histone H3 phosphorylation is highly conserved, there are some differences in its chromosomal distribution between different species. In non-plants eukaryotes phosphorylation of histone H3 serine 10 and 28 starts in the late G2 phase in the pericentromeric region from where it is distributed homogeneously throughout the chromosomes as the mitosis proceeds (Goto et al. 1999). Phosphorylation of histone H3 threonine 3 initially overlaps with the distribution of phosphorylated serine 10 but later it is localized mostly in the central region of the metaphase plate (Polioudaki et al. 2004). Also, phosphorylation of histone H3 threonine 11 seems to be concentrated mostly in centromeric region during metaphase (Preuss et al. 2003). All together those modifications suggested that phosphorylation of histone H3 in mammal cells can play a role in chromosome condensation and segregation. In plants the distribution of phosphorylated serine 10 and 28 during mitosis is high in pericentromeric regions but low along chromosomes arms (Fig. 1) (Houben et al. 1999; Manzanero et al. 2000). On the opposite, phosphorylation on threonine 3 and 11 starts in the pericentromeric region but then is distributed along the entire chromosome arms. Interestingly during meiosis in plants the distribution of Ser 10 and Ser 28 phosphorylation varies between the two meiotic divisions (Manzanero et al. 2000). These results led to the hypothesis that in plants H3 phosphorylation at both serine positions is involved in sister chromatid cohesion, while threonine phosphorylation seems to be involved with chromosome condensation (Houben et al. 2005).

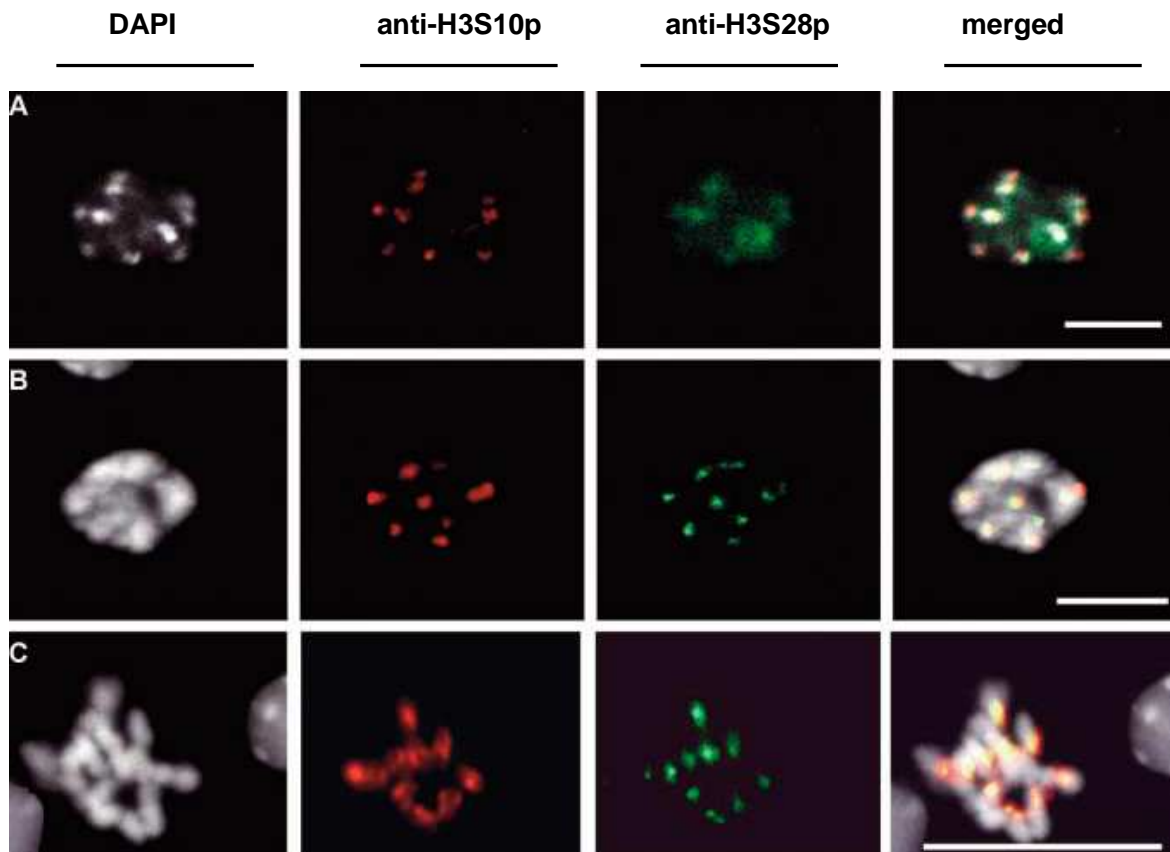


Figure 1: Immunostaining on *Arabidopsis thaliana* chromosomes showing the phosphorylation at histone H3 serine 10 and serine 28 at early prophase (A), late prophase (B) and metaphase (C). In the merged pictures DAPI-signals are indicated in grey, phosphorylated H3 at serine 10 in red, phosphorylated H3 at serine 28 green. Bar represents 10 μ m (Gernand et al. 2003).

1.2 - Histone H3 is phosphorylated by different kinases

Different kinases are involved in the phosphorylation of histone H3 including: mitogen and stress activated protein kinase 1 and 2 (MSK 1/2) (Kouzarides 2007; Vermeulen et al. 2009), death-associated protein (DAP)-like kinase (Dlk) (Preuss et al. 2003), Haspin kinase (Dai et al. 2005), Aurora B kinase (Adams, Maiato et al. 2001) and NIMA kinase (De Souza et al. 2000). MSK 1/2 are phosphorylating histone H3 at position serine 10 has response to the activation of mitogen stimulated immediate-early response genes such as *c-fos* and *c-jun* (Mahadevan et al. 1991; Strelkov and Davie 2002; Soloaga et al. 2003). Dlk is able to phosphorylate histone H3 at position threonine 11, rather than serine 10. This modification occurred during mitosis, from prophase to early anaphase (Preuss et al. 2003). Phosphorylation of histone H3 by haspin kinase happens

during mitosis at position threonine 3 (Dai et al. 2005), the timing of the phosphorylation suggest that it can play a role in sister chromatid cohesion (Markaki et al. 2009). Aurora kinases are a family of serine/threonine kinases whose activity peak during cell division and that has been shown to play key roles in regulating chromosome segregation and cytokinesis. Those findings were supported by the observation that members of this family are overexpressed in several types of tumors (Bischoff et al. 1998). The Aurora kinase family comprises three members in human and mouse, two in *Drosophila* and *C. elegans* and one in *Saccharomyces cerevisiae* and *Schizosaccharomyces pombe* (Meraldi et al. 2004). Non-plant Aurora kinases were divided in three classes based on their role and localization: Aurora A, B and C (Adams, Carmena et al. 2001). The founding members of the family are budding yeast Ipl1 and *Drosophila* Aurora A (Glover et al. 1995). The exact role of Aurora A is not known, but several studies suggested that its function is related to centromere separation and spindle assembly (Bischoff et al. 1998; Giet et al. 2002). Also overexpression of Aurora A produces extra copies of centrosomes, defects in cell division and consequent formation of tetraploid cells (Zhou et al. 1998; Meraldi et al. 2002; Stenoien et al. 2003). Yeast aurora kinase Ipl1 can phosphorylate histone H3 at serine 10 *in vitro* (Hsu et al. 2000) and *Saccharomyces cerevisiae* mutant lacking the Ipl1 present a phenotype similar to the H3Ser10 Ala mutant (Wei et al 1999). Aurora kinase B is involved in several mitotic regulatory pathways and displays the behavior of a chromosomal passenger protein (Bischoff et al. 1998). In mammals it first associates with the centromere/kinetochore, forming a complex with the proteins INCENP and Survivin (Adams, Carmena et al. 2001; Adams, Maiato et al. 2001). Then during cytokinesis it relocates to the midbody region between dividing cells (Crosio et al. 2002). Overexpression of catalytically inactive Aurora B causes defects in the organizations of the spindle microtubules and in the interaction of kinetochore with microtubules, including loss of kinetochore associated motor proteins dynein and CENP-E from kinetochore, suggesting that Aurora B plays a role in kinetochore assembly (Murata-Hori et al. 2002; Murata-Hori and Wang 2002). Also in mammals the histone H3 like kinetochore protein CENP-A is

phosphorylated by Aurora B kinase (Zeitlin et al. 2001). In addition to its role in kinetochore assembly and microtubule dynamics, Aurora B mediates chromosome condensation and sister chromatid cohesion in *C. elegans* (Kaitna et al. 2002). Aurora B of *C. elegans* (Hsu et al. 2000), *Drosophila* (Adams, Maiato et al. 2001; Giet and Glover 2001) and mammals (Crosio et al. 2002) are able to phosphorylate histone H3 at positions serine 10 and serine 28 (Goto et al. 1999; Goto et al. 2002; Sugiyama et al. 2002). Plant Aurora kinases were characterized in *A. thaliana* (Demidov et al. 2005). Arabidopsis encodes for three Aurora like genes (*AtAurora*) labelled as *AtAurora 1*, *AtAurora 2* and *AtAurora 3*. The catalytic domain of the different *AtAurora* kinesis is highly similar to the Ipl1 and Aurora from *Drosophila*, showing 64% to 95% identity. The three *AtAurora* kinases share a similar expression pattern, with their transcripts particularly abundant in organs rich of dividing cells like callus, roots and flowers. Analysis of the cell cycle dependant expression shows that the mRNA level of *AtAurora* kinases reach a peak of expression during mitosis, in particular for *AtAurora1* which has approximately a fivefold increase. Localization experiments with GFP reporter gene indicates that during mitosis *AtAurora* kinases associate mostly with dynamic structures, like microtubule spindles and centrosomes. In addition *AtAurora1* is able to phosphorylate *in vitro* histone H3 at position serine 10, although does not seems to be able to phosphorylate serine 28, threonine 3 and threonine 11.

1.3 - Role of NIMA kinases in the regulation of mitosis

NIMA (*Never in Mitosis A*) kinase was first discovered in the fungus *A. nidulans* by screening of temperature- sensitive mutants that exhibits cell cycle mutations. Some of these mutants were completely unable to initiate mitosis (Morris et al, 1976). Soon was discovered that such mutation involves a gene denoted as *nimA*; such mutants arrested late in G2 with duplicate spindle bodies (Osmani et al. 1987). Analysis of the cDNA sequence indicated that *nimA* encode a protein kinase designated as NIMA (Osmani et al. 1988). NIMA is a 79 kDa protein that contains at the N-terminal the serine/threonine specific kinase domain. The C-

terminal domain seems to be involved in the regulation of the kinase and includes also the putative Cdc2 phosphorylation sites, it also contains several PEST motifs (that seems to direct NIMA degradation via ubiquitin-dependent proteolysis) and a coiled coil region close to the catalytic domain that might be important for interactions with other proteins (Fry and Nigg 1995). NIMA may be essential for mitotic entry as it is required to localize the mitotic regulator Cdc2/cyclin B to the nucleus. The mechanism by which NIMA promotes the uptake of Cdc2/cyclin B seems to involve the interaction SONA and SONB, two components of the nuclear pore complex identified via screening for allele-specific suppressors of *nimA* (Wu et al. 1998; De Souza et al. 2003; O'Regan et al. 2007). However Cdc2 is completely functional even in *nimA* mutants arrested in G2, indicating that NIMA is not part of the activation pathway of Cdc2 (Osmani et al. 1991). It was postulated that NIMA could be activated directly by phosphorylation from Cdc2/cyclin B, but a basal level of phosphorylated NIMA protein was detected also in *A. nidulans* mutants in whom the activation of Cdc2/cyclin B was blocked, thus rejecting this hypothesis (Osmani et al. 1991). However, when Cdc2/cyclin B is active it can phosphorylate NIMA, increasing dramatically its activity during the G2 phase (Ye et al. 1995). So it could be concluded that the activities of both NIMA and Cdc2/cyclin B kinases are strictly coordinated through positive feedback loop, which is part of the mitotic regulatory pathways (O'Connell et al. 2003). Another function of NIMA kinase during mitosis seems to be the regulation of chromatin condensation. Overexpression of *nimA* triggers the condensation of chromatin in *A. nidulans*, no matter where the nuclei are in the cell cycle (Osmani et al. 1988). Interestingly overexpression of NIMA can cause premature and abnormal chromatin condensation also in *Schizosaccharomyces pombe*, *Xenopus* oocytes and human cells (O'Connell et al. 1994). In addition it was demonstrated that expression of the carboxy-terminal domain of NIMA by itself produces a dominant-negative phenotype and that accumulation of such mutant proteins causes arrest in G2 phase in *A. nidulans* and human cells (Lu and Means 1994; Lu and Hunter 1995).

It was later discovered that NIMA kinase can regulate chromatin condensation by phosphorylating histone H3 at the position serine 10 (De Souza et al. 2000), by performing indirect immunostaining with an antibody specific for histone H3 phosphorylated at serine 10 (Hendzel et al. 1997) on a strain of *A. nidulans* carrying a temperature sensitive mutation that reversibly block Cdc2/cyclin B (Ye et al. 1995). At the arrest point the cells exhibited uncondensed DNA and no histone phosphorylation, but when they were shifted to the permissive temperature to start phosphorylation of histone H3 Ser 10 occurred simultaneously to DNA condensation. Successive experiments confirmed that NIMA is directly responsible for the phosphorylation of histone H3 serine 10 in *A. nidulans*, without any involvement of Cdc2/cyclin B kinase. However, a functional Cdc2/cyclin B kinase is required for a proper chromosome condensation (De Souza et al. 2000; O'Connell et al. 2003).

Because of the highly conserved nature of cell cycle regulators it was expected to find NIMA related kinases (Nrk) in other organisms of the eukaryotic kingdom. Homology based screens for NIMA-like genes have uncovered a large family of Nrk proteins that includes also yeasts Nrk protein, vertebrate Nek proteins and various plant NIMA like proteins. The homologue of *nimA* in yeast was labeled *Fin1* (Krien et al. 1998). *Fin1* is a cell cycle-regulated protein, controlled at both transcriptional and post transcriptional level, and it is particularly abundant in spindle pole bodies during mitosis G2 phase. *Fin1* activity as protein kinase mirrors its abundance, because it is low throughout interphase and maximal during mitosis, in the same way as NIMA. Overexpression of *Fin1* resulted in a premature chromosome condensation in any point of the cell cycle, independently by the activity of Cdc2 and of the rest of mitotic machinery (Krien et al. 1998). The most prominent differences with NIMA are that phosphorylation of histone H3 is not affected by activity of *Fin1* and that deletion of *Fin1* results only in a modest cell cycle delay on G2, while inactivation of NIMA completely blocks mitosis in *A. nidulans* (Krien et al. 2002). However, the localization of *Fin1* in the mitotic spindle pole bodies and the screening of temperature sensitive

mutants suggested that Fin1 is required for the formation of a functional mitotic spindle (Grallert and Hagan 2002; Krien et al. 2002).

In mammals eleven NIMA-related kinases, labeled as Neks, has been found, although they tend to share similarity only in the catalytic domain. Of all the NIMA related kinases from vertebrates, human Nek2 is the protein most closely related to NIMA, having a 45% similarity in the catalytic domain (Fry 2002). Human Nek2 is a 48 kDa protein that comprises the serine/threonine catalytic domain at the N-terminal, and two coiled coil regions at the C-terminal, one close to the catalytic domain and the other at the extreme of the C-terminal. Several studies indicate that Nek2 resides at the proximal ends of the centrioles and is involved in the organization of centrosomes and in the formation of a functional mitotic spindle. Anyway, despite their structural similarity, there are several differences between NIMA and Nek2. The first point is that Nek2 does not contain Cdc2 phosphorylation sites neither PEST motifs. Also, while NIMA activity is maximal in mitotically arrested cells, Nek2 activity rises in G₁/S and G₂/M phase and decreases upon entering in mitosis; such activity levels mimic the abundance of Nek2 during cell cycle (Fry et al, 1995). Overexpression of Nek2 results in the splitting of centrioles instead of inducing abnormal chromatin condensation like NIMA or Fin1. Finally, its expression in *A. nidulans* does not complement a mutation in *nimA*, it is also unable to complement a mutation in *fin1* in yeast cells (O'Connell et al, 2003).

Other characterized mammalian NIMA-related kinases are Nek1 and Nek6. Murine Nek1 is the longest documented member of the NIMA kinase family and the analysis of its full-length sequence show many similarities with the fungal NIMA, suggesting that Nek1 is performing similar activities. Overexpression of a truncated fragment of Nek1 induces chromatin condensation, although this is not associated with histone H3 phosphorylation (Feige et al. 2006). Nek6 is a protein of 338 amino acids and its catalytic domain shares 57% sequence similarity to *A. nidulans* NIMA, with a peak activity is in G₁/M phases. *In vitro* kinase assay demonstrated that, unlike other mammalian NIMA related kinases, Nek6 is able

to phosphorylate effectively histones H1 and H3 (Kandli et al. 2000; Hashimoto et al. 2002). This result raises the possibility that, like the fungal NIMA kinases, mammalian Nek6 could have a specific role in regulating chromosome condensation through histone phosphorylation. Overall, although NIMA-related kinases in mammals had diverged in a certain degree from NIMA in structure and function, they are still able to regulate chromosomes condensation and assembly in higher eukaryotes.

1.4 - NIMA-like kinases in plants

Few NIMA-like genes were described in plants until now. A single NIMA related gene was found in *Antirrhinum majus* (Zhang et al. 1996) and in *Lycopersicon esculentum* (Pnueli et al. 2001), while an entire gene family was discovered in *Arabidopsis thaliana*, populus species and *Oryza sativa* (Vigneault et al. 2007). *AmnimA* of *A. majus* was recovered as a partial 500 bp-long cDNA fragment of the catalytic kinase domain. Even if its sequence similarity with the fungal gene suggested some involvement in cell division, the function of *AmnimA* is still unknown (Zhang et al. 1996). SPAK of tomato was found to be involved in the signaling system that regulates shoot architecture and flowering, this happens through binding with both self-pruning (SP) and 14-3-3 proteins. Suppression of SPAK also causes an abnormal fruit elongation (Pnueli et al. 2001). 14-3-3 are highly conserved proteins involved in many cellular processes through protein-protein interactions, most of these interactions requires the presence of phosphorylated residues (Yaffe et al. 1997; Fu et al. 2000). Poplar NIMA related kinase PNek1 was discovered to interact with 14-3-3 in poplar. Its predicted protein structure contains a kinase catalytic domain with conserved sub-domains typical of serine/threonine protein kinases that belongs to the NIMA family (Schultz et al. 1994). Secondary motif prediction includes a PEST degradation motif, a coiled-coil domain and three putative 14-3-3 binding motifs, typical of the C-terminal extension of Neks (O'Connell et al. 2003).

A genome-wide search performed on *A. thaliana*, using PNek1 as bait, uncovered seven putative ORF, labeled as AtNek 1-7, and showing homology

with the NIMA family. The catalytic domain of PNek 1 has a 90% identity with SPAK and the putative AtNek 1 and a 45% identity with human Nek4 (Cloutier et al. 2005). The expression pattern of *PNek1* was analyzed using a suspension of poplar cells synchronized with aphidicolin and it was found that the transcript amount of *PNek1* is particularly high during the transition through G₁/S and G₂/M phases, but almost undetectable during S phase. In addition *PNek1* expression levels are relatively high in meristematic tissues, like apical meristems, buds and cambium. Subcellular localization using GFP constructs shows that PNek1 accumulates in both nucleus and cytoplasm. Overexpression of PNek1 in *A. thaliana* caused several morphological anomalies, that includes flowers with shorter stamens, shorter carpels, atrophied or absent petals and siliques that carried few seeds or no seeds at all. All the findings suggested that PNek1 is involved in the regulation of plant development, while its expression is probably cell cycle regulated, although there are no indications of a PNek1 involvement in the phosphorylation of histone H3 (Cloutier et al. 2005).

Plant Nek genes are scattered through the genomes, with the various members located in different chromosomes. However in each species Nek 1, 2 and 3 seems to be closely related orthologues, also in each of those sub groups a pair of paralogues can be identified. In addition the intron-exon distribution seems to be highly conserved between the same Neks in the different species. Overall plant Neks seems to be originated from a common ancestor, while the similarity in the intron-exon structure and the presence of paralogues suggested that a duplication event took place before the divergence between the three plants species raised. *In silico* analysis shows that plant Neks expression profiles are correlated with organ development patterns, in particular localization experiments performed with GUS reporter gene indicated that PNek1 expression is related with the vascularization process (Vigneault et al. 2007). The first *A. thaliana* NIMA-like kinase to be characterized was AtNek6. It was hypothesized that AtNek6 may interact with ARKs (Armadillo repeat kinesin), which are involved in root hairs and epidermal cells morphogenesis, through the Armadillo repeat domains. Loss of function experiments performed with different T-DNA

and RNAi lines revealed that inactivation of *AtNek6* affects the epidermal cells morphogenesis causing a leftward slant of the primary roots, abnormal protrusions on the surface of the hypocotyls and alterations on the branching of leaf trichomes. A similar phenotype was obtained by treating *Arabidopsis* seedling with the microtubule drugs taxol and propyzamide, suggesting an involvement of *AtNek6* in the regulation of microtubule dynamics (Sakai et al. 2007).

Those findings were further expanded by the work of Motose and colleagues (2008) that described also a class of *AtNek6* mutants which have protuberances on the surfaces of their hypocotyls and petioles originating from local outgrowth of epidermal cells. Sequence analysis of *AtNek6* identified a serine/threonine protein kinase domain at the N-terminus, which has significant homology to the kinase domain of the NIMA-related proteins of various organisms. The kinase domain of *AtNek6* is followed by three PEST degradation motifs and a coiled-coil domain near the C-terminus. Transient expression of *AtNek6* fused at N-terminal with GFP in *N. benthamiana* allowed to observe strong fluorescence in small dots aligned with microtubules structures. Treatment with the microtubule stabilizing drug taxol intensified the fluorescence on the filamentous structures, while treatment with oryzalin (microtubule depolymerizing drug) caused the structures to disappear leaving only the fluorescent dots (Motose et al. 2008). The latest data support the hypothesis that the role of *AtNek6* kinase is related to the pathways of cell expansion and through an interaction with cortical microtubules, probably with the coiled coil domain contained in its C-terminal region. Basing on those findings it seems that some of the NIMA related kinases in plants are more involved in the processes of plant development and cell morphogenesis rather than cell-cycle regulation. However the function of the other members of the Nek family remains to be analyzed.

2. Aims of the work

The questions addressed in this work are focused in the characterization of the family of AtNIMA kinases, the definition of their functions and their putative involvement in the phosphorylation of histone H3. To answer these questions the following approaches were employed.

2.1 - Phylogenetic analysis of the NIMA-like family in *A. thaliana* and identification of the AtNIMA kinases closely related to the fungal NIMA.

To better understand the origin and the evolution of AtNIMA kinases a genome-scale investigation was conducted on the entire database of Viridiplantae. In addition the sequences of the individual AtNIMA kinases were analyzed and compared with the fungal NIMA, to select the proteins that have the highest degree of similarity with the founding member of the NIMA family.

2.2 - Investigation of the transcriptional activity of previously selected AtNIMA kinases and determination of their role through gain and loss of functions mutations.

The transcriptional activity of the selected AtNIMA genes was analyzed *in silico* and/or via RT-PCR in the various organs during different stages of the development and through the progression of cell cycle. The role of AtNIMA genes was further determined by using different T-DNA and RNAi lines and analyzing the phenotype of the loss of functions mutants. In addition a construct designed to over-express the AtNIMA genes was employed, to investigate the gain of function mutations on the plant phenotype.

2.3 - Subcellular and organ specific localization of AtNIMA kinases.

To analyze the organ specific distribution of AtNIMA kinases, constructs designed to express AtNIMA genes and promoters fused with YFP and GUS reported gene were used. In addition, antibodies against AtNIMA specific peptide sequences were produced, in order to determine the sub cellular distribution of AtNIMA kinases.

2.4 - Investigation of the putative role of AtNIMA kinases in the phosphorylation of histone H3.

To determine if AtNIMA kinases are involved in the cell cycle-dependent phosphorylation of histone H3, immunostaining with antibodies specific for histone H3 phosphorylated at position serine 10 was performed on mitotic cells prepared from plants carrying loss of function mutations of AtNIMAs.

3. Material and methods

3.1 - Plant material and growth conditions

Wild-type *Arabidopsis thaliana* plants (ecotype 'Columbia-0' (Col-0)) were used for most of the studies. *A. thaliana* lines containing a T-DNA insertion designed for inactivate AtNIMA genes were identified via Signal website (<http://signal.salk.edu/cgi-bin/tdnaexpress>). The lines used (Salk_054652 for AtNIMA 5, Salk_093269 and Salk_012284 for AtNIMA 2, Salk_056986 and Salk_123055 for AtNIMA 3) were ordered from NASC (<http://arabidopsis.info/>) (Fig. 2). Seedlings were grown in a 1:1 mixture of potting substrate and sterilized soil, at first in short day conditions (8 h of light). After three weeks plants were moved into long day conditions (16 h of light).

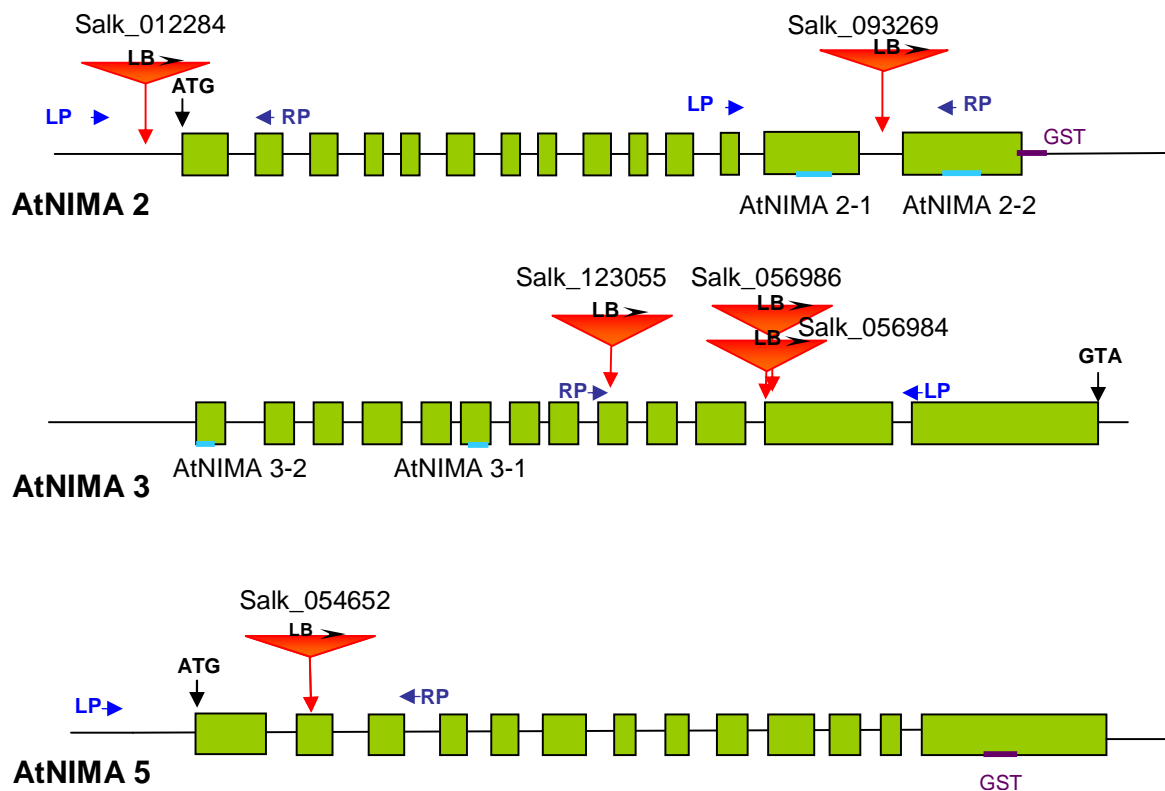


Figure 2: Intron-exon structure of genes AtNIMA 2, 3 and 5. The blue segments represent the position of the peptide sequences selected for productions of anti AtNIMA antibodies. The red arrows show the position of the different T-DNA insertions. The right (RP) and left (LP) border primer and the gene specific tag (GST) for RNAi are also indicated.

3.1.1 - Seed sterilization and plating conditions

Seeds were sterilized by leaving them in 70% ethanol for 10 min on a shaking plate at RT and then for 15 min in a solution of 3% Sodium-hypochlorite (Roth) and 0.005% Tween-20 (Serva). After 3x 10 min washes in sterile H₂O seeds were resuspended in sterile 0.1% agarose (Invitrogen) and plated on growth medium. Seeds were germinated in MS medium (0.5 g/l MES, 2.2 g/l MS (Duchefa), pH 5.8 with K, 1.5% Agar) and left in growth chambers in a 12 h light-dark cycle at 20°C. Different selective agents (16 mg/l phosphinotricin, 25 mg/l hygromycin) were added to the medium for selection of transformed seeds.

3.2 - Sequence processing and primer design

AtNIMA sequences were identified using BLAST (Basic Local alignment Search Tool) <http://www.ncbi.nlm.nih.gov/BLAST/> and the following databases:

TAIR - <http://www.arabidopsis.org/>

TIGR - <http://www.tigr.org/tdb/e2k1/ath1/>

SIGnAL - <http://signal.salk.edu/cgi-bin/tdnaexpress>.

Sequences were processed using the software 'Editseq' and aligned using 'MegAlign', from DNASTar Lasergene 7. Primer sequences for AtNIMA genes were designed using the Operon calculation tool. Each primer was designed with GC content between 30-60%, length of ~22 bp, T_m ~60 °C and designed using a sequence that overlaps two exons, in order to avoid annealing with genomic DNA. Primers for Salk T-DNA lines were designed according to the protocol for Salk T-DNA primer design and verified using the Salk T-DNA verification tool (<http://signal.salk.edu/tdnaprimers.2.html>). RP and LP were respectively the right and left genomic primers while LB indicates the T-DNA insertion left border primer. Primer sequences for verification of RNAi vectors (Agri primers) were obtained by Agrikola (http://www.agrikola.org/index.php?o=/agrikola/html/pAGRIKOLA_validation).

Oligonucleotides were synthesized by Operon (see Table 1) and stored as 100

μ M stock solutions. For PCR a primer concentration of 10 μ M was employed. *In silico* data about the expression behavior of AtNIMA genes were obtained from Genevestigator (<https://www.genevestigator.com/gv/index.jsp>).

Table 1: List of primers specific for AtNIMA genes, Salk T-DNA lines or reporter genes. Melting temperatures (T_m) are given in the last column.

Primer N	Primer name	Primer sequence	T_m
1)	At3g04810 For	5'- AAAGGAGGAGACATGGCGGAAGC -3'	66°C
2)	At3g04810 Rev	5'- GAGACCTCGGAAGGCAGCAGAAT -3'	66°C
3)	AtNek2 new For	5'- TTTGGTCGCTAGGATGTTGTATG -3'	61°C
4)	AtNek2 new Rev	5'- GAAACAGGAAGTTGACCAAGGT -3'	60°C
5)	At5g28290 For	5'- TTGGGTTGAGAAA GGTTGCTATG -3'	61°C
6)	At5g28290 Rev	5'- CCAACCACTGAAGAAGCAAGGTC -3'	64°C
7)	At5g28290-2 For	5'- CTCAGACCAAGCGCTTCTGATCT -3'	64°C
8)	At5g28290-2 Rev	5'- CCGCAGGTTTAGCAGACCACCA -3'	68°C
9)	At3g20860 For	5'- GTCCGAGAGACGAAAGTATGTGG -3'	64°C
10)	At3g20860 Rev	5'- CAAAGTCACCTAACCGAACCTCG -3'	64°C
11)	Agri 51	5'- CAACCACGTCTTCAAAGCAA -3'	55°C
12)	Agri 56	5'- CTGGGGTACCGAATTCCTC -3'	55°C
13)	Agri 64	5'- CTTGCGCTGCAGTTATCATC -3'	55°C
14)	Agri 69	5'- AGGCGTCTCGCATATCTCAT -3'	55°C
15)	N244762 For	5'- ACCTTGGTCAACTTCCTGTTTC -3'	61°C
16)	N244762 Rev	5'- ACCAAATAAGCACCAAAATAGAAT -3'	56°C
17)	N239401 For	5'- TCAAGGCTCCTGACATGGCAGC -3'	66°C
18)	N239401 Rev	5'- TTAAATATTGTTTCATCATCG -3'	53°C
19)	At5g19510 For	5'- AAACCTACATCTCCGGGATCAATT -3'	60°C
20)	At5g19510 Rev	5'- ACAGAAGACTTTCCACTCTCTTTAG -3'	60°C
21)	Salk_054652 RP	5'- GCCGCTAGATAACGAGCTTTG -3'	63°C
22)	Salk_054652 LP	5'- CGACCCAAACATAATAACAAAAAC -3'	58°C
23)	Salk_093269 RP	5'- CATAACCGCCTTCATAATCG -3'	61°C
24)	Salk_093269 LP	5'- CTCCGGAATAATCCAGAACTC -3'	61°C
25)	Salk_012284 RP	5'- AAGCAACCTCTTGATGAGCAG -3'	61°C
26)	Salk_012284 LP	5'- TCATTTCGTTTTCTTCCAATGC -3'	57°C
27)	Salk_056986 RP	5'- TTGCGTTCAGGTTGTTGTATG -3'	58°C
28)	Salk_056986 LP	5'- CGATTCTTGCGAGTTTACTG -3'	60°C
29)	Salk_056984 RP	5'- TTGCGTTCAGGTTGTTGTATG -3'	58°C
30)	Salk_056984 LP	5'- CGATTCTTGCGAGTTTACTG -3'	60°C
31)	Salk_123055 RP	5'- CCGGTTTATCCTGTTGATCAG -3'	60°C
32)	Salk_123055 LP	5'- TGTCGCTCTGGTGTATGTTTG -3'	60°C
33)	LBa1	5'- TGGTTCACGTAGTGGGCCATCG -3'	71°C
34)	LBb1	5'- GCGTGGACCGCTTGCTGCAACT -3'	71°C
35)	LBb1.3	5'- ATTTTGCCGATTTCCGAAC -3'	56°C
36)	S. blot probe left	5'- GGTCTTGCGAAGGATAGTGG -3'	58°C
37)	S. blot probe right	5'- GGTGGAGCACGACACACTT -3'	58°C
38)	35 S Forward	5'- AAGGAAGTTCATTTTATTG -3'	52°C
39)	Gateway AtNIMA 2F	5'-CACCATGGAGAATTACGAGGTTCTTGAGCAA -3'	67°C
40)	Gateway AtNIMA 2R	5'- TCAATCTCCAGCTTAGTAGTAGTGGT -3'	64°C

41)	Gateway AtNIMA 3F	5'- CACCATGGAGCATTACGAGGTTCTTGAGCAA - 3'	68°C
42)	Gateway AtNIMA 3R	5'- TCAATCTTCTTCCAAGTTACTAGGACT -3'	61°C
43)	Promoter AtNIMA 2F	5'- CACCGTGAGATTGCTAGACAACATA -3'	63°C
44)	Promoter AtNIMA 2R	5'- ATTCTCCATTGACAAACTCTG -3'	56°C
45)	Promoter AtNIMA 3F	5'- CACCCCCATTGTTGGTTATTTCTCA -3'	63°C
46)	Promoter AtNIMA 3R	5'- GAAGAAGATTGAAAAACAGGG -3'	56°C
47)	YFP Forward	5'- CGCACAATCCCACTATCCTTCGCA -3'	66°C
48)	YFP Reverse	5'- TTTACGTCGCCGTCCAGCTCGAC -3'	68°C
49)	GUS Forward	5'- ATGTGCTGTGCCTGAACCGTTATTAC -3'	64°C
50)	GUS Reverse	5'- AGGTCGCAAAATCGGCGAAATTC -3'	62°C
51)	GFP Forward	5'- TCTCCCGTTACCCTGATCATATGAAG -3'	64°C
52)	GFP Reverse	5'- TTGTATTCCAACCTTGTGGCCGAG -3'	62°C
53)	BAR Forward	5'- ATGCCAGTTCCCGTGCTTGAAG -3'	64°C
54)	BAR Reverse	5'- CATCGTCAACCACTACATCGAGAC -3'	64°C

3.3 - Extraction of plant genomic DNA

Genomic DNA was extracted from 100 mg of leaf material frozen in liquid N₂, grinded and resuspended in 1.5 ml isolation buffer (0.1 M Tris, 0.7 M NaCl, 0.05 M EDTA at pH 8.0) pre warmed at 65°C for 15 min. After adding 0.65 ml of isoamylethanol: chloroform (1:24), the mix was shaken for 5 min and centrifuged for 2 min at 14.000 rpm at RT. The supernatant was transferred in a new tube and mixed with 10 µl of RNase (10 mg/ml stock) at RT, and then the DNA was precipitated by adding 700 µl isopropanol, shaking for 2 min at RT and centrifuging 10 min at 14000 rpm at RT. The pellet was washed with 1 ml of 70% ethanol, then dried and dissolved in 50 µl double distilled H₂O for 10 min at 65°C (Souza 2006). Extractions were also performed using Mini Plant DNA Extraction kit (Quiagen), according to the company's protocol, in order to obtain DNA of higher purity. The DNA quality and quantity was verified using a 0.8% agarose gel 1X TAE buffer.

3.4 - Extraction of plant total RNA

Samples from different *A. thaliana* tissues (young leaves, adult leaves, open flowers, stems and siliques) were harvested, frozen in liquid nitrogen, crushed and stored at -80°C. Total RNA from the various tissues was isolated using the TRIzol method (Chomczynski P 1987), which was modified according to the protocol of the DNA Microarray Core Laboratory (<http://ipmb.sinica.edu.tw/microarray/protocol.htm>, Institute of Plant and Microbial Biology, Taipei, Taiwan). The RNA quality and quantity was monitored using a MOPS-formaldehyde gel electrophoresis (Sambrook et al. 1989), mixing the probes with RNA loading buffer (95% formamide, 0.025% xylene cyanol, 0.025% bromophenol blue, 10mM EDTA, and 0.025% sodium dodecyl sulphate) in a 1:1 ratio (v/v) and denaturing them for 20 min at 65°C.

3.4.1 - Determination of the concentration of RNA and DNA

The concentration of RNA and DNA was determined via spectrophotometric measurement (SmartSpec Plus, Bio-Rad) on the wavelength between 260/280 nanometres; samples were diluted 1:100 in DEPC-ddH₂O at pH ≥7.5.

3.4.2 - DNase treatment and cDNA synthesis

Contamination from genomic DNA was removed by treating RNA with DNase I, RNase free (Fermentas) according to manufacturer's protocol. The absence of genomic DNA contamination was assayed with PCR using primers 41 and 42 on DNase treated RNA prior to reverse transcription reaction. The cDNA was synthesized using “RevertAid H minus First Strand cDNA Synthesis Kit” (Fermentas).

3.4.3 - Verification of the T-DNA insertion position via genomic PCR

The presence of the T-DNA insertion on the transformed plants was verified by setting up two paired PCR reactions, RP+LP and RP+LB, for each genomic DNA sample. For each Salk T-DNA line a gene-specific primer pair was used (see table 1). RP and LP were used to amplify DNA sequences lacking of a T-DNA insertion, while RP+LB were amplifying sequences containing the T-DNA insertion. Wild type plants were producing amplicons only in the RP+LP reaction while homozygous lines (with the T-DNA insertion located in both homologous chromosomes) only in the RP+LB reaction. Heterozygous lines (with the T-DNA insertion located only in one of the homologous chromosomes) were giving products with both primer pairs. For each PCR reaction 1 µg of genomic DNA extracted from leaf tissue was used. The PCR mix contained: 0.4 µM of primers, 0.1 mM dNTP (Bioline), 1x reaction buffer A (with 1.5 mM MgCl₂), 1U of Taq polymerase (Segetetic); the volume of each reaction was 25 µl. The PCR program used was: 2 min 95 °C ; 30 cycles: 60 sec 94 °C, 60 sec X °C, 1.30 min 72 °C; 5 min 72 °C. The annealing temperatures were depending on the primer pair employed, PCR were performed in Thermal Cycler (Bio-Rad). The products were analyzed in a 0.8% TAE agarose gel, using the mi-100 bp+ DNA Marker Go (Metabion) as size marker.

3.4.4 - Reverse transcription-PCR (RT-PCR)

1 µg cDNA from different tissues was used for each RT-PCR reaction. The primer pair for elongation factor (At5g19510, primer 19 and 20) was used in order to assay the quality and quantity of the cDNA. The PCR mix contained: 0.4 µM of primers, 0.1 mM dNTP (Bioline), 1x reaction buffer A (with 1.5 mM MgCl₂), 1 U of Taq polymerase (Segetetic); the volume of each reaction was 25 µl. The PCR conditions were: 4 min 95 °C ; 25 cycles: 60 sec 94 °C, 60 sec 60 °C, 1.30 min 72 °C + 5 sec/cycle; 10 min 72 °C. For the various AtNIMA primer combinations the annealing temperatures were different (see table 1). The products were analyzed in 0.8% or 1.2% TAE agarose gels, depending on the

expected size of the products, using the mi-100 bp+ DNA Marker Go (Metabion) as size marker.

3.5 - Cloning procedures of constructs

3.5.1 - Full length cDNA isolation

Full length sequences were amplified by using total cDNA from wild type leaf tissues as template for PCR, performed with proof reading High-Fidelity DNA Polymerase (Phusion). The PCR mix contained: 1x Phusion HF buffer (with 2.5 mM MgCl₂), 0.4 µM of primers, 0.1 mM dNTP, 0.6 U of Taq polymerase; the volume of each reaction was 25 µl. The PCR conditions were: 30 seconds 98°C; 30 cycles: 10 seconds 98°C, 30 seconds X °C, 30 seconds 72°C; 10 minutes 72°C. The annealing temperature was varying depending on the AtNIMA primer combination: primer 37 and 38 for AtNIMA 2 (product size ~1.8 kb) and primer 39 and 40 for AtNIMA 3 (product size ~2 kb). The -CACC- sequence added to 5' region of all forward primers allowed an easier ligation reaction with the pENTR D-TOPO entry vector. The size and the concentration of the products were determined via 0.8% agarose gel electrophoresis, using the MI-1kb DNA Marker Go (Metabion) as size marker.

3.5.2 - Isolation of putative AtNIMA 2 and AtNIMA 3 promoter regions

Putative promoter sequences were amplified with the procedure described above, but using genomic DNA from wild type leaf tissues as template. The primers 41 and 42 were used for amplification of the suspected promoter of AtNIMA 2. The primer combination 43/44 was used for amplification of the suspected promoter of AtNIMA 3 (product size ~ 1.2 kb).

3.5.3 - DNA extraction from agarose gel and ethanol precipitation

The DNA was isolated using a QIAquick Gel Extraction Kit (Quiagen) and further concentrated via precipitation according to the Kitto Lab

(<http://kitto.cm.utexas.edu/research/Kittolabpage/Protocols/Microbiology/ethanolPpt.html> University of Texas at Austin, Austin, Texas).

3.5.4 - Preparation of competent bacteria cells

E. coli cells of the strain DH5 α and *A. tumefaciens* cells of the strain LHA 4404 were grown overnight until they reached OD= 0.8 - 1, then they were centrifuged 20 min at 9000 rpm, 4°C. The supernatant was removed, the pellet resuspended in ice cold sterile ddH₂O, using the same volume of the starting bacteria culture, and centrifuged for 20 min at 9.000 rpm, 4°C. This step was repeated a second time using half of the volume of ddH₂O. The pellet was then resuspended in 10 ml of ice cold 10% glycerol and centrifuged for 20 min at 9.000 rpm, 4°C; this step was repeated two times. After the last centrifugation, the cells were resuspended in 1 - 2 ml of 10% glycerol and divided on ice in 50 μ l aliquots using 1.5 ml safe lock tubes that were immediately frozen in liquid nitrogen and stored at -80°C.

3.5.5 - Cloning of AtNIMAs and transformation of *E. coli* bacteria via electroporation

AtNIMAs full cDNA sequences and promoters were inserted separately into pENTR vector (Fig. 3), that contains the gene for kanamycin resistance, using the pENTR/D-TOPO cloning kit (Invitrogen) following the manufacturer's instruction. Each construct was transferred via electrotransformation into *E. coli* DH5 α competent cells, employing an Easyject Prima electroporator (Equibio) at 2500 V and 2 μ l of TOPO cloning reaction. Bacteria were left to grow for 1 h at 37°C in SOC medium for *E. coli*, before spreading on prewarmed petri dishes containing LB+50 mg/l kanamycin.

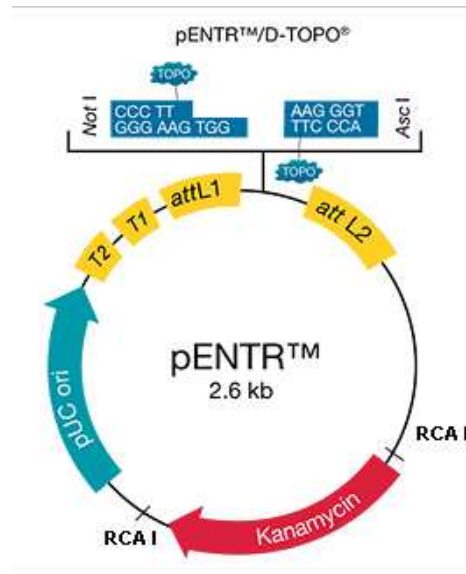


Figure 3: Plasmid map of the pENTR vector used for cloning of AtNIMAs cDNA sequences and promoters. The position of Rca I restriction site is indicated in bold.

3.5.6 - Plasmid DNA extraction and sequencing

E. coli colonies were individually inoculated in liquid LB medium with kanamycin 50 mg/l and left to grow overnight at 37°C. The next day, cells were centrifuged and the plasmid DNA extracted using a QUIAGEN Mini Prep kit according to manufacturer's instructions. Plasmids for *A. tumefaciens* cells were extracted with the same method, except for employing for each sample a double amount of buffer compared to *E. coli*. The plasmids were checked for the correct size of the insertion via PCR using the primer described above. Sequencing was performed using facilities at IPK (Gatersleben) or at Eurofins MWG Operon Biotech AG.

3.5.7 - pENTR plasmid digestion

The selected pENTR vectors were digested with *Rca I* (Roche) following the manufacturer's protocol, in order to inactivate the gene responsible for kanamycin resistance. The digested DNA was run on a 0.8% agarose gel and the DNA fragments of interest were isolated using a QUIAGEN gel extraction kit.

3.5.8 - Recombination of AtNIMA sequences into destination vectors

The AtNIMA-fragments were recombined into various destination vectors using the LR Clonase II kit (Invitrogen), according to manufacturer's protocol. The chosen destination vectors were:

1. pEarleyGate 100, containing 35S promoter for producing over-expressed constructs (Earley K.W. 2006)
2. pEarleyGate 104, to produce YFP reporter constructs with N-terminal fusion (Earley K.W. 2006)
3. pMDC107, for promoter test with GFP N-terminal fusion (Brand L 2006)
4. pMDC162, for promoter test with GUS N-terminal fusion (Brand L 2006)

3.5.9 - Analysis of the destination vector constructs

Recombinant plasmids were digested using the following restriction enzymes to further confirm their sequences, according to manufacturer's protocol (Fig. 4).

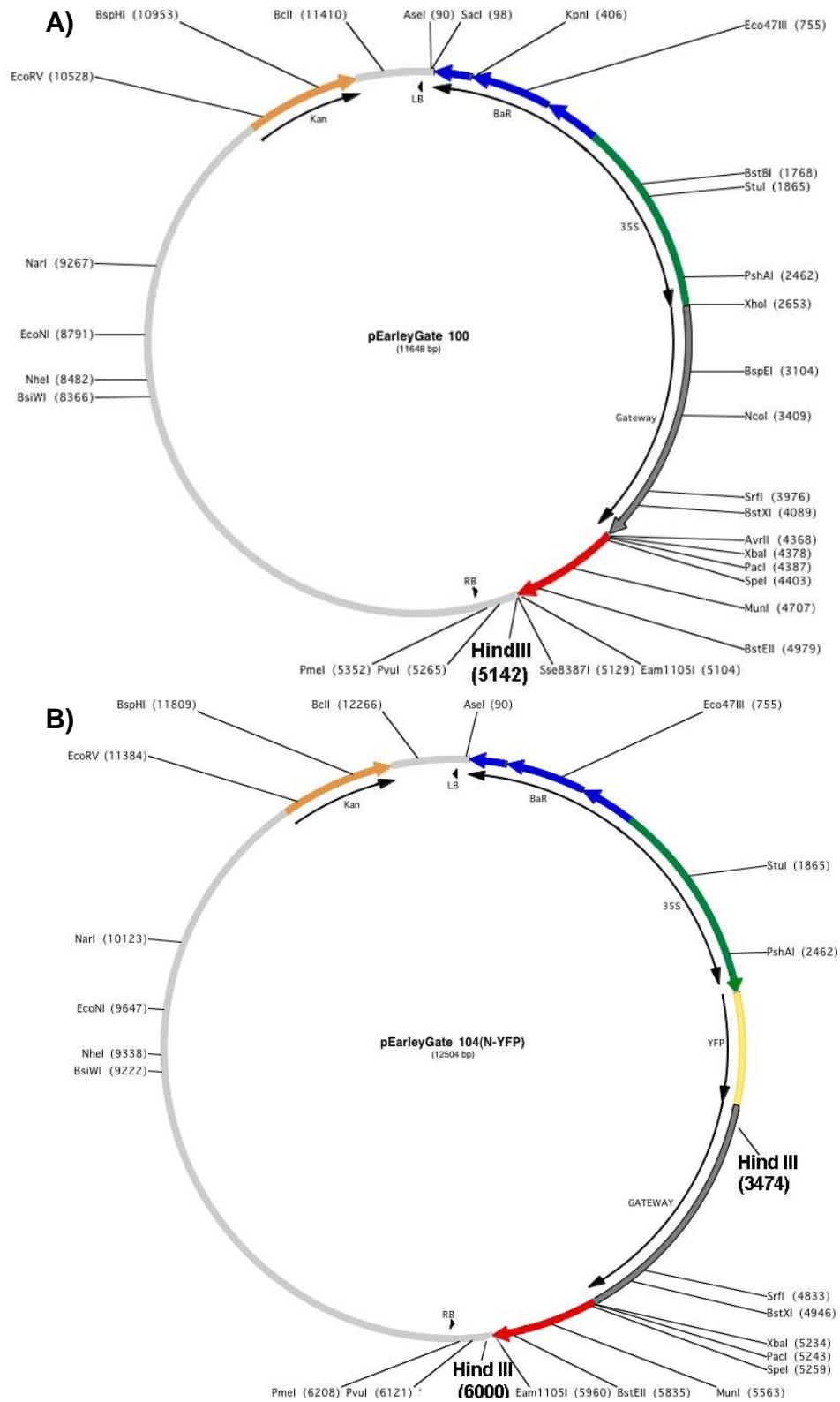
- *Hind* III (Fermentas) for pEarley vectors,
- *Hind* III and *Xho* I (Fermentas) for pMDC vectors.

Further analyses of the vector's sequences were performed via PCR using the following primer combinations:

- 36+38 for pEarleyGate plasmids with AtNIMA 2,
- 36+40 for pEarleyGate plasmids with AtNIMA 3,
- 41+48 for pMDC162 with the promoter of AtNIMA 2,
- 43+48 for pMDC162 with the promoter of AtNIMA 3,
- 41+50 for pMDC107 with the promoter of AtNIMA 2,
- 43+50 for pMDC107 with the promoter of AtNIMA 3.

The selected constructs were transformed into *A. tumefaciens* strain LBA 4404 via electroporation and then plated into petri dishes containing YEB+kanamycin (50mg/l) and left 2 days at 28°C. The resulting colonies were further verified by PCR and digested with restriction enzymes. Positive colonies were grown in

liquid media of YEB+50 mg/l kanamycin + 100 mg/l rifampicin in order to perform subsequent plant transformation.



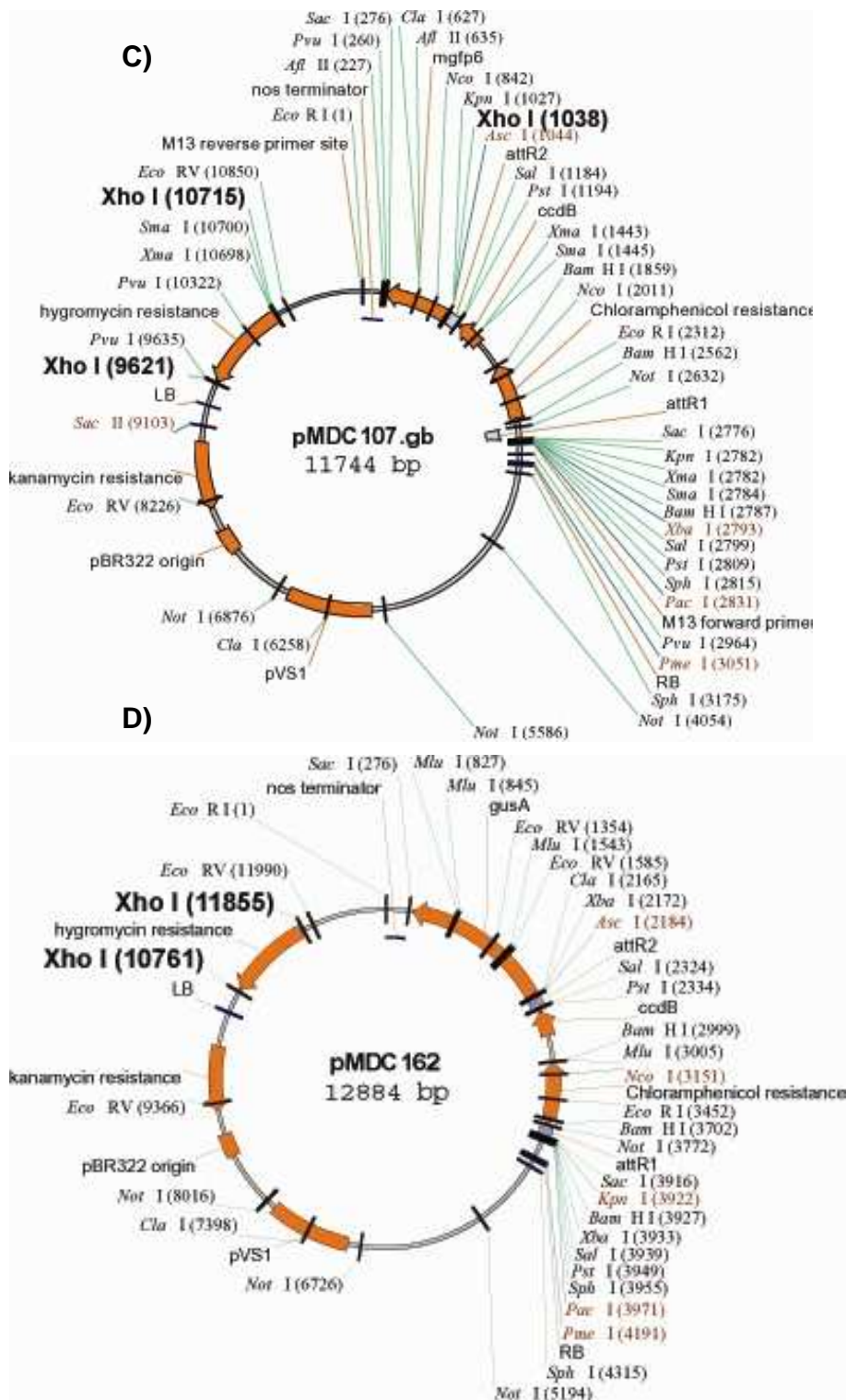


Figure 4: Plasmid maps of the destination vectors used for analysis of AtNIMAs gene. The restriction sites used for verification are indicated in bold. A) pEarley 100, B) pEarley 104, C) pMDC 107, D) pMDC 162.

3.6 - Stable transformation of *A. thaliana* via floral dip

Wild-type *A. thaliana* plants were transformed using the floral dip method (Clough S.J. 1998). A preculture of recombinant *A. tumefaciens* was prepared with 5 ml YEB+50 mg/l kanamycin + 100 mg/l rifampicin and left to grow at 28°C overnight. The following day the bacteria were used to inoculate 500 ml YEB+50 mg/l kanamycin + 100 mg/l rifampicin and left to grow under the same conditions. When the culture reached OD₆₀₀ 0.8 – 1.0 it was centrifuged 20 min at 5.500 g, 4°C and then resuspended in 500 ml of infiltration medium (5% sucrose, 0.05% Silwet L-77). In case the OD₆₀₀ of the culture was higher the volume of infiltration medium was changed accordingly, in order to have a bacteria solution of OD₆₀₀ ~1 for plant transformation. Six weeks old *A. thaliana* Columbia-0 plants were inverted in the recombinant *A. tumefaciens* solution so that their inflorescences were submerged for ~1 min with some brief shaking. After, the plants were left overnight lying on trays shielded by light. The next day the inflorescences were shielded with aracorns and the plants were further cultivated.

3.7 - RNAi-based knockdown of AtNIMA genes

3.7.1 - Design of the constructs

RNAi vectors were obtained by the Agrikola consortium (<http://www.agrikola.org/index.php>), and ordered via NASC.

The following clones were used:

- N244762 for AtNIMA 2
- N239401 for AtNIMA 5

The corresponding GSTs sequences were identified through the CATMA database (<http://www.catma.org/>). The position of GSTs is shown in figure 1.

3.7.2 - Transformation of bacteria with AtNIMA RNAi constructs

Recombinant pAgrikola vectors were transferred via electroporation into cells of the *A. tumefaciens* strain GV3101:pMP90:pSOUP. Bacteria were spread in petri dishes containing LB+50 mg/l kanamycin + 5 mg/l tetracycline and left to grow two days at 28°C. For validation plasmid were extracted from several colonies using a QUIAGEN Mini Prep kit.

3.7.3 - Validation of recombinant pAgrikola vectors used for plant transformation

Validation of recombinant pAgrikola vectors was performed via PCR using the following conditions: 5 minutes 94 °C; 35 cycles: 45 seconds 94 °C, 45 seconds 55 °C, 2 minutes 72°C; 5 minutes 72°C. For each construct we performed four paired PCR reactions following the Agrikola validation protocol

(http://www.agrikola.org/index.php?o=/agrikola/html/pAGRIKOLA_validation).

The Agri primers were used in the following combinations:

- Mix 1 = Agri 51+56
- Mix 2 = Agri 51+64
- Mix 3 = Agri 56+69
- Mix 4 = Agri 64+69

The products were analyzed in a 1.2% TAE agarose gels using the mi-100 bp+ DNA Marker Go (Metabion) size marker. The validated cultures were used to transform *A. thaliana* plants via floral dip.

3.7.4 - Selection and validation of AtNIMA RNAi plants

Seeds from transformed plants were germinated in petri dishes with MS + 16 mg/l phosphinotricin, including wild-type seeds on non selective and selective medium as positive and negative controls. In order to confirm the presence of the RNAi construct genomic DNA was extracted from the selected plants and the

GSTs sequences were amplified via PCR, using the same conditions as described under 3.7.3.

3.7.5 - Analysis of RNAi-based down regulation of AtNIMA genes

Down regulation of the AtNIMA genes expression was assayed via RT-PCR using primer pair 15-16 for AtNIMA 2-GST and 17-18 for AtNIMA 5-GST, using wild type cDNA as control. Primer pair for elongation factor (n° 19-20) was also used as control.

3.7.6 - Analysis of the phenotype of RNAi-based down regulated AtNIMA plants

Cross sections of stem and leaf tissues coming from down regulated lines and wild type plants were comparatively analyzed by confocal microscopy. Length of primary root and cotyledon size of two weeks old seedlings were determined using a SZX12 stereo microscope (Olympus).

3.8 - Southern hybridization of genomic DNA

Southern hybridization was performed according to (Sambrook et al. 1989). 10 µg of genomic DNA from plants was digested overnight with the following restriction enzymes: *EcoR* I, *Kpn* I, *Hind* III (Fermentas) according to the company's instruction. The digested DNA was size-fractionated by gel electrophoresis (0.8% agarose in 1X TAE buffer, 24-30 hours at 25V). The gel was denatured in denaturation buffer (1.5 M NaCl, 0.5 M NaOH) for 30 minutes, rinsed shortly in distilled H₂O and neutralized for 15 min twice in neutralization buffer (1.5 M NaCl, 1 M TrisHCl (pH7.2), 0.001 M EDTA). Next the gel was blotted onto Hybond-N⁺ membrane (Amersham) by capillary transfer in 20x SSC overnight; the platform was covered with Whatman 3MM filter paper saturated with 20x SSC. The successive day the membrane was washed first with 2x SSC, then left 20 min in 0.4M NaOH to allow DNA denaturation. After a brief wash in

5x SSC the membrane was covered, still moist, in Glad Wrap and left at 4°C. Prehybridisation and hybridization were performed in Church buffer (7% SDS, 10 mM EDTA, 0.5 M phosphate buffer (pH 7.2), at 64 °C; herring sperm DNA (10 mg/ml) was employed for prehybridisation. Probes (100 ng) were labeled with 5 µl [α -³²P] CTP, 125 µCi P³² (GE Healthcare) using the HexaLabel™ DNA Labeling Kit (Fermentas). After overnight hybridization the membrane was washed first for 20 min in 2x SSC+ 0.5% SDS buffer, then for 20 min in 1x SSC+ 0.5% SDS buffer, all washing steps were performed at 65°C. The membranes were exposed to Fujifilm imaging plates which were scanned using the Phospho-Imager (Fuji).

3.9 - Indirect immunostaining and Western blotting

3.9.1 - Generation of putative AtNIMA-specific polyclonal antibodies

Antibodies were ordered by Eurogentec. The candidate peptide sequences were first analyzed via BLAST (<http://www.ncbi.nlm.nih.gov/BLAST/>) in order to find sequences specific for AtNIMA 2 and 3 and avoid the binding to different members of the AtNIMA family. For each AtNIMA protein the following peptide sequences were selected (see Figure 1):

AtNIMA	2-1	H2N-	ESA	RRN	SFP	EQR	RRP	A	-	CONH2	(16 AA)
AtNIMA	2-2	H2N-	DAY	LED	RSE	SSD	QNA	T	-	CONH2	(16 AA)
AtNIMA	3-1	H2N-	CES	ERR	SSY	PQQ	RKR	T	-	CONH2	(16 AA)
AtNIMA	3-2	H2N-	CSK	SFK	ESS	PSN	LEE	D	-	COOH	(16 AA)

Each couple of peptides was injected in two different rabbits, and then pre-immune serum and three different bleeds (small bleed, large bleed and a final bleed) were harvested in a period of time of three months.

3.9.2 - Preparation of squashed mitotic cells

The seeds were germinated on moist filter paper at 22-24°C under long day light conditions for 3-4 days. The root tips were fixed in freshly prepared 4%

paraformaldehyde solution (dissolved in 1x PBS) for 20 min on ice, then washed 3x 15 min in 1x PBS on ice. Cell walls were digested by treating the root meristems with an enzyme mix (2.5% Pectinase, 2.5% Cellulase R-10, 2.5% Pectolyase Y-23 dissolved in 1x PBS) at 37°C until the material become soft (about 5-10 min). The material was then washed several times in 1x PBS. The squashing was performed in 1x PBS between slide and cover slip, then the slides were immersed into liquid nitrogen and after immediate removal of the cover slip collected in a glass coplin jar with 1x PBS. For longer storage the slides were kept in 100% glycerol at 4°C. Flower buds (between 0.3-0.7 mm) were fixed as the root tips and washed 3x10 minutes in 1x PBS at room temperature. After enzymatic digestion (performed as above) the material was washed 3x10 minutes in MTSB. Flower buds were squashed in a drop of MTSB and stored with the same procedure used for the root tips.

3.9.3 - Preparation of chromosome suspension from *Vicia faba*

Seeds from *V. faba* were germinated on wet filter paper for three days in a desiccator in a dark room. Afterwards the seedlings were incubated for 18 h in Hoagland solution and then treated for 18 h in Hoagland solution with 1.25 mM hydroxyurea to block the cells in S-phase. After a short wash with ddH₂O the seedlings were incubated for 6 h in fresh Hoagland solution, then for 3 h in 0.05% colchicine to arrest cells at metaphase. After rinsing in ddH₂O the seedlings were fixed with 4% (v/v) formaldehyde in 15 mM Tris buffer pH 7.5 for 20 min on ice in vacuum and then washed twice for 15 min in Tris buffer at 4°C. The meristems of root tips were separated with a sharp scalpel and homogenized in 1 ml Isolation buffer (15 mM Tris-HCl, 80 mM KCl, 20 mM NaCl, 2 mM disodium EDTA, 0.5 mM spermine, 0.1% Triton X-100, 15 mM mercaptoethanol, pH 7.5; (Dolezel et al. 1989)). This suspension of released chromosomes and nuclei was passed through a 35 µm nylon filter to remove larger cellular fragments (Schubert et al. 1993)

3.9.4 - Indirect immunostaining of cells and seedlings

First 100 µl blocking solution (8% BSA, 0.1% Tween 100, 1x PBS) was applied to slides containing cells or whole seedlings, covered with parafilm and incubated at room temperature for 30 min, then washed 2x 5 min in 1x PBS. The slides were left to drain for a short moment before the primary antibodies, diluted in 1x PBS and 1% BSA, were separately applied in following dilutions: 1:300 for anti-histone H3S10ph (Upstate Biotechnology, USA), 1:500, 1:200 and 1:100 for anti-AtNIMA 2 and 3 (Eurogentec) in 1x PBS, 1% BSA. The slides were then incubated at 4°C. After 12 hours the material was washed 2x 5 min in 1x PBS, then the secondary anti-rabbit antibody conjugated to Cy3 (Jackson ImmunoResearch) was applied. The slides were covered with parafilm and incubated for 1 hour in a humid chamber at 37°C followed by washing 3x 5 minutes in 1x PBS in darkness. Then they were mounted with 10 µl of antifade containing 10 µg/ml DAPI (4', 6-diamidino-2-phenylindole) and covered with cover slips. The slides were analyzed with an Olympus BX61 fluorescence microscope equipped with an ORCA-ER CCD camera. Images were analyzed using the SIS software (Olympus).

3.9.5 - Anti-tubuline staining of leaf cells

Leaf material from *N. benthamiana* was fixed in 4% paraformaldehyde dissolved in MTSB, treating the material first for 10 minutes in vacuum and subsequently for 20 minutes without vacuum at room temperature. Samples were then washed 3x 10 minutes in MTSB. The specimens were then prepared by squashing the leaf fragments as described in 3.8.1, only without enzymatic digestion. After adding the blocking solution (see 3.8.3) the anti- α tubuline primary antibody (Sigma), diluted 1:100 in 1x PBS and 3% BSA, was applied to the slides. After 14 hours the material was washed 2x 5 minutes in 1x PBS, then the secondary anti-mouse antibody conjugated to Alexa₄₈₈ (Invitrogen) was applied in a dilution 1:100 in 1XPBS 3% BSA. The preparation then was continued as described in 3.8.3.

3.9.6 - Extraction of proteins

Proteins were extracted by adding 250 µl of protein extraction buffer (112 mM Na₂CO₃, 112 mM DTT, 4% SDS, 24% Saccharose, 4mM EDTA, bromophenol blue) to 100 mg of leaf material frozen in liquid N₂ and grinded. The samples were incubated at 65°C for 20 min and then centrifuged for 5 min at 14000 rpm RT. Proteins were collected as supernatant in new 1.5 ml tubes and stored at -20 °C.

3.9.7 - Western Blotting

Proteins were separated using a vertical Tricine-SDS-Polyacrylamide gel electrophoresis (Schagger and von Jagow 1987) with 10% acrylamide (stacking gel: 50% acrylamide, 20% SDS buffer, 1.3% APS, 0.13% Temed, dH₂O; separating gel: 50% acrylamide, 20% SDS buffer, 50% glycerin, 0.7 % APS, 0.07% Temed, dH₂O). Samples were denaturated for 5 min at 95 °C prior to the loading on the stacking gel, the electrophoresis was run for 2 h at 100 V using 5 µl of PageRuler Prestained Protein Ladder (Fermentas) as size marker. Blotting on PVDF membrane was performed using PEGASUS Semi-Dry-Blotter at 0.8 mA/cm² for 1.30 h. The membrane was blocked by leaving it in a solution of PBST (1xPBS +0.1% Tween-20) +5% milk powder for 1 h, before moving it in a tube containing the primary antibody solution (1:500) and leaving in a rotor at 4°C ON. The next day the membrane was washed 3x10 min in PBST before applying the secondary antibody (1:5000) for 1 h at RT, then was washed again 3x10 min in PBST and stored in a lead cassette.

3.10 - Quantification of seed setting

Siliques were harvested and fixated overnight using an ethanol: acetic acid (9:1 v/v) solution. After fixing, the tissues were washed with 80% ethanol and 70% ethanol and then left over night in clearing solution (chloralhydrate:H₂O:glycerol

(8:3:1 w/v/v)). Observation was performed using a SZX12 stereo microscope (Olympus). Data was plotted using Microsoft Office Excel 2003.

3.11 - Alexander staining of pollen

Anthers from mature flowers were isolated and collected on glass slides. Few drops of Alexander stain (10 ml ethanol 95%, 1 ml malachite green (1% in 95% ethanol), 5 ml Fuchsin acid (1% in water), Orange G (1% in water), 5 g phenol, 5 g chloral hydrate, 2 ml acetic acid (ice cold), 25 ml glycerol, 50 ml dH₂O) were added, the cover slip was put on with a slight pressure and the slides were left to rest for 15 min. Observation was performed using a light microscope equipped with phase contrast (Zeiss).

3.12 - Transient expression of AtNIMA::YFP constructs in *Nicotiana benthamiana* leaves

3.12.1 - Preparation of AtNIMA::YFP constructs and plant infiltration

6 weeks old *N. benthamiana* plants were selected for infiltration. *A. tumefaciens* colonies from the strain LBA 4404 containing the plasmids 35S::YFP::AtNIMA 2, pEarley 104 and 35S::H2B::YFP (Boisnard-Lorig et al. 2001) were grown in 5 ml YEB + Kan 50 mg/ml and Rif 10 mg/ml at 28°C over night. In parallel, *Agrobacterium* with “helper” plasmid (pBinAR with Hc-Pro), one for each culture with a plasmid of interest, were grown at the same conditions. At OD ~1 growth was stopped and each culture containing a plasmid with a reporter gene was mixed together with a culture containing the “helper” plasmid in a 1:1 ratio (v/v) and centrifuged at 5.500 g for 15 min at room temperature. Supernatant was removed and the bacteria resuspended in 10 ml buffer containing 10 mM MgSO₄ and 10 mM MES (the volume was adjusted in order to keep the OD ~1). The infiltrations were performed by piercing the top leaves of *N. benthamiana* with a needle and injecting the bacteria using a 10 ml syringe. Each leaf was injected 2-4 times, and then the plants were left two days in the greenhouse at long day conditions.

3.12.2 - Analysis of transiently expressed AtNIMA::YFP proteins in *N. benthamiana*

Leaf fragments of ~2 cm² were cut from the inoculated plants and moved on glass slides, with few drops of water. The specimens were analyzed with an Olympus BX61 fluorescence microscope equipped with an ORCA-ER CCD camera. Images were analyzed using the SIS software (Olympus).

3.12.3 - Treatment of leaf cells with tubuline inhibitors

To analyse the tubuline organization, leaf pieces were placed in 0.1% colchicine (Merck) in 10% DMSO (Sigma), 10 µM oryzalin (Sigma) in 10% DMSO or 10 µM Latrunculin B (Calbiochem) in 10% DMSO and left 15 min in a vacuum (using Concentrator 5301 (Eppendorf)), then incubated for 3 hours at RT. After incubation, slides were prepared as described above. As negative control, 10% DMSO was applied as described above.

3.13 - GUS histochemical staining

The expression of the AtNIMA promoters via GUS activity on transformed plants was analyzed with the procedure developed by Kim and colleagues (Kim et al. 2002). Briefly, tissues of interest (entire seedlings, roots and stem sections, leaves, flowers or siliques) were harvested in 2 ml tubes and fixated at room temperature for 20-30 min (depending on the size) with a cold solution of acetone:H₂O mix (9:1, v/v). Each sample was then washed three times on ice with GUS staining buffer (50 mM sodium phosphate buffer pH 7.0, 0.2% Triton X-100, 2 mM potassium ferrocyanide, and 2 mM potassium ferricyanide), before adding the GUS staining solution (containing 1 mM X-Gluc (Fermentas) dissolved in GUS staining buffer). Samples were infiltrated by leaving 5 minutes in vacuum and incubated over night at 37°C with gentle agitation. The next day they were washed several times in 70% ethanol to remove chlorophyll. Hoyer's

solution (5 ml H₂O, 3 g gum arabicum (Sigma, G9752), 2 ml glycerol, 20 g chloral hydrate) was used for permanent histological preparation. Tissues were analyzed using a SZX12 stereo microscope (Olympus) equipped with an Exwave HAD digital camera (Sony), implementing the software Cell A-Soft Imaging System (Olympus).

4. Results

4.1 - Identification of AtNIMA genes in *A. thaliana*

The NIMA related kinases in *A. thaliana* were identified via BlastP using the entire protein sequence of *A. nidulans* nimA kinase as bait (accession number XP_868886). It was found that the genome of Arabidopsis encodes for a family of NIMA related kinases that comprises seven members.

- 1) AtNIMA 1 = *At1g54510*
- 2) AtNIMA 2 = *At3g04810*
- 3) AtNIMA 3 = *At3g20860*
- 4) AtNIMA 4 = *At3g63280*
- 5) AtNIMA 5 = *At5g28290*
- 6) AtNIMA 6 = *At3g44200*
- 7) AtNIMA 7 = *At3g12200*

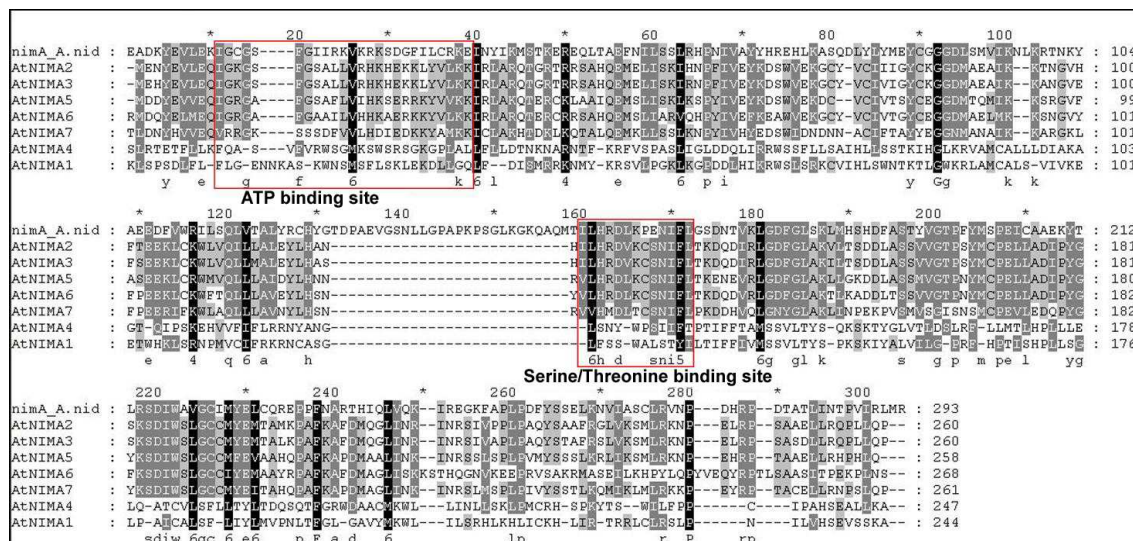


Figure 5: Amino acid sequence alignment of the catalytic domains of nimA of *A. nidulans* and AtNIMAs of *A. thaliana*. The *in silico* predicted different active sites of the catalytic domains are highlighted in the red boxes.

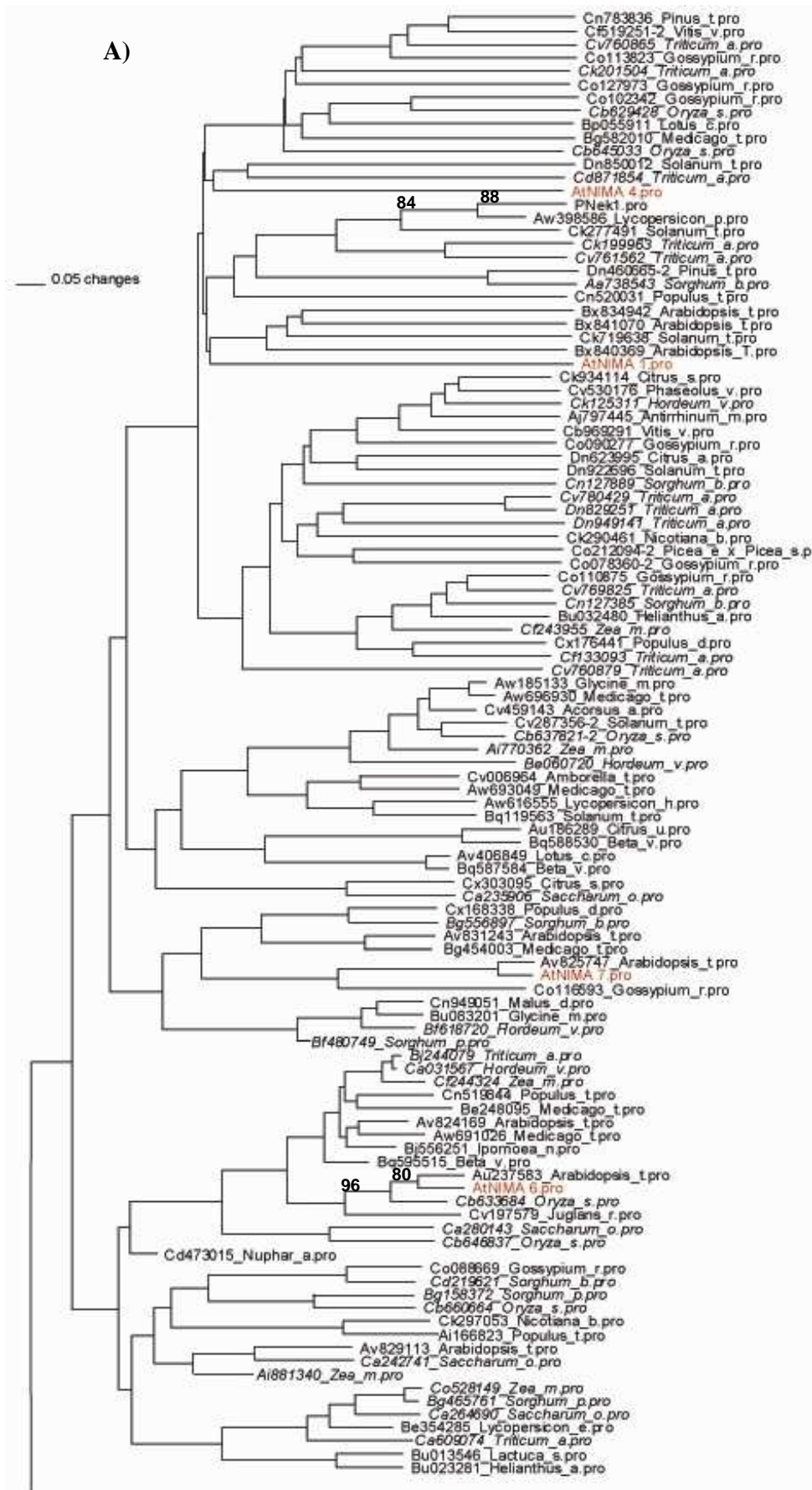
By using the software GeneDoc the catalytic domain of the different AtNIMAs were aligned with the one of nimA from *A. nidulans* (Fig. 5). The alignment shows that the catalytic domains of NIMA-like proteins are highly conserved, in particular AtNIMA 2, 3, 5 seems to be more closely related to the fungal nimA.

Due to this reason those members of the *A. thaliana* NIMA family were selected for further molecular studies.

4.2 - Phylogenetic relationship of AtNIMAs with NIMA related kinases from other plants

A phylogenetic study was conducted in order to improve the knowledge about NIMA related kinases origin and distribution in other plant species. Alignment of the nimA kinase catalytic domain of *A. nidulans* (Pfam: PF00069.18) with other putative NIMA-like proteins revealed that NIMA homologues are found in a number of plant species. Using the nucleotide and protein sequences of AtNIMA 2, 3 and 5 as baits to search the *Viridiplantae* database (a subset of GeneBank) it was possible to obtain around 500 ESTs encoding NIMA-like genes in 20 different organisms, including: *Zea mays*, *Oryza sativa*, *Hordeum vulgare*, *Triticum aestivum*, *Lycopersicon esculentum*, *Populus thricocarpa* and *Vitis vinifera*. The identified EST sequences were subsequently aligned and trimmed to remove redundancy. The resultant 200 sequences were analyzed to isolate the portions encoding for the catalytic domain, identified between the amino acid residues n° 145 and 550. The putative sequences for the catalytic domain of the different NIMA like proteins were used to generate a phylogenetic tree (Fig. 6). The tree is divided in four major branches. Three of them contain plant species and are further separated in various sub-clusters; the fourth contains the fungal *nimA*. AtNIMA kinases do not cluster together, but instead occur in two of the main clusters. A closer observation shows that each AtNIMA kinase is located in a different branch of the phylogenetic tree, clearly separated from the other members of the family. The exceptions are the pairs AtNIMA 1-4 and AtNIMA 2-3, that show close phylogenetic relationships, particularly AtNIMA 2 and 3. This indicates relative recent duplication events of these AtNIMA family members. In addition the separation between monocots and dicots is evident in each minor cluster containing an AtNIMA kinase. This suggests that NIMA like kinases in plants already differentiated into a gene family before the split of monocots from early dicots. Most of the species analyzed, in monocots and dicots, posses

multiple members of the NIMA-like gene family, for example *P. trichocarpa* encodes for nine NIMA-like genes while *O. sativa* possesses six (Vigneault et al. 2007). All together these results indicate that the NIMA like kinases family was conserved through the evolution, suggesting a major role for plant development.



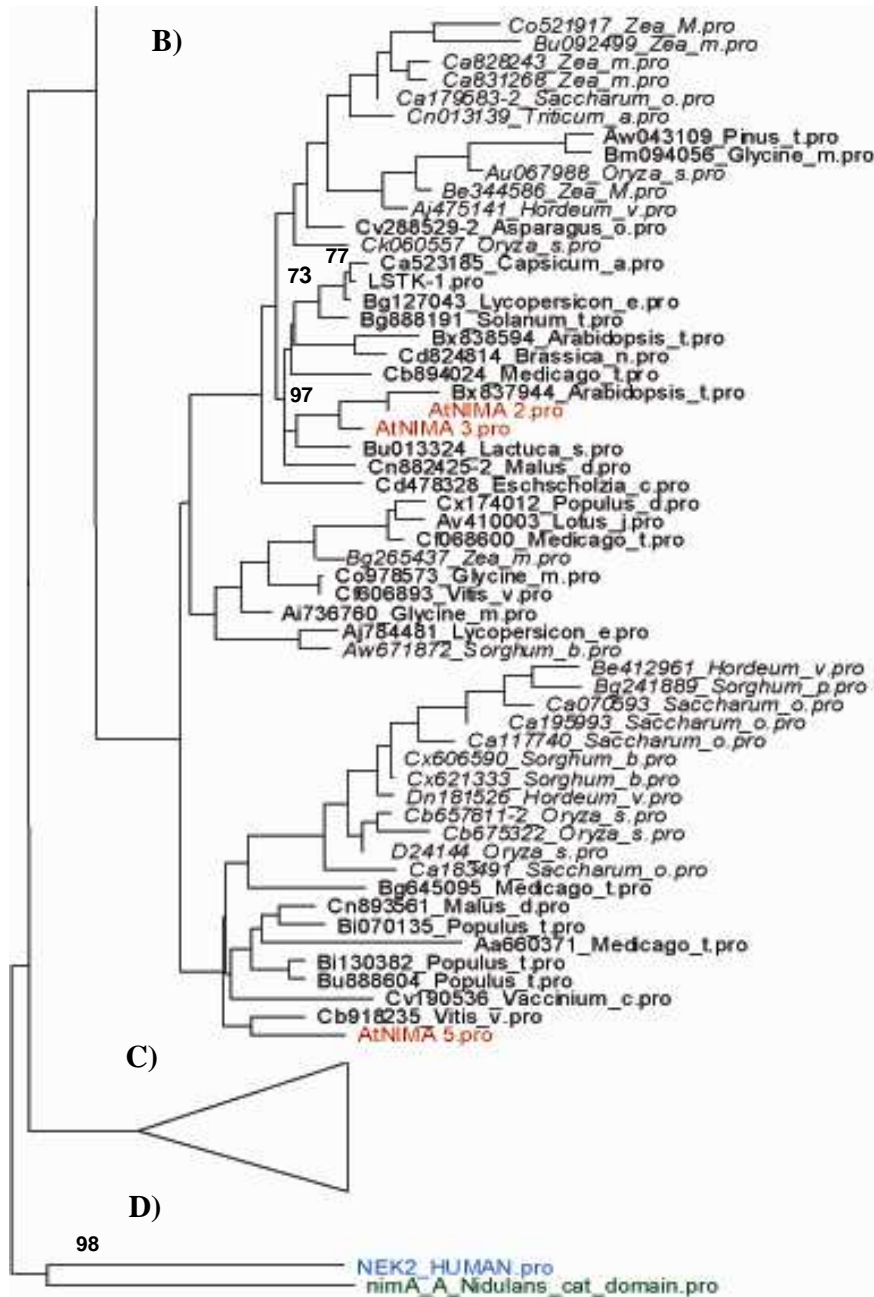
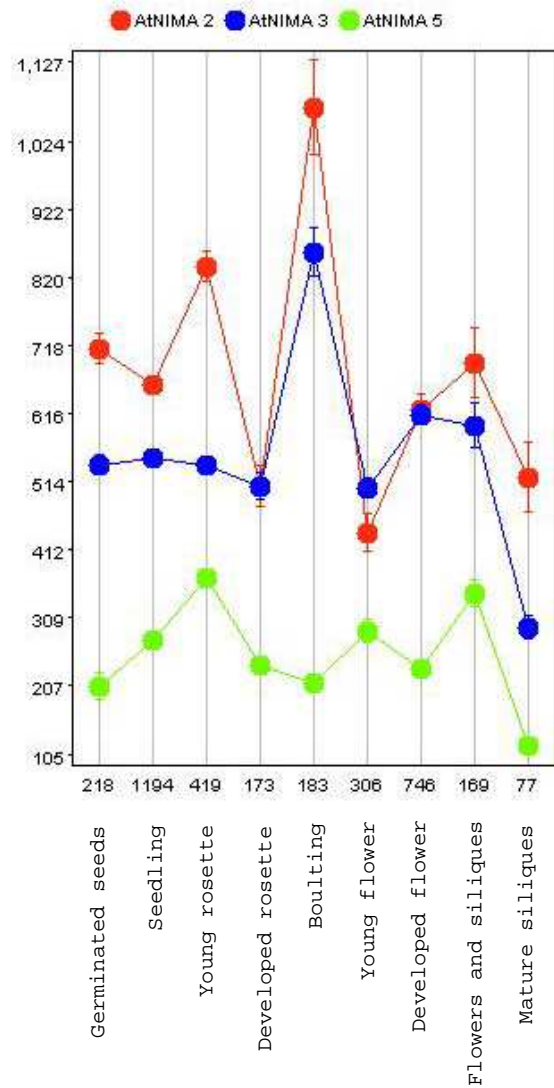
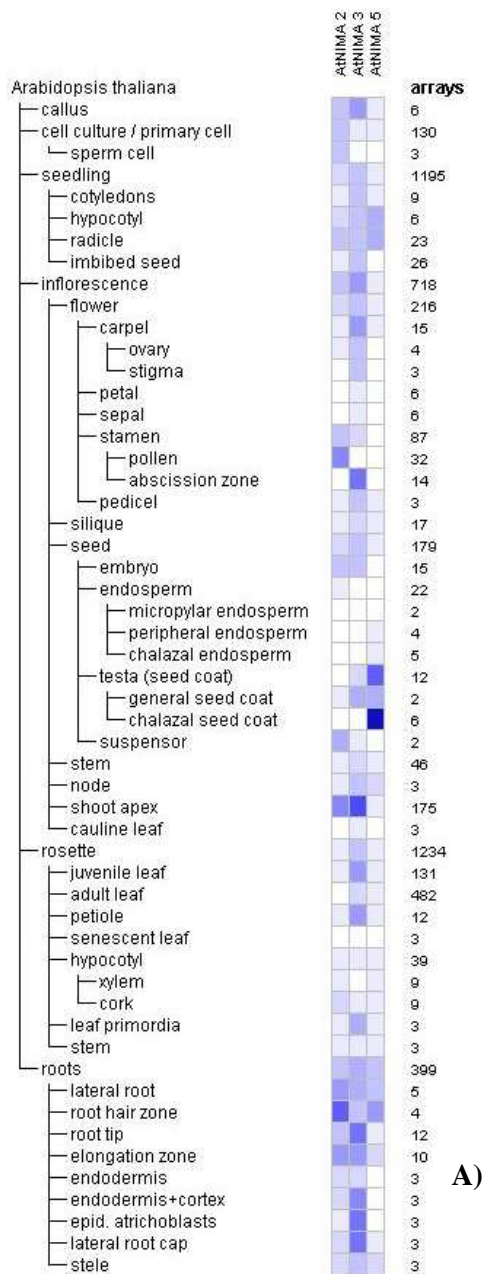


Figure 6: Neighbour joining tree calculated from amino acid residues n° 145-550 of different plants NIMA like kinases. The tree is divided in four major branches. AtNIMA family members (indicated in red) are located in clusters **A)** and **B)**. AtNIMA kinases are separated from each other inside different minor clusters with the exception of AtNIMA 2-3 and AtNIMA 1-4, which seem to maintain a major conservation in the catalytic domain. Monocots are written in italic. Cluster **C)** does not contain any AtNIMA protein and is described in the Supplemental material. **D)** Human NEK2 indicated in blue (accession number P51954) and nimA of *A. nidulans* indicated in green (accession number P18837) were used as outgroup. The Genbank accession numbers are indicated in front of the species names. Bootstrap values are indicated on the nodes.

4.3 - Organ specific expression of AtNIMA 2, 3 and 5

The expression pattern of the selected members of the AtNIMA family was firstly analyzed *in silico*. A gene expression database, which is based on results of microarray hybridization experiments with RNA samples extracted from a large variety of *A. thaliana* organs and plants grown under different conditions, was processed using the software “Genevestigator” (<https://www.genevestigator.ethz.ch>) (Zimmermann et al. 2005). The first observation about AtNIMA gene expression pattern obtained by the computational analysis (Fig. 7 A) is that all of them are transcribed in almost all organs of *A. thaliana* (leaves, stems, flowers, roots). In particular AtNIMA 2 and 3 seems to have a similar expression at the same stages of plant development, especially during growing of inflorescence, embryo and shoot apex. The plant development dependent gene expression profile (Fig. 7 B) shows that the AtNIMA genes seem to be active in all stages of *A. thaliana* growth, although the total expression of AtNIMA 2 and 3 is in the average two fold higher than AtNIMA 5. Interestingly, it reaches highest activity during the bolting stage, corresponding to the final stages of the rosette growth and the beginning of formation of the primary stem. The transcription activity of AtNIMA genes during the mitotic cell cycle was analyzed using publicly available microarray data (Menges et al. 2005), which were deduced from a cell cycle synchronized *A. thaliana* cell suspension (Menges et al. 2003). The onset of mitosis is indicated by the strong expression of Cyclin B1 (At2g26760) (Fig 7 C). Based on this data set, AtNIMA 2 seems to have a constant expression during all stages of the cell cycle. Instead AtNIMA 5 has a peak of activity during S phase, before stationary expressed during the rest of the cell cycle. On the opposite, AtNIMA 3 has a very low expression during all phases of the cell cycle. Anyway, none of the AtNIMA genes has an increased expression during G2 phase with a peak at mitosis, like the expression profile of Cyclin B1. Hence, the transcription activity of AtNIMA 2, 3 and 5 is no cell cycle dependent.



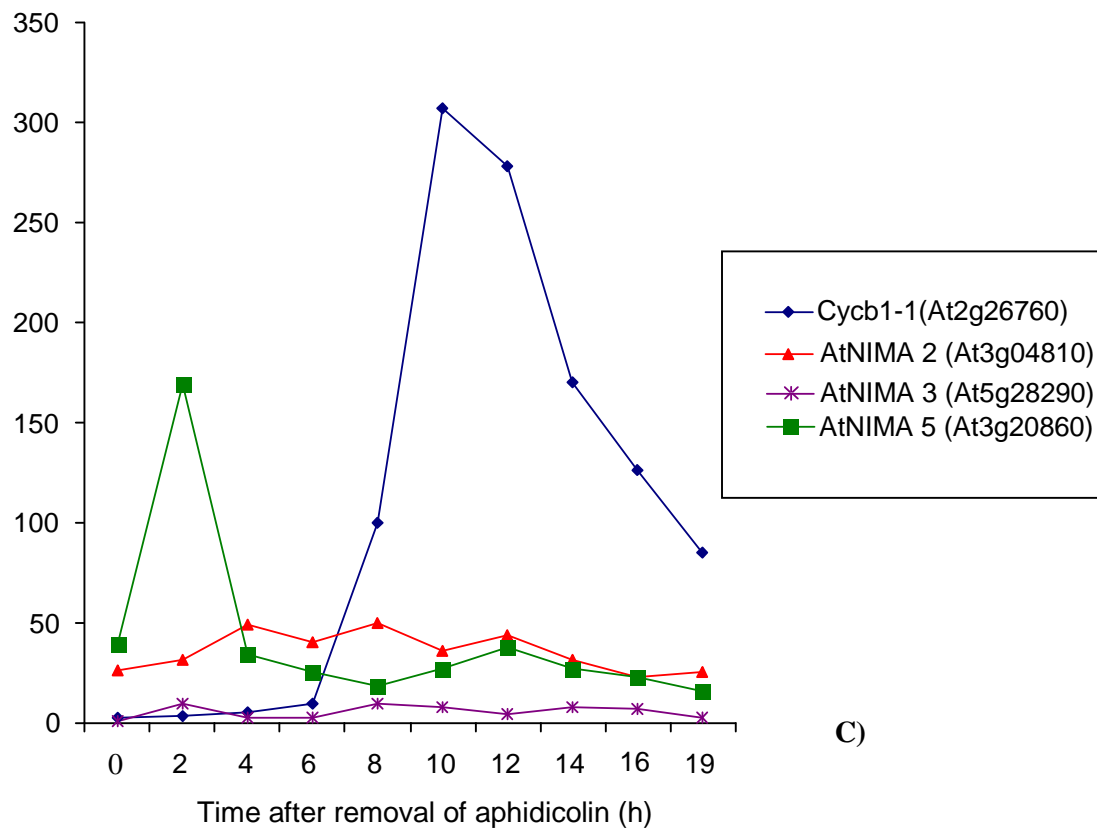


Figure 7: *In silico* gene expression analysis of AtNIMA 2, 3 and 5 based on Genevestigator (update from September 2009).

A) Organ-type specific expression behaviour of AtNIMA 2, 3 and 5. A darker color indicates a high transcription activity of a gene.

B) Expression dynamics of AtNIMA 2, 3, and 5 during plant development. Horizontal axis shows the stages of development and the number of microarray used; vertical axis indicates relative gene activity.

C) Transcription profiles of AtNIMA 2,3, and 5 and Cyclin B1 (Cycb1-1) during the mitotic cell cycle deduced from publicly available microarray data of synchronized *Arabidopsis* suspension cells (Menges et al. 2003). Hours 0 - 4 correspond to S phase, hours 6 - 8 to G2 phase, hours 10 - 14 to mitosis, hours 16 -19 to G1 phase. Vertical axis indicates relative gene activity.

To confirm the *in silico* data of organ distribution of *AtNIMA* expression a semi-quantitative RT-PCR was performed using total RNA isolated from juvenile leaves, adult leaves, stems, siliques and open flowers. Primers specific for the different *AtNIMA* genes (n° 1-2 for *AtNIMA* 2, n° 5-6 for *AtNIMA* 3, n° 9-10 for *AtNIMA* 5, see Table 1) were employed. To demonstrate equal amounts of cDNA, a primer pair specific for the nearly constitutively expressed elongation factor 1B alpha-subunit (n° 19-20) (Becher et al. 2004) was used for RT-PCR

control experiments. RT-PCR shows that AtNIMA genes share a similar pattern of expression (Fig. 8). In all genes the amount of transcripts is higher in stem, juvenile leaves and flower, than in siliques or adult leaves. The RT-PCR results are in accordance with the *in silico* profiles (Fig 4 A and B). AtNIMA 2, 3 and 5 genes are transcribed mostly during leaf development, bolting and flower development, while their activity decreases in older leaves and siliques. All together the data seems to indicate that the expression of AtNIMA genes 2, 3 and 5 is particularly high in differentiated organs with an elevate level of cell proliferation. This could suggest an involvement of AtNIMA 2, 3 and 5 in the process of organ differentiation.

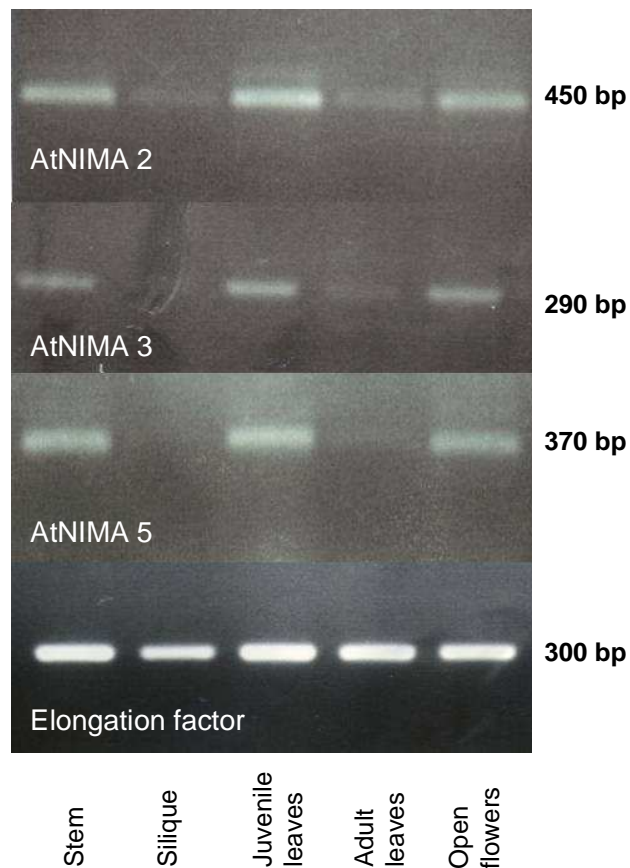


Figure 8: Transcriptional activity of *AtNIMA* 2, 3 and 5 assessed via semi-quantitative RT-PCR in different *Arabidopsis* organs. Size of the PCR products is indicated on the right side. The genes seems to be similarly active in an organ specific way. Elongation factor 1B was used as a control.

4.4 - Inactivation of AtNIMA 2, 3 and 5 via T-DNA insertions

Several *A. thaliana* T-DNA insertion lines were tested to identify plants with inactivated members of the AtNIMA gene family. When possible lines were selected in which the T-DNA insertion was located inside an exon of AtNIMAs (Table 2). In order to identify homozygous T-DNA plants of each line genomic PCR was performed, using the specific LP/RP/LB primers for each line (see 3.4.3 and Table 1).

Table 2: List of T-DNA lines used to identify inactivated AtNIMA 2, 3 or 5. Names of T-DNA lines are indicated with the TAIR code. Genes are indicated also with their AGI code. Unconfirmed T-DNA insertion indicates that the PCR failed. Normal expression means that the target gene was still activate, while no expression indicates a successful inactivation of the target gene. Normal phenotype indicates no differences between mutant and wild type plants.

T-DNA Line (TAIR)	Gene name (AGI)	AtNIMA kinase	Insertion position	Insertion presence (PCR)	Expression of target gene in homozygous plants	Phenotype in homozygous line
Salk_093269	At3g04810	AtNIMA 2	intron	confirmed	no expression	lethal
Salk_012284	At3g04810	AtNIMA 2	promoter	confirmed	normal	normal
Salk_054652	At3g20860	AtNIMA 5	exon	confirmed	no expression	normal
Salk_056986	At5g28290	AtNIMA 3	exon	unconfirmed	not determined	not determined
Salk_056984	At5g28290	AtNIMA 3	exon	unconfirmed	not determined	not determined
Salk_123055	At5g28290	AtNIMA 3	exon	confirmed	normal	normal

AtNIMA 5

The T-DNA insertion of line Salk_054652 falls into the second exon of the gene AtNIMA 5 (Fig. 2). From this line we identified 10 homozygous T-DNA, 2 heterozygous T-DNA and 11 wild type plants. RT-PCR (Fig. 9) shows that AtNIMA 5 of this line is completely inactivated in homozygous T-DNA plants, while the same gene was still active in the heterozygous T-DNA and wild type plants. The presence of target cDNA is demonstrated by using elongation factor primers as control. Due to an unequal amount of cDNA prepared from a heterozygous genotype it is impossible to conclude on a reduced level of AtNIMA 5 transcripts in heterozygous T-DNA plants. Although the inactivation of AtNIMA 5 was successful there were no obvious differences in the phenotype between homozygous T-DNA plants and wild type plants, which were grown under normal environmental conditions.

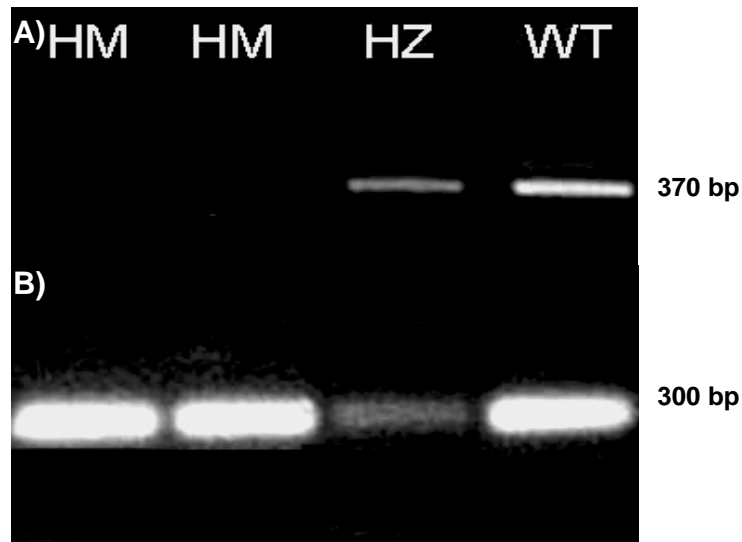


Figure 9: RT-PCR performed on cDNA from plants wild type (WT), homozygous (HM) and hemizygous (HZ) for the Salk_054652 T-DNA insertion. **(A)** Primers specific for AtNIMA 5 and, **(B)** elongation factor 1B (as control) were used. Transcripts are present in wild type (WT) and hemizygous (HZ) plants but missing in homozygous plants (HM). Note the different cDNA amount used for the analysis of hemizygous material.

AtNIMA 3

Based on the data provided by the Sequence Viewer of TAIR (<http://www.arabidopsis.org/servlets/sv?action=closeup>) the T-DNA insertions of the lines Salk_056984, Salk_056986 and Salk_123055 should be located in one of the exon of AtNIMA 3. Unfortunately, it was not possible to confirm the presence of the T-DNA insertions in the lines Salk_056984 and Salk_056986. Most likely due to a reorganization of the T-DNA inserts the genomic PCR using RP and LB primers did not work for these lines. In difference, genomic PCR on the line Salk_123055 succeeded and 15 plants were identified as homozygous for the T-DNA. Subsequent RT-PCR demonstrated that this T-DNA insertion was not able to inactivate the gene AtNIMA 3 (Fig. 10).

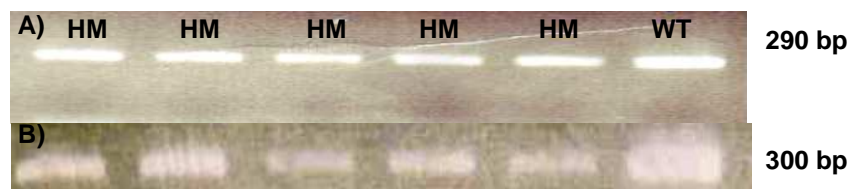




Figure 10: RT-PCR performed on cDNA from plants wild type and homozygous (HM) for the T-DNA line Salk_123055. **(A)** Primers specific for AtNIMA 3 and, **(B)** elongation factor 1B (as control) were used. The relative amount of AtNIMA 3 transcripts of homozygous T-DNA and of wild type is similar.

AtNIMA 2

T-DNA lines Salk_012284 and Salk_093269 were chosen to analyze the transcription activity of AtNIMA 2. The T-DNA of Salk_012284 is inserted before the start codon of the gene, in the promoter region. Four homozygous T-DNA plants were identified by the genomic PCR but subsequent RT PCR revealed transcription activity for AtNIMA 2. No homozygous T-DNA plant was identified for the line Salk_093269. The T-DNA of this line is inserted in the last intron of the gene AtNIMA 2. Genomic PCR showed that this AtNIMA 2 specific line produced only wild type and heterozygous plants. This outcome was observed also during the screening of the progeny of hemizygous T-DNA plants. Basing on the Mendelian inheritance a 25% of the total population was expected to be composed of homozygous mutants. Instead analysis of the F1 generation (approximately 90 plants) shows that 60% of the progeny was composed by heterozygous T-DNA plants and 40% by wild type (see Table 3). The absence on any viable homozygous T-DNA mutant of line Salk_093269 demonstrates that the complete knockout of AtNIMA 2 is lethal for the plant, suggesting that the activity of this gene is required for the development of *A. thaliana*.

Table 3: Scheme of segregation of Salk 093269 T-DNA insertion in the progeny of AtNIMA 2 heterozygous plants.

	AtNIMA 2 Wild type	AtNIMA 2 Salk 093269
	Wild type	AtNIMA 2 heterozygous
AtNIMA 2 Wild type		
AtNIMA 2 Salk 093269	AtNIMA 2 heterozygous	lethal phenotype

The absence on any viable homozygous T-DNA mutant of line Salk_093269 demonstrated that the complete knockout of AtNIMA 2 is lethal for the plant, suggesting that this gene could be a fundamental one for the survival of *A. thaliana*.

4.4.1 - Characterization of AtNIMA 5 T-DNA plants

4.4.1.1 - AtNIMA 5 knock out mutant plants does not show major differences in the phenotype

Seeds from AtNIMA 5 knock-out plants were harvested and planted, in order to compare the development of homozygous T-DNA plants with wild type plants. Approximately 30 mutant and ten wild type plants were grown under the same environmental conditions. The presence of the T-DNA insertion Salk_054652 was tested via genomic PCR using primers n° 21-34, the inactivity of AtNIMA 5 was verified via RT-PCR using primers n° 9-10. The phenotype of homozygous T-DNA plants and wild type plants was compared at different stages of development. Therefore, the number of rosette leaves was counted in different time points and their size compared. It was found that AtNIMA 5 knockout plants produce in the average slightly less leaves in the rosette compared with wild type plants of the same age (Fig. 11 and table 4). Although no obvious differences in the phenotype between mutant and wild type plants were registered during the bolting phase and the flower production. Therefore, it is possible to conclude that under normal environmental conditions the gene AtNIMA 5 does not play a major role in the pathways of plant development, or other members of the AtNIMA gene family are able to compensate the missing activity of AtNIMA 5 on homozygous Salk_054652 T-DNA plants.

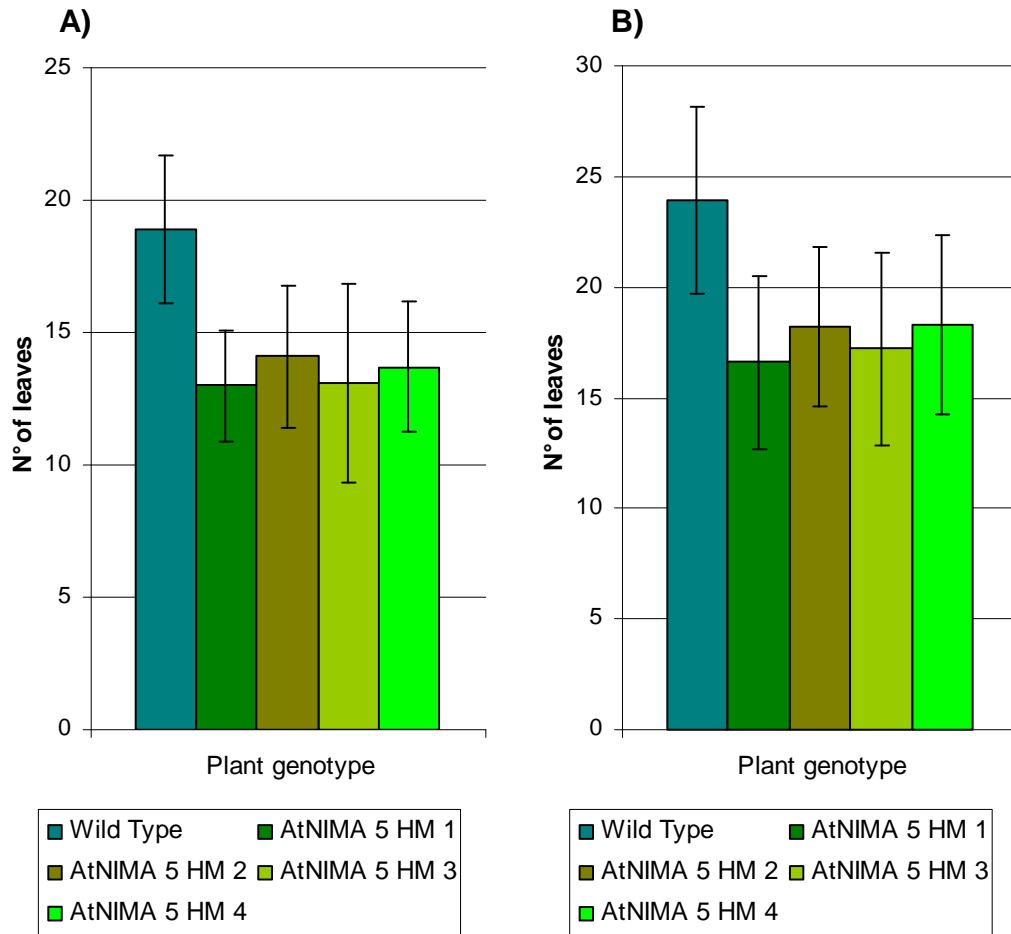


Figure 11: Number of rosette leaves counted in wild type and AtNIMA 5 homozygous plants (plant 1 – 4) after four (A) and five (B) weeks from germination.

Table 4: Statistical data of leaves difference, four weeks after germination, between wild type and AtNIMA 5 knock out plants. Basing on a T-test analysis the difference it is statistically relevant, rejecting the null hypothesis.

	Average leaves n°	Standard deviation	T test	Degrees of freedom n	T at P = 5% with $n = 9$
Wild type	18.9	2.806738	X	X	X
AtNIMA 5 knock out 1	13	2.108185	4.849	9	1.833
AtNIMA 5 knock out 2	14.1	2.685351	4.261	9	1.833
AtNIMA 5 knock out 3	13.6	2.951459	3.820	9	1.833
AtNIMA 5 knock out 4	13.7	2.451757	3.526	9	1.833

4.4.1.2 - Inactivation of AtNIMA 5 does not influence the cell cycle dependent phosphorylation of histone H3 at position serine 10

In order to test whether AtNIMA 5 is involved in the cell cycle dependent phosphorylation of histone H3S10 immunostaining using antibodies against histone H3S10ph and tubuline was performed on cells prepared from plants with inactivated AtNIMA 5. Flower buds were collected from wild type and homozygous plants (T-DNA line Salk_054652) in order to prepare mitotic cells. In wild type plants strong immunofluorescence signals specific for the phosphorylated histone H3Ser10 were only detected in mitotic cells as previously reported (Houben et al. 2007). The highest accumulation of histone H3S10ph was found in the pericentromere of metaphase chromosomes. In parallel, anti-tubuline staining was performed to confirm the correct characterization of the mitotic stages. As expected, interphase nuclei did not display histone H3S10ph specific signals (Fig. 12). Mitotic cells of AtNIMA 5 mutant plants displayed the same distribution of phosphorylated histone H3S10 and no obvious alteration of the mitotic segregation behavior of chromosomes was found. Hence, the function of AtNIMA 5 is not essential for the cell cycle dependent phosphorylation of histone H3 at serine 10. This result is in accordance with the mRNA profile obtained from cell cycle- synchronized suspension cells (Fig. 7 C).

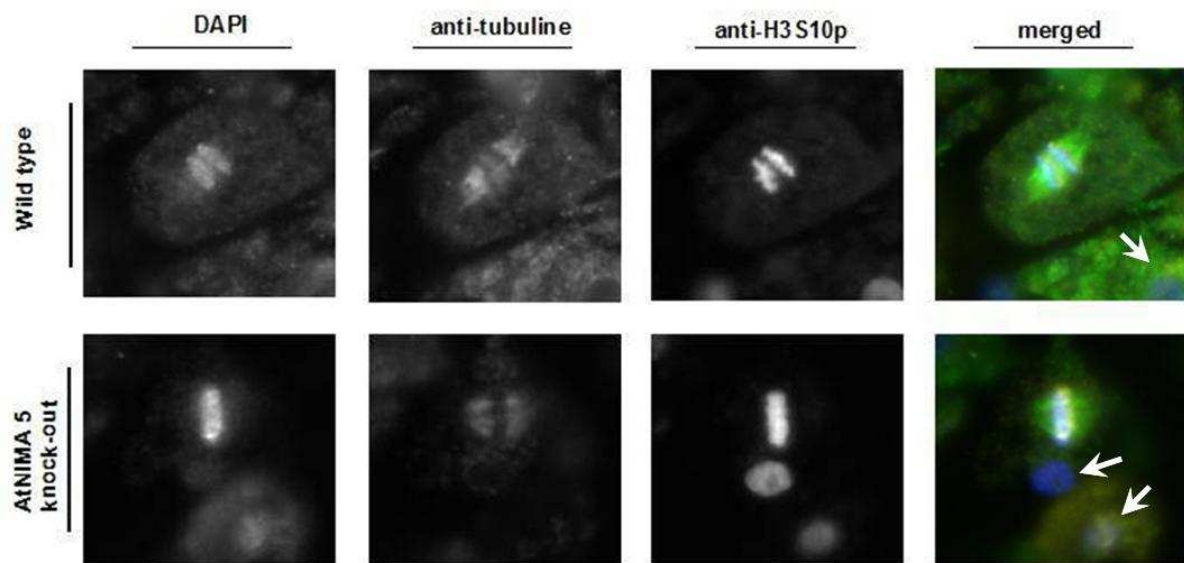


Figure 12: Immunostaining of mitotic cells from wild type and AtNIMA 5 knock-out plants using antibodies against tubuline and histone H3S10ph. Anti-tubuline staining indicates the position of the mitotic spindle. Anti-H3S10ph staining localized on condensed chromosomes. In the merged picture DAPI-signals are indicated in blue, anti-tubuline signals in green, and anti-H3S10ph signals in red. Interphase nuclei are indicated by arrows.

4.4.2 - Characterization of AtNIMA 2 T-DNA plants

4.4.2.1 - Reduced seed setting of AtNIMA 2 T-DNA heterozygous plants

To identify the possible role of AtNIMA 2 in the embryogenesis pathway the seed settings of wild type and heterozygous T-DNA (Salk_093269) plants was determined. Siliques from genotyped wild type and heterozygous plants were collected (approximately 10 plants per line, 10 siliques per plant) and the number of developed and aborted seeds was determined (Fig. 13 A). Siliques of heterozygous T-DNA plants contained around 25% of aborted seeds, while siliques of wild type displayed 5% of aborted seeds (Fig 13 B). The values obtained from the seeds counting were also analyzed with the χ^2 test, in order to confirm that the difference was statistically relevant (Table 5). All together this data indicate that seeds containing the insertion in both homologous chromosomes are aborted early in the development, suggesting a role of AtNIMA 2 in the mechanism of embryogenesis.

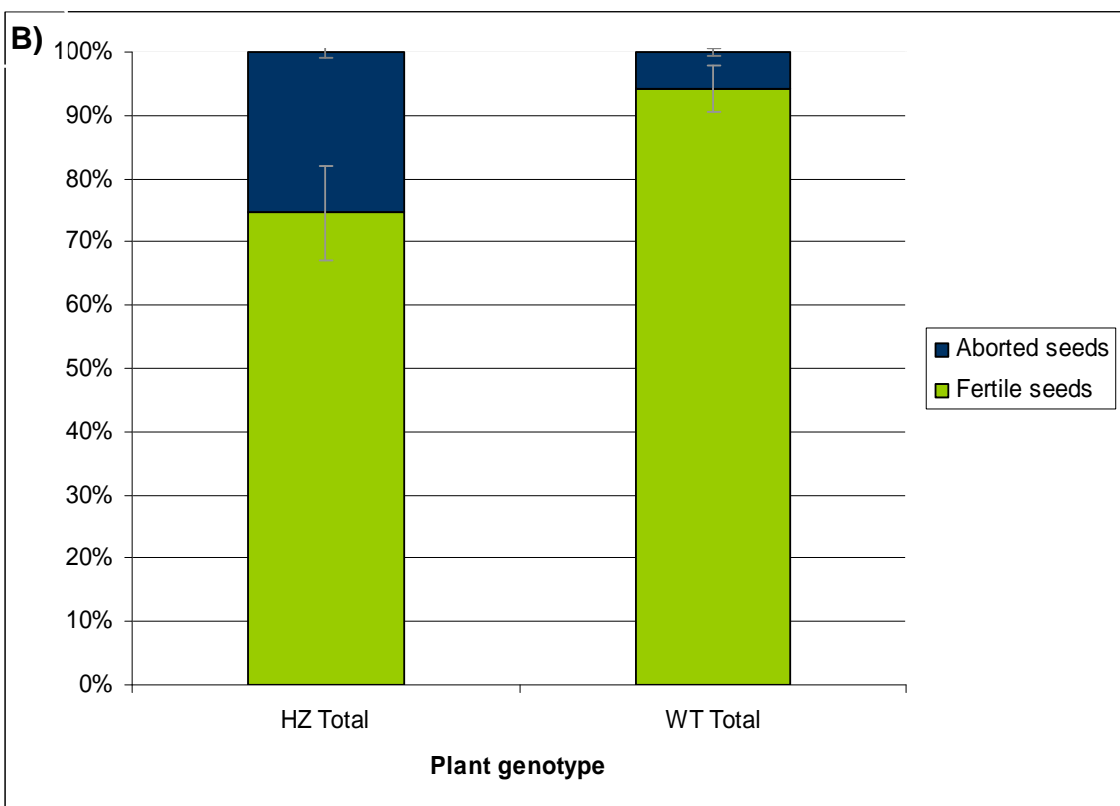
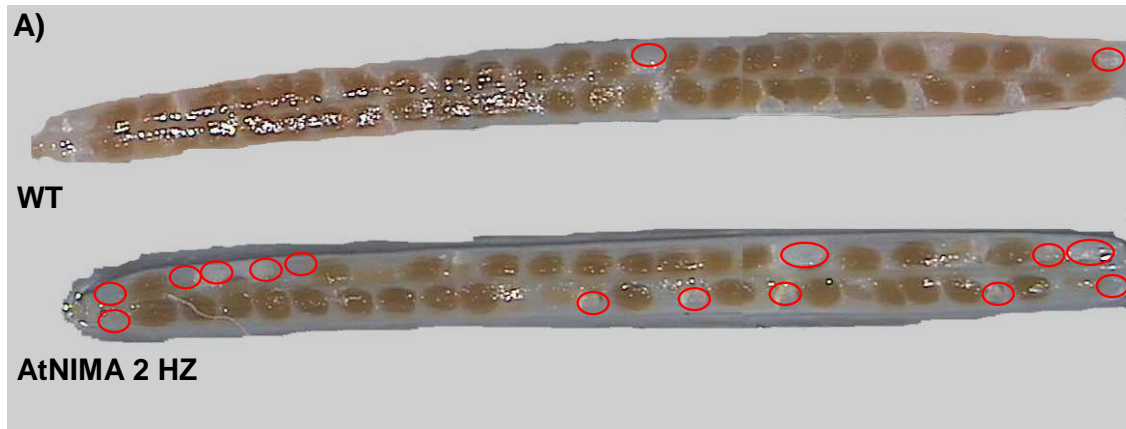


Figure 13: Characterization of the seed setting of wild type and *AtNIMA 2* mutant plants.
A) Bleached siliques collected from wild type (**WT**) and heterozygous T-DNA Salk 093269 (**AtNIMA 2 HZ**) plants. Red circles indicate the position of aborted seeds. Comparison of the seed setting shows that the amount of missing seeds is much higher in the mutant plants.
B) Data plots of the total seeds number counted in wild type and T-DNA siliques, each showing the percentage of fertile and aborted seeds. Mutant plants show around 25% of aborted seed, while this value is around 5% for wild type plants. Around 3000 seeds were analyzed from both WT and HZ plants.

Table 5: Average number of sterile and fertile seeds, counted from wild type and AtNIMA 2 heterozygous plants. χ^2 test shows that the difference is statistically relevant.

	Average fertile seeds	Average sterile seeds	Degrees of freedom (<i>n</i>)	χ^2 of fertile seeds	χ^2 of sterile seeds	χ^2 of <i>P</i> = 5% with <i>n</i> = 1	χ^2 of <i>P</i> = 1% with <i>n</i> = 1
HZ	232	107.75	1	68.381	22.65	3.84	6.64
WT	397.333	68					

4.4.2.2 - Sequence analysis of Salk_093269 confirms T-DNA position in the AtNIMA 2 gene

The amplicons produced by PCR from genomic DNA from AtNIMA 2 heterozygous plants using primers n° 23 and 34 were sequenced to confirm the T-DNA insertion position in line Salk_093269. A BLASTn search confirmed that the gene-specific part of the amplicons was derived from the fourteenth exon of AtNIMA 2 (Fig. 14). *In silico* analysis also proved sequence similarity between the T-DNA-specific part of the amplicons and the sequence of the T-DNA construct present in the pROK2 plasmid (Fig 15). In between the parts derived from the T-DNA construct and the AtNIMA 2 gene are 28 “filler” nucleotides of unknown origin. Thus, it was confirmed that the T-DNA insertion of Salk_093269 is positioned inside the AtNIMA 2 gene.

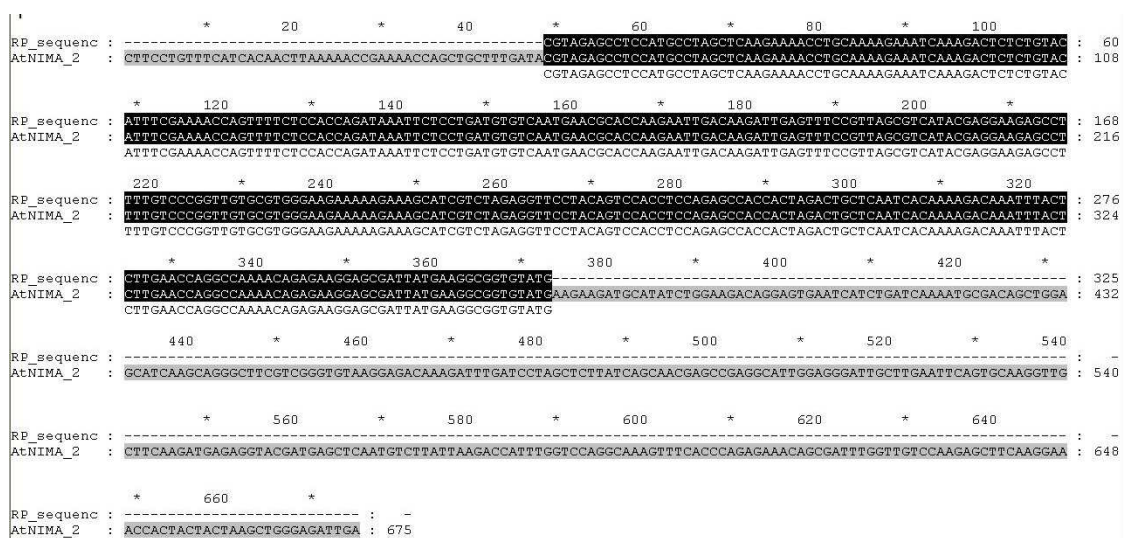


Figure 14: Nucleotide sequence alignment of the RP side part from the Salk_093269 RP-LB amplicon with the AtNIMA 2 gene.

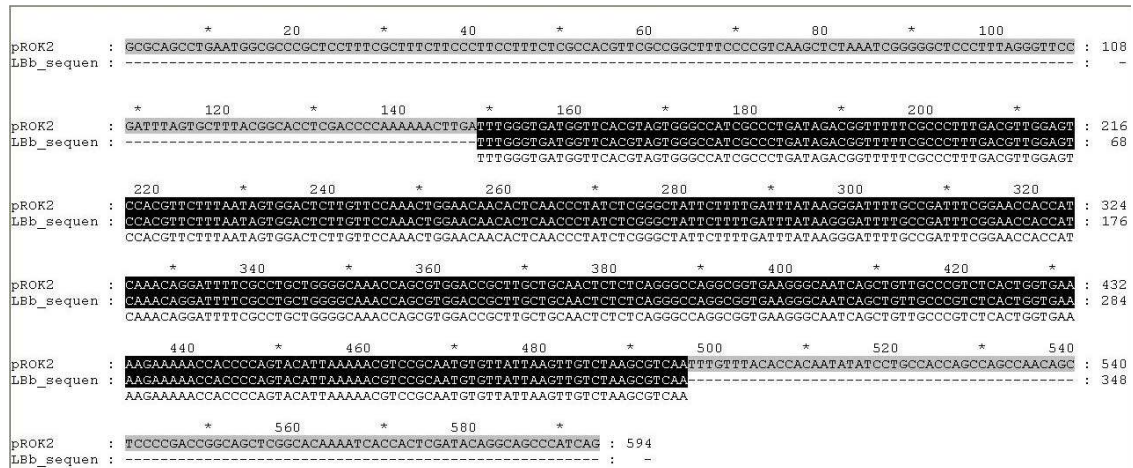


Figure 15: Nucleotide alignment of the LB side part from the Salk_093269 RP-LB amplicon with part of the sequence of the T-DNA construct, corresponding to the position of pROK2 comprised between 6247-6841 bp.

4.4.2.3 - Salk_093269 line could contain two tandemly oriented T-DNA copies inserted in AtNIMA 2

Salk_093269 plants heterozygous for the T-DNA insertion were analyzed by Southern hybridization to determine the number of T-DNA copies present in the plant genome. *KpnI* or *HindIII* digested genomic DNA of plants containing the T-DNA insertion and non-transformed control plants were hybridized with a 35S promoter-specific probe. Analysis of the Southern blots revealed identical patterns with two major hybridization signals for all transgenic plants and no signals for non-transgenic plants (Fig. 16 and data not shown). An identical band of ~3.5 kb was detected for DNA samples cleaved with either *KpnI* or *HindIII*. The second band detected had a size of ~2.5 kb after digestion with *HindIII* and of ~5.5 kb when using *KpnI*. The 3.5 kb fragment almost corresponds to the size of the T-DNA construct in pROK2 that was used to establish the SALK T-DNA insertion collection. Its detection after cleavage with *HindIII* and *KpnI* indicates the presence of two *HindIII* and *KpnI* sites in equal distance from each other, which would be consistent with the presence of two copies of the T-DNA in a tandem repeat arrangement (Fig. 17). This hypothesis was confirmed by performing a PCR using primers 35S R and NPT II R. This primer combination allows amplification of a PCR product only if two T-DNA copies are inserted in

close proximity in a tandem repeat orientation. The PCR product of ~1.7 kb obtained from the reaction (Fig. 18) approximately corresponds to the distance between the 35S promoter of the one T-DNA copy and the NPT II gene of the other T-DNA copy in the assumed tandem repeat (Fig. 17). It should be noted that the bands from the Southern hybridization and the PCR product have a size slightly smaller than the one expected from the *in silico* analysis, suggesting that some parts of the T-DNA copies are missing in between the 35S promoter and the NPT II gene.

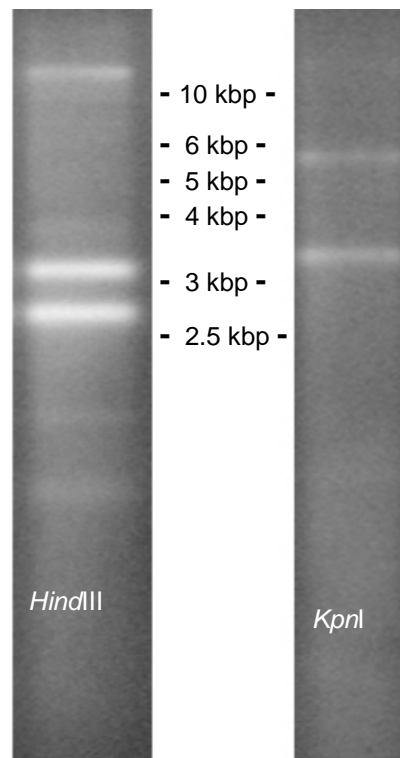


Figure 16: Southern hybridization on genomic DNA of plants heterozygous for the T-DNA insertion in line Salk_ 093269. DNA samples were cleaved with *HindIII* (left) or *KpnI* (right), separated by agarose-gel electrophoresis, blotted on membrane and hybridized to a probe based on the 35S promoter. The hybridization on *HindIII*-cleaved DNA resulted in three bands, a ~2.7 kb band, a 3.5 kb band and a faint band above 10 kb. Hybridization on *KpnI*-cleaved DNA produced two bands, at ~3.5 kb and at ~5.5 kb.

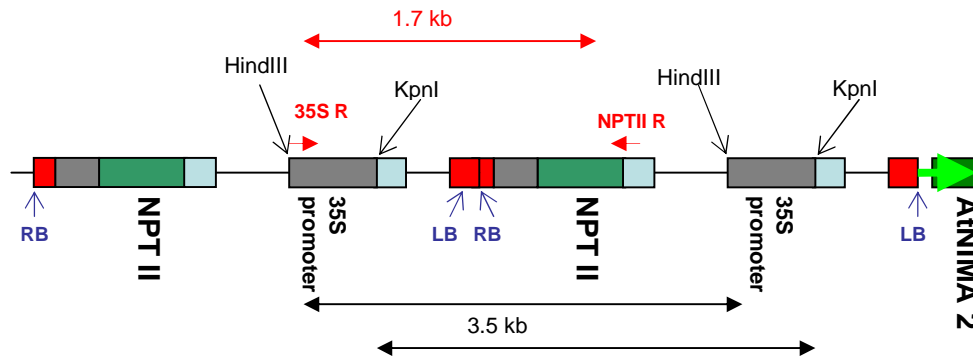


Figure 17: Scheme of the assumed T-DNA tandem repeats in line Salk_093269. The T-DNA construct in pROK2 had a length of ~4.2 kb from the right border (RB) to the left border (LB). The positions of the restriction sites, the NPT II gene, the 35S promoter and the primers are indicated. The red double-headed arrow indicates the size of the PCR amplicon from 35S R and NPT II R. The black double-headed arrow marks the size of the restriction fragments obtained from *HindIII* and *KpnI* cleavage.

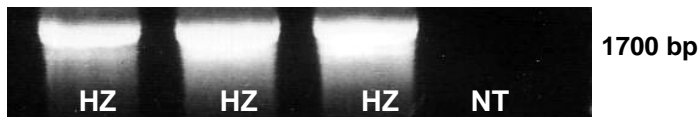


Figure 18: Genomic PCR on DNA from non-transgenic (NT) plants and plants heterozygous for the T-DNA insertion in line Salk_093269 (HZ) using 35S R and NPT II R primers.

4.5 - Down regulation of AtNIMA 2 gene using an RNAi construct

In order to generate viable plants with a reduced activity of AtNIMA 2 the corresponding gene was down regulated via the RNAi approach. *A. thaliana* plants were transformed using the AtNIMA 2-specific RNAi construct N244762. Antibiotica selected plants were first analyzed via genomic PCR (see 3.7.3) to verify the presence of the RNAi construct using the Agri primers (n° 11-12-13-14) (Fig. 19). For the T0 generation approximately 40 transgenic plants were obtained. Subsequently, RT-PCR was performed on RNAi-positive plants, at first using the primer pair for elongation factor (n° 19-20) to equalize the amount of cDNA, then using a GST-specific primer pair in order to assay the down regulation of AtNIMA 2 gene (n° 15-16). RT-PCR was also performed using the primer pair specific for AtNIMA 3 (n° 5-6), to assure that the RNAi construct is not influencing the expression of other members of the AtNIMA family (Fig. 20). RT-PCR results proved that the RNAi construct N244762 is able to reduce the

expression of AtNIMA 2 in half of the analyzed plants. Also, the selected GST sequence used for RNAi is highly specific for AtNIMA 2 and is not affecting the expression of the related NIMA-member AtNIMA 3. The level of down regulation is not uniform between the samples and is probably influenced by the number and chromosomal position of copies of the T-DNA insertions present in the genomic DNA of each plant.



Figure 19: PCR performed on genomic DNA extracted from RNAi transformed plants. Different combinations of Agri primers were used to identify the plants containing the insertion. Mix 1 contains primers Agri 51+56, Mix 2 primers Agri 51+64, Mix 3 primers Agri 56+69, Mix 4 primers Agri 64+69 (see in 3.7.3). Plasmid DNA of the construct N244762 was used as control.

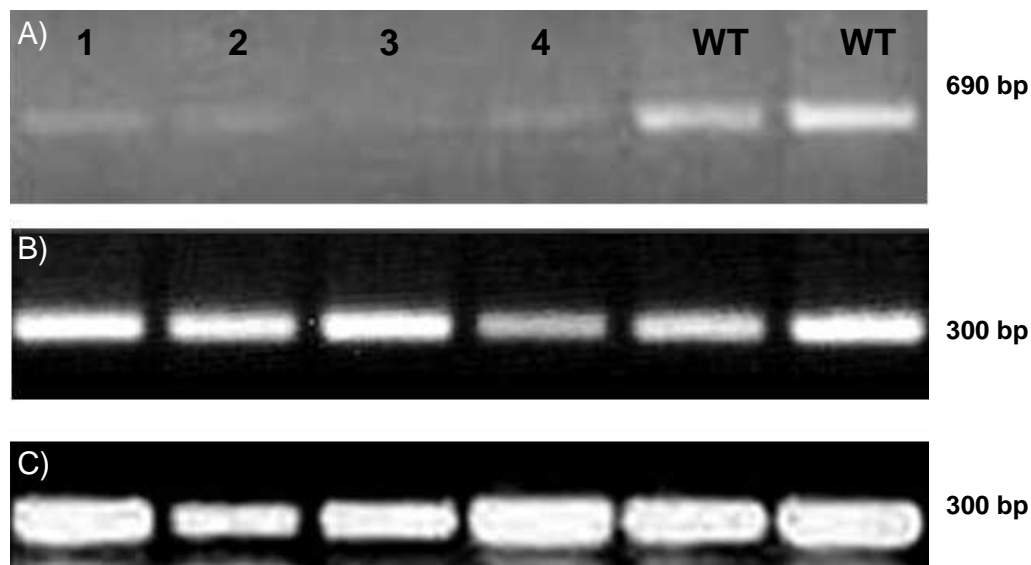


Figure 20: RT-PCR performed on cDNA transcribed from wild type (WT) and AtNIMA 2 RNAi down regulated plants (1-4). Reactions were performed using A) AtNIMA 2 GST specific primers, B) AtNIMA 3 primers and C) elongation factor primers. Expression of AtNIMA 2 amplicons is much lower in RNAi plants (1 to 4) in comparison with wild type. In contrast the same amount of amplicons was obtained in all samples using AtNIMA 3 and elongation factor primers.

4.5.1 - AtNIMA 2 RNAi mutants are delayed in plant development

Analysis of six different lines of plants transformed with the RNAi construct N244762 demonstrated that down regulation of AtNIMA 2 is influencing the phenotype of *A. thaliana* already in the early stages of plant development. Comparison between wild type and AtNIMA 2 RNAi seedlings revealed that F1 plantlets from plants with down regulated AtNIMA 2 activity are smaller in size. In detail, while two week old wild type seedlings have formed five to six leaves greater than 1 mm in length, AtNIMA 2 down regulated plants developed only three to four leaves no more than 1 mm in length (Fig. 21 A). Analysis of root growth shows that in RNAi mutant plants the primary roots are shorter and with a less developed branching, compared with the roots of wild type plants (Fig. 21 B). By plotting the data on the phenotype of roots and leaves it was found that RNAi mutant seedlings are delayed in development (Fig. 21 C and table 6).

Table 6: Statistical data of comparison between wild type and RNAi seedlings on the root length A) and leaf number B). The t-test for both data set is higher than the value at P=0.01%, rejecting the null hypothesis.

A)	N°of samples	Average root length (cm)	Std Dev	t-test	Degrees of freedom (n)	t at P = 5% with n = 38	t at P = 1% with n = 38
Wild type	20	5.037	0.314	27.992	38	1.686	2.429
AtNIMA 2 RNAi	20	2.628	0.223				

B)	N°of samples	Average leaves n°	Std Dev	t-test	Degrees of freedom (n)	t at P = 5% with n = 38	t at P = 1% with n = 38
Wild type	20	6.5	0.889	11.671	38	1.686	2.429
AtNIMA 2 RNAi	20	3.5	0.759				

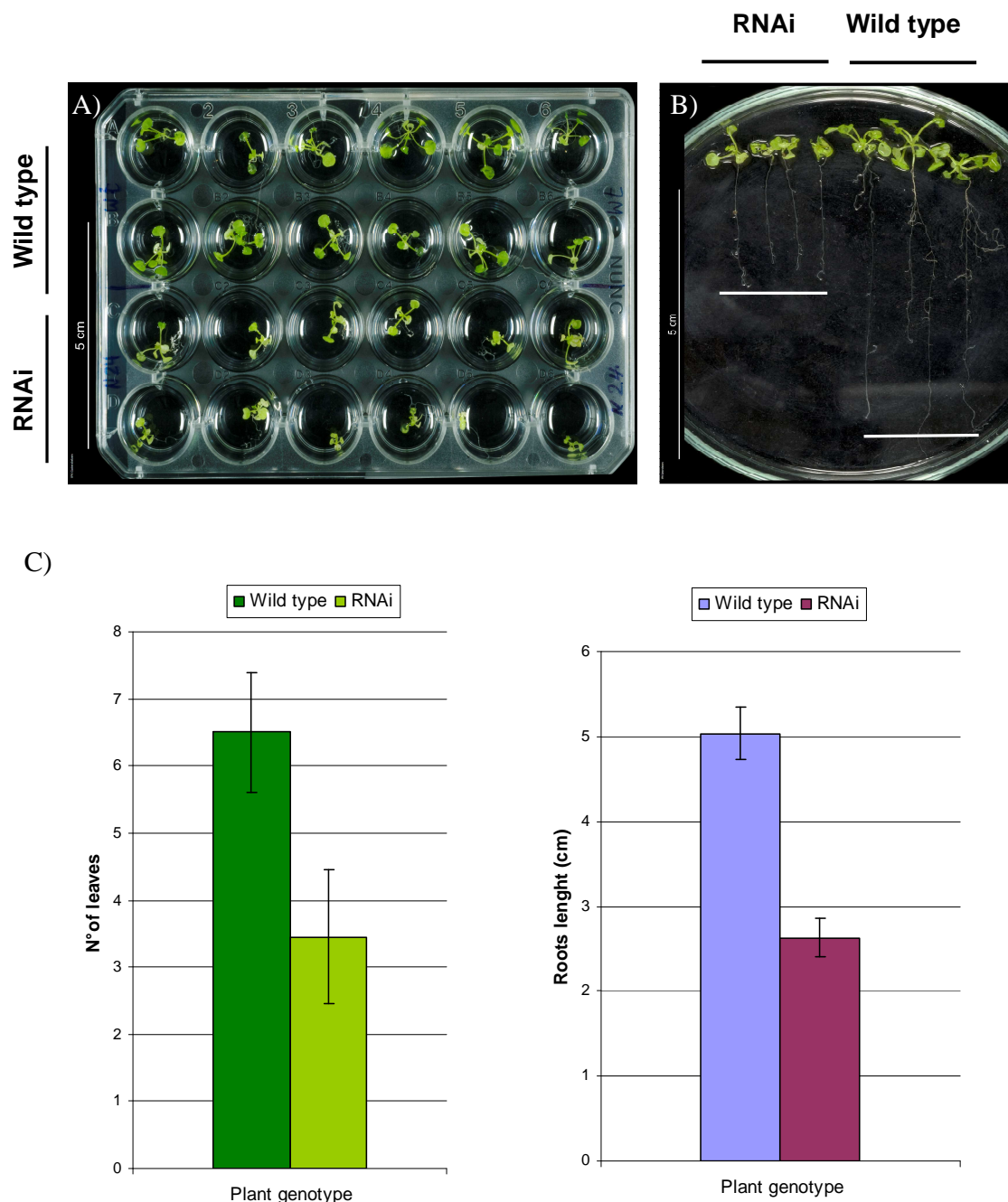


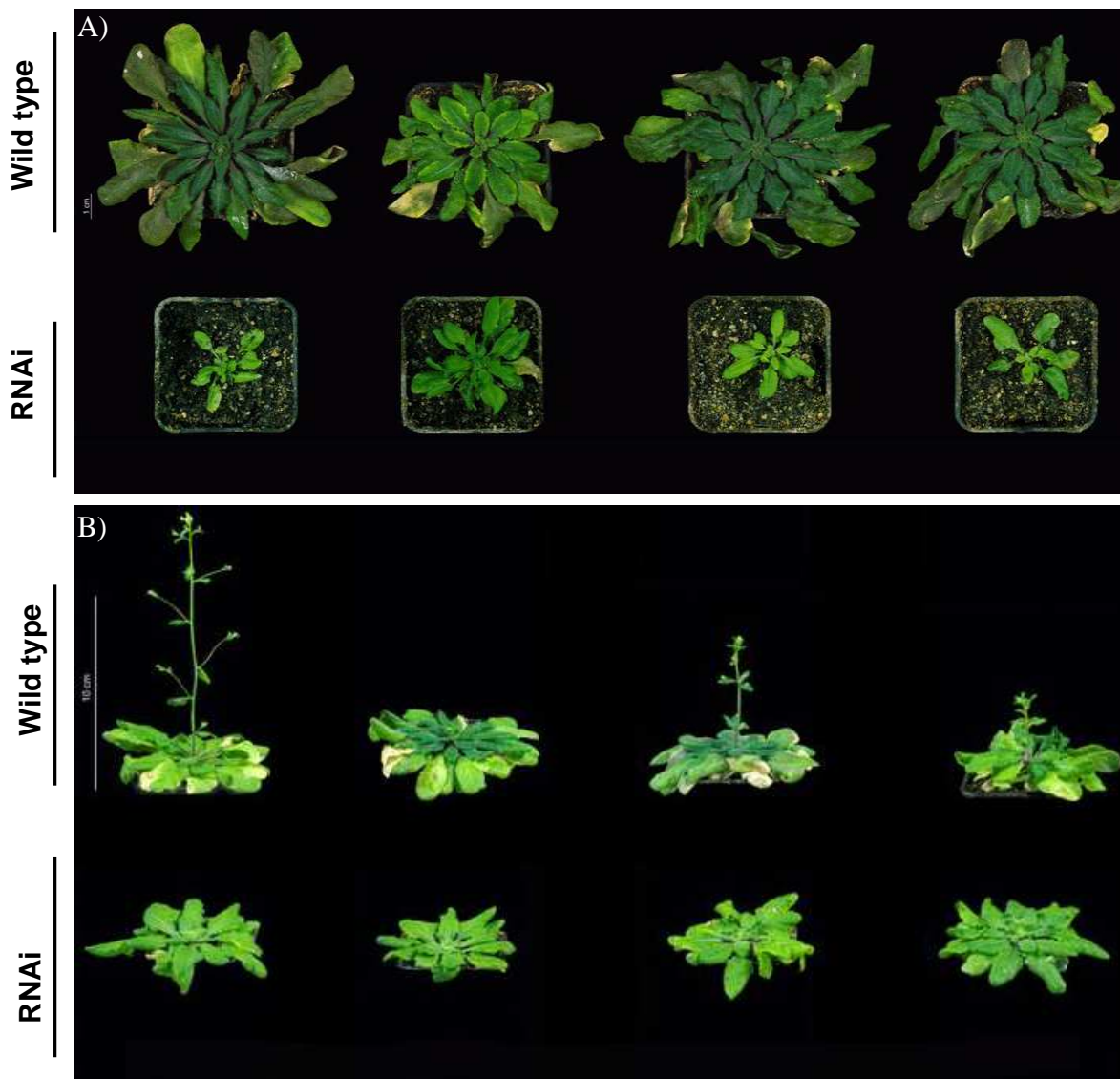
Figure 21: Phenotype analysis of AtNIMA 2 RNAi and of wild type plants.

A) Size comparison between wild type (top) and RNAi down regulated (bottom) seedlings two week old. Mutants were cultivated in selective medium with phosphinothricin, while wild type plants were grown on MS medium only.

B) Analysis of root length. RNAi seedlings have shorter roots in comparison with wild type. The extremities of the roots are indicated with a white bar.

C) Data plots of differences between total leaf number (left) and roots length (right) measured on wild type and RNAi two week old seedlings. Analysis was performed on 20 wild type and RNAi plantlets.

The development of RNAi down regulated plants is delayed also in the successive stages of development, after four weeks many mutants still do not have a completely formed leaf rosettes (Fig. 22 A). Moreover, bolting and the emergence of the inflorescence are also proceeds with roughly half of speed in comparison with wild type (Fig. 22 B-C and table 7). However, although detained, the development of mutant plants goes through all the stages of growth, including production of siliques with seeds, until senescence. Also seeds from RNAi down regulated plants were proved to be fertile.



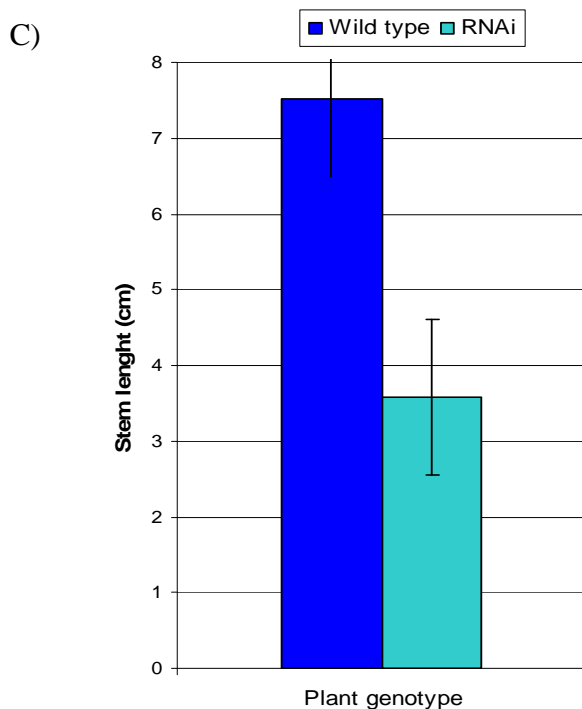


Figure 22: Comparison between wild type (WT) plants and AtNIMA 2 RNAi down regulated plants.

A) Four week old material, rosette of mutant plants is approximately half the size of wild type.

B) Five week old material, inflorescence is emerged in wild type plant but not yet in mutant ones.

C) Data plot comparing differences in the length of the stem between wild type and RNAi mutants. Analysis was performed on 19 plants five week old.

Table 7: Statistical data of comparison between stem length in wild type and RNAi plants. The T-test result is higher than the value at $P=0.01\%$, rejecting the null hypothesis.

	N°of samples	Average stem length (cm)	σ	t-test	Degrees of freedom (n)	t at $P = 5\%$ with $n = 36$	t at $P = 1\%$ with $n = 36$
Wild type	19	7.526	1.026	11.894	36	1.688	2.434
AtNIMA 2 RNAi	19	3.579	1.020				

These results suggest that AtNIMA 2 plays a role in the regulatory mechanism of plant growth. When the expression of AtNIMA 2 is reduced via RNAi silencing, the plants exhibit a slowing down in the development and a slight reduction in overall size but are still able to survive and produce fertile seeds. However, the presented RNAi AtNIMA 2 phenotype is not uniform. Around half of the RNAi plants show a phenotype similar to the wild type. Those RNAi mutant plants with a phenotype different from that of the wild type, always show various degrees of

delayed development. The extend to which development in individual plants was delayed coincided with the level of AtNIMA 2 silencing in these plant as analysed by RT-PCR (Fig. 20 and Table 8).

Table 8: Summary about AtNIMA 2 RNAi mutants, based on data obtained from 60 plants. The fraction of plants in the total population is indicated presenting a certain degree of delay in growth, in comparison with wild type. The phenotype is correlated to the level of silencing of AtNIMA 2 transcript.

<u>Phenotype</u>	<u>% of plants</u>	<u>Expression of AtNIMA 2 amplicons</u>
highly delayed development	30%	amplicons almost absent
less delayed development	20%	weaker than wild type
similar to wild type	50%	Strong as wild type

4.5.2 - Histological analysis of AtNIMA 2 RNAi mutants

Morphological and histological studies were performed in collaboration with Dr. T. Rutten (IPK, Gatersleben) to determine, if the distorted development of the AtNIMA 2 RNAi plants was reflected in an altered organization of cells and tissues. For this purpose semi thin sections of plastic embedded leaves and stems were analyzed under the light microscope. Additionally, leaf surfaces were studied under the scanning electron microscope. A total of 25 plants were screened by RT-PCR and those with the highest level of AtNIMA 2 gene-silencing selected. The first impression is that transgenic leaves are somewhat smaller and slightly thinner than wild type leaves. The underlying reason for this, so the histological studies show, is a disturbed organization of the chlorenchymal tissues. The palisade layer in the RNAi down regulated leaves comprises fewer cells, and these tend to be round-shaped instead of cylindrical. The spongy parenchymal tissues are also severely affected. Whereas in wild type leaves the spongy parenchyme comprises of three loosely organized cell layers (Fig. 23 A), in RNAi plants there are only one to two cell layers with much larger intercellular spaces (Fig. 23 B-C). The effect on the epidermal cell layers was revealed by scanning electron microscopy recordings of leaf surfaces. The micrographs show a lower trichome and stomata density in RNAi leaves as compared to wild type

leaves (Fig. 24 A-F). Trichomes and stomata density was analyzed using the Fisher variant of the χ^2 test, assuming as null hypothesis that the difference between wild type and mutant was not related to the down regulation of AtNIMA 2. The results of the test (Table 9) rejected this assumption, linking the phenotype observed to the RNAi activity. Interestingly normal epidermal cells were substantially larger in RNAi leaves as compared to wild type. Per surface area the number of epidermal cells in wild type leaves was about twice the number found in transgenic leaves (Fig 24 D-F and G-I). If we look at the ratios of stomata/epidermal cells and trichomes/epidermal cells it transpires that these ratios are virtually similar between transgenic and wild type leaves (Fig. 25). Similar to the leaves, also the stems of RNAi plants are somewhat smaller in diameter than stems of wild type plants (Fig. 26). A histological analysis of the cross sections through this organ shows the same degree of organization in wild type and transgenic lines. With the exception of an extremely dwarfed specimen, transgenic plants and wild type have a similar number of identically organized vascular bundles. The only difference observed being a marked reduction in the total amount of parenchymal pith cells. In summary, superficially down regulation of AtNIMA 2 only marginally affects the overall morphology of the plants. A histological analysis shows, however, that the organs of the RNAi plants are made up of substantially fewer cells than in the wild type, thus affecting the internal organization of tissues.

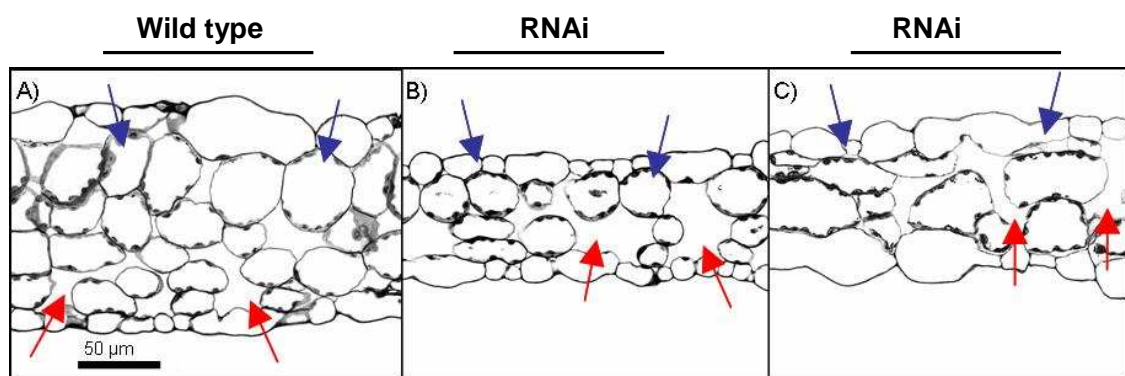


Figure 23: Cross section of cauline leaves of wild type (Wt) and AtNIMA 2 RNAi plants. **A)** Blue arrows indicates the palisade layer, red arrows the sponge tissue. In sample **B)** the palisade layer is reduced to a few round shaped cells, while the sponge parenchyma loosely organized cell layers. Note also that large intercellular spaces span the distance from upper to lower epidermis. In sample **C)** the transition from palisade into spongy parenchyma is almost fluent, the latter comprising of a single cell layer only.

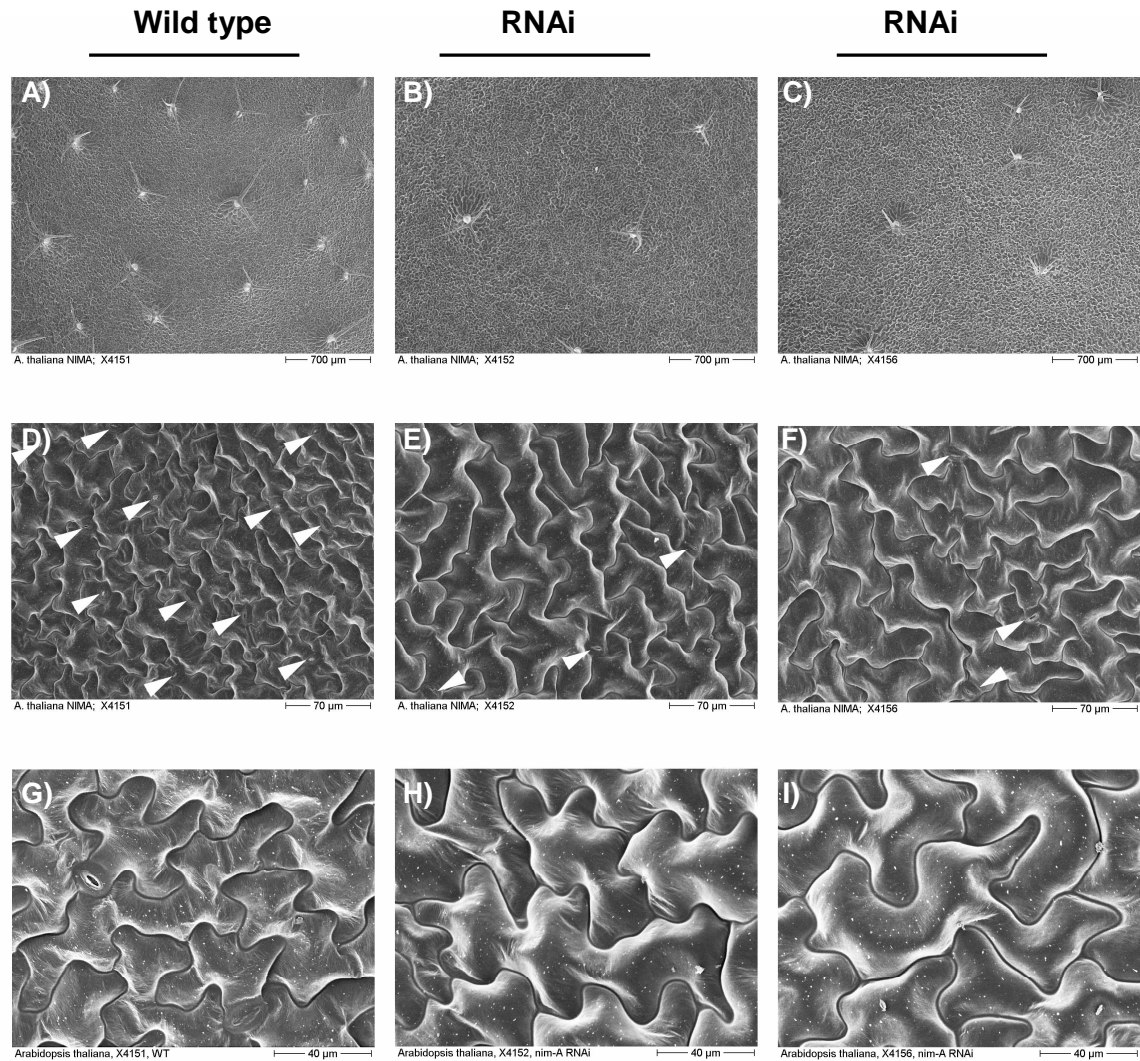


Figure 24: SEM recordings of leaf surfaces of wild type (WT) and AtNIMA 2 RNAi plants. (A-C) Overview images show wild type leaf to have a significantly higher density of trichomes compared to RNAi plants. (D-F) Epidermis cells at 500x magnification. Density of stomata (white arrowheads) is also much higher in wild type material. (G-I) Magnification at 800x reveals epidermal cells to be larger in the transgenic lines compared to the wild type.

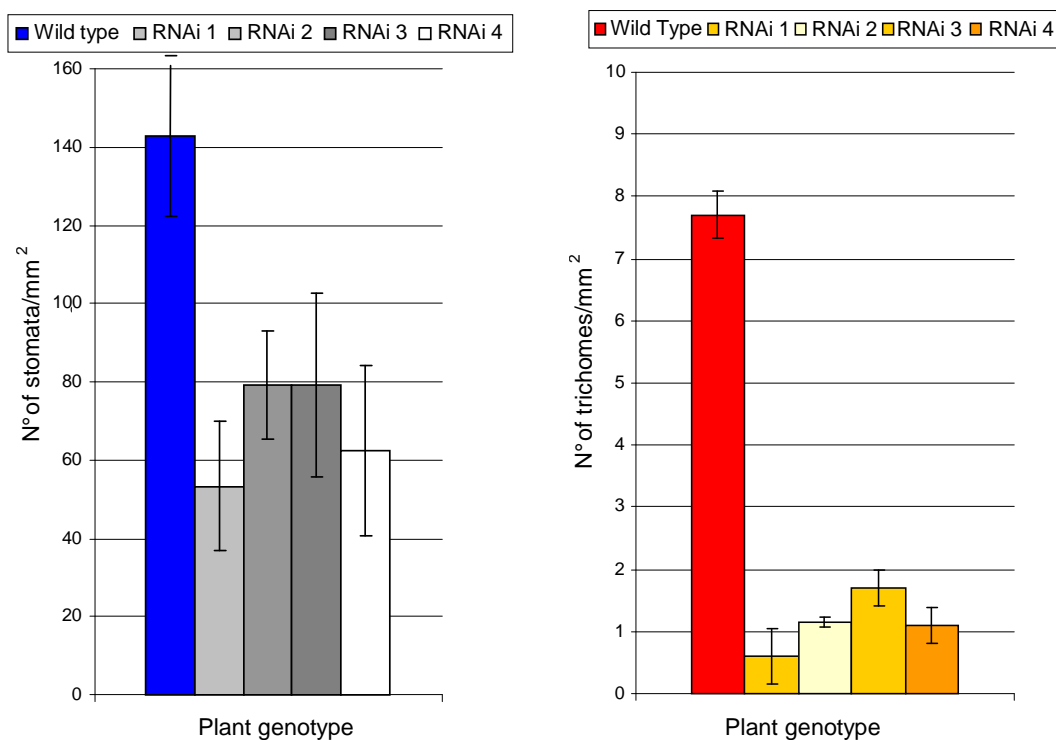


Figure 25: Data plots based on the counting of trichomes and stomata per mm² in epidermal cells of wild type and RNAi leaves.

Table 9: Statistical analysis of stomata (A) and trichomes (B) counting in wild type and RNAi seedlings. The t-test for both data set is higher than the value at P=0.01%, rejecting the null hypothesis.

A)	N° of photos	Average stomata mm ²	Std Dev	t-test	Degrees of freedom (n)	t at P = 5% with n = 9	t at P = 1% with n = 9
WT	10	142.7	20.5	X	X	X	X
RNAi 1	10	53.4	16.5	10.555	9	1.833	2.821
RNAi 2	10	79	13.8	7.529	9	1.833	2.821
RNAi 3	10	79.1	23.4	7.518	9	1.833	2.821
RNAi 4	10	62.4	21.9	7.418	9	1.833	2.821

B)	N° of photos	Average trichome mm ²	Std Dev	t-test	Degrees of freedom (n)	t at P = 5%	t at P = 1%
WT	3	2,6	0,38	X	X	X	X
RNAi 1	3	0,6	0,17	16.364	2	2.92	6.965
RNAi 2	3	1.1	0.1	6.285	2	2.92	6.965
RNAi 3	4	1.7	0.28	3.974	3	2.353	4.541
RNAi 4	3	1.1	0.3	5.634	2	2.92	6.965

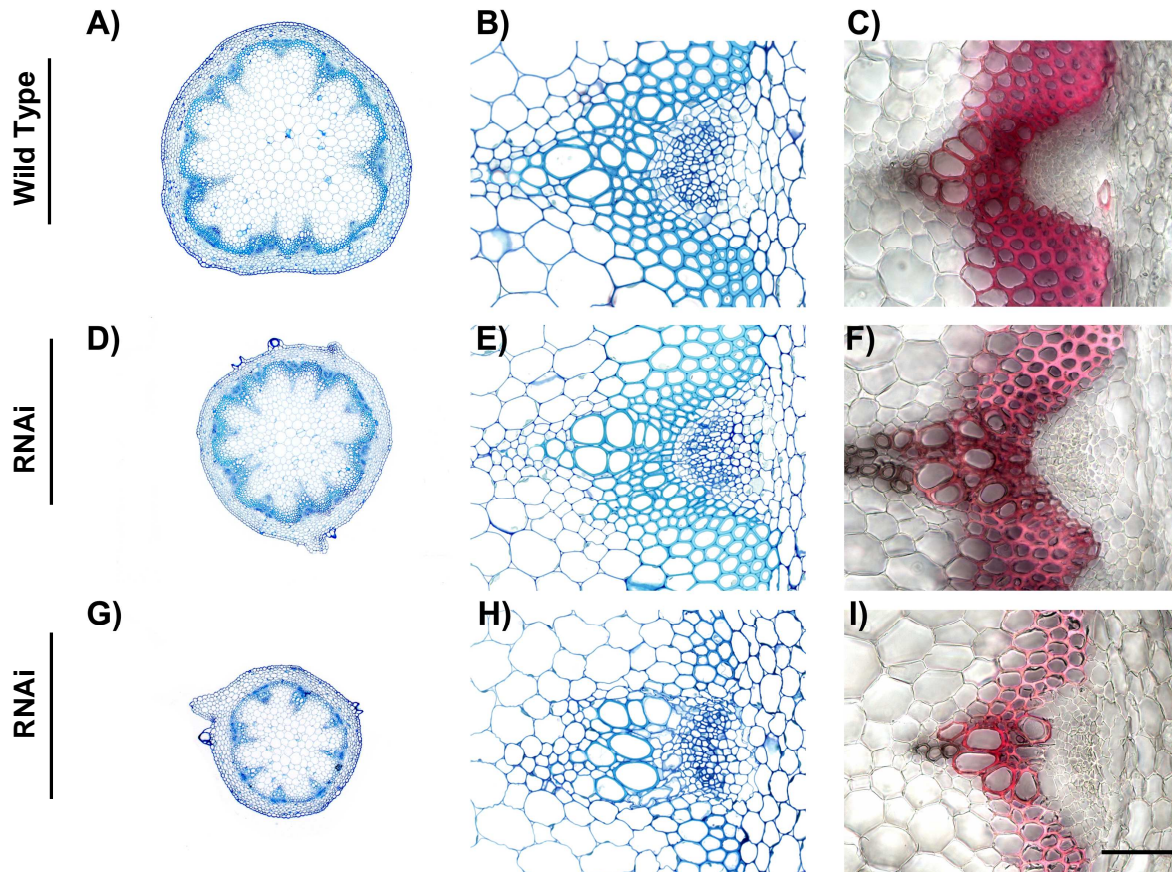


Figure 26: Cross sections through stems of wild type and AtNIMA 2 RNAi plants. Wild type stem (A) has a distinctly larger diameter than AtNIMA 2 RNAi stems (D, G). Detailed views of the vascular bundles after methylenblue/azur II (B, E, H), or after phloroglycin staining (C, F, I) shows that apart from extreme cases of dwarfism (H, I), the internal organization is similar between wild type and RNAi plants. Bar = 200 μ m for a, d, g; 25 μ m for all others.

4.5.3 - The vascularisation process of cotyledons is affected in AtNIMA 2 RNAi mutants

The correct development of the vascular network has a fundamental role in the growth of the plant. The organization of vascular bundles in the RNAi mutants was investigated, to evaluate whether down regulation of AtNIMA 2 is influencing the vascularisation process of seedlings. Seedlings from wild type and AtNIMA 2 RNAi plants, grown for one week in short day conditions, were analyzed by dark field microscopy. In seven day-old wild type seedlings the vascular network of cotyledons normally comprises a median primary bundle from which departs secondary bundles that divides the leaf in four lobes (Fig. 27 A). The cotyledons

of seven day-old AtNIMA 2 RNAi seedlings often showed an incomplete pattern of vascularisation (Fig 27 B). Here the vascular network formed only three, two or even just one single lobe, and occasionally only the primary bundle was present. The relative abundance of each type of pattern in RNAi and wild type plants is plotted in Figure 27 C. The data indicate that the majority of AtNIMA 2 down regulated leaves having an incomplete vascularisation network. It should be noted that also in wild type cotyledons there is a limited amount of incomplete vascularisation after one week. However, those findings are in accordance with the previous one on the RNAi material, reinforcing the hypothesis of a role of AtNIMA 2 in the plant development pathway.

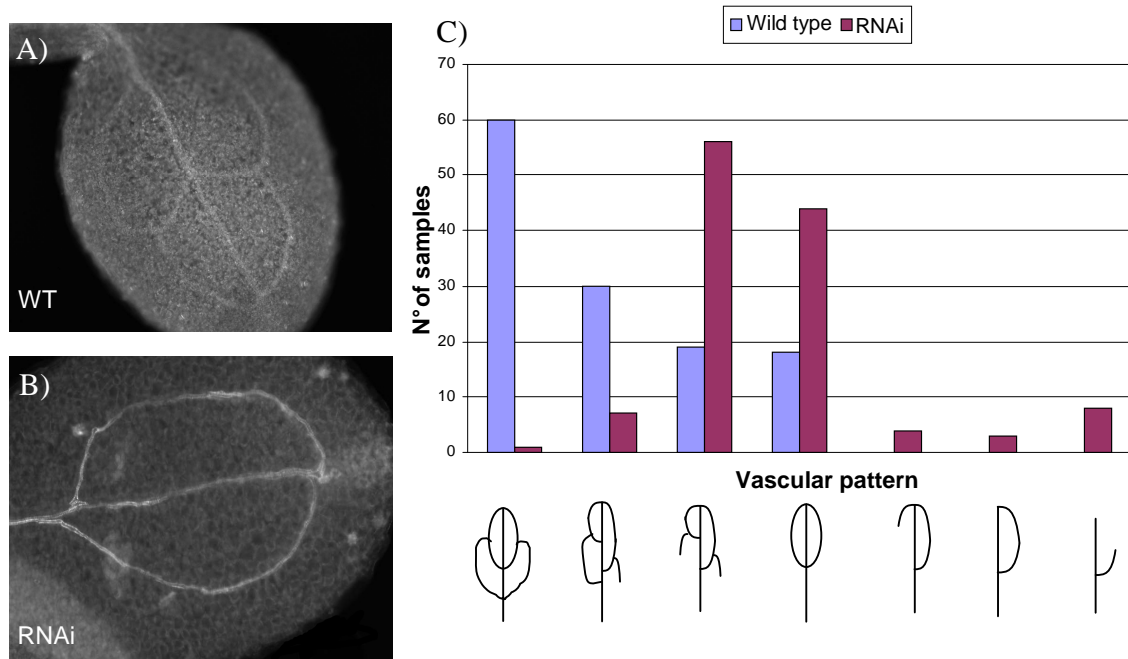


Figure 27: Comparative analysis of the vascularisation process of AtNIMA 2 RNAi and wild type cotyledons.

A) Typical vascular pattern of a wild type cotyledon (WT), clearly showing the primary bundle in the middle of the leaf with secondary ones delimiting four lobes.

B) Vascular pattern of an RNAi mutant cotyledon, the primary bundle is present but the secondary are incomplete, delimiting only two lobes.

C) Data plot showing the different types of vascular patterns (horizontal axis) and their relative abundance in wild type (in blue) and RNAi mutants (in red). Approximately 120 cotyledons each from wild type and RNAi plants were analyzed.

4.5.4 - RNAi down regulation of AtNIMA 2 does not influence the cell cycle dependent phosphorylation of histone H3S10.

Immunostaining using antibodies against histone H3S10ph was performed on RNAi plants to test whether AtNIMA 2 down regulation was affecting histone H3S10 phosphorylation. Cells were prepared using flower buds harvested from plants showing the highest level of down regulation of AtNIMA 2. Analysis via fluorescence microscopy shows that the RNAi silencing of AtNIMA 2 is not producing any significant change in the level of phosphorylation of histone H3S10. Signals specific for histone H3S10ph were of the same intensity as in wild type cells (Fig. 28). Those findings seem to exclude any significant involvement of AtNIMA 2 in the process of cell cycle dependent phosphorylation of histone H3S10.

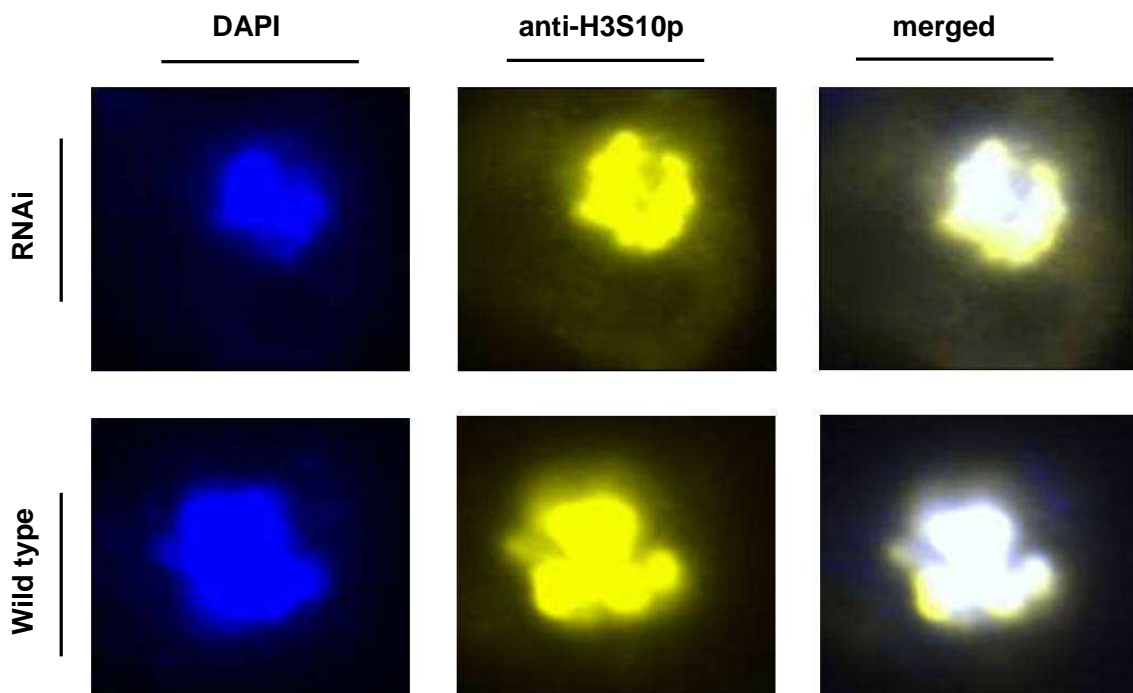


Figure 28: Immunostaining of mitotic metaphase cells prepared from wild type and down regulated AtNIMA 2 plants. Immuno fluorescence signals specific for the phosphorylated serine 10 of histone H3 were of the same intensity and distribution in wild type and AtNIMA 2 RNAi cells. In merged pictures blue indicates DAPI staining, yellow the fluorescence signal from Cy3-conjugated secondary antibody

4.6 - Cloning of the full length AtNIMA 2 cDNA

Amplicons of full-length AtNIMA 2 cDNA of gene AtNIMA 2 were ligated into the pENTR/D-TOPO (Invitrogen) vector. The construct was propagated in *E. coli* and subsequently cleaved with *RcaI* prior to the recombination reaction to destroy the selection kanamycin marker which is present also in the destination vectors. To verify the correct size of the recombinant product the construct was digested with different combinations of restriction endonucleases, Restriction analysis revealed that the recombination reaction was successful (Fig. 29).

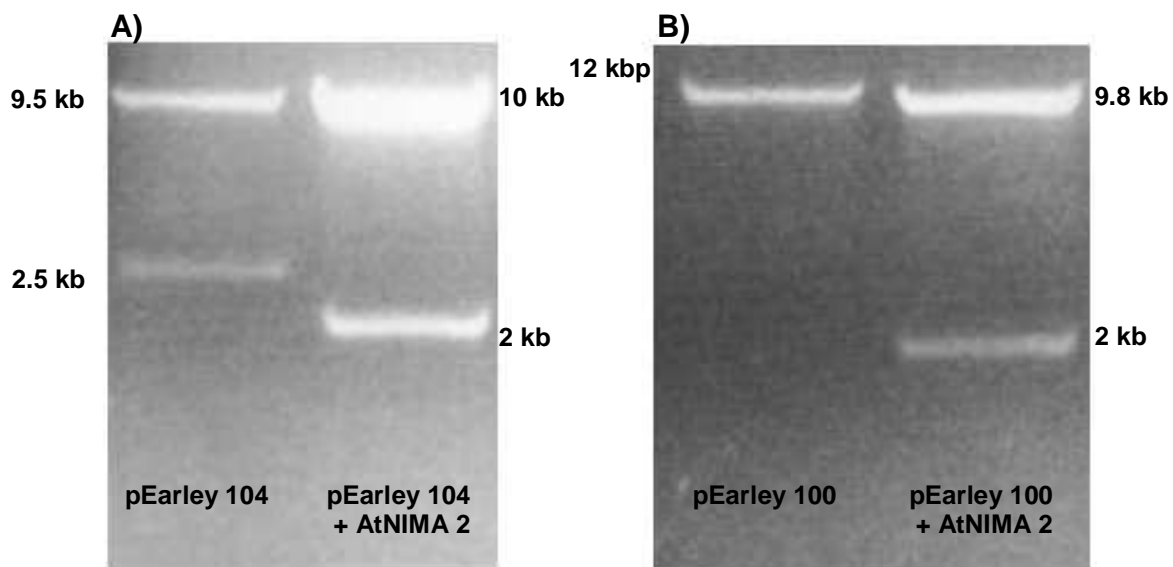


Figure 29: Digestion of recombinant and native plasmids pEarley 104 and 100 with *HindIII*. **A)** Cleavage of pEarley 104 without insertions produced two fragments of 9.5 and 2.5 kb. After recombination with the full amplicon of AtNIMA 2 the cleavage products has a length of 10 and 2 kb. **B)** Cleavage of pEarley 100 without insertion produced a linear plasmid of 12 kb, due to the presence of a single restriction site for *HindIII*. After recombination with AtNIMA 2 amplicon two fragments of 9.8 and 2 kbp were obtained.

4.7 - Characterization of putative AtNIMA 2 and 3 specific antibodies

Peptide antibodies were chosen to overcome the absence of recombinant AtNIMA proteins and as a more accurate tool for localize the target protein without cross reaction with other members of the AtNIMA family. The peptide sequences selected for the immunization belongs to the thirteenth and fourteenth exon of AtNIMA 2 and to the first and sixth exon of AtNIMA 3 (see 3.9.1, Fig. 2).

In order to distinguish between specific and unspecific signals the pre-immune sera of the rabbits used for immunization with AtNIMA peptides were used for indirect immunostaining experiments first (Fig. 30). Analysis revealed that the signals caused by the pre-immune sera of the rabbit are weakly diffuse in the cytoplasm and almost absent in the nuclei. Signals caused by the pre-immune sera of the rabbit used to generate AtNIMA 3 are of weaker intensity. Cytoplasm and nuclei were weakly labeled (Fig. 30).

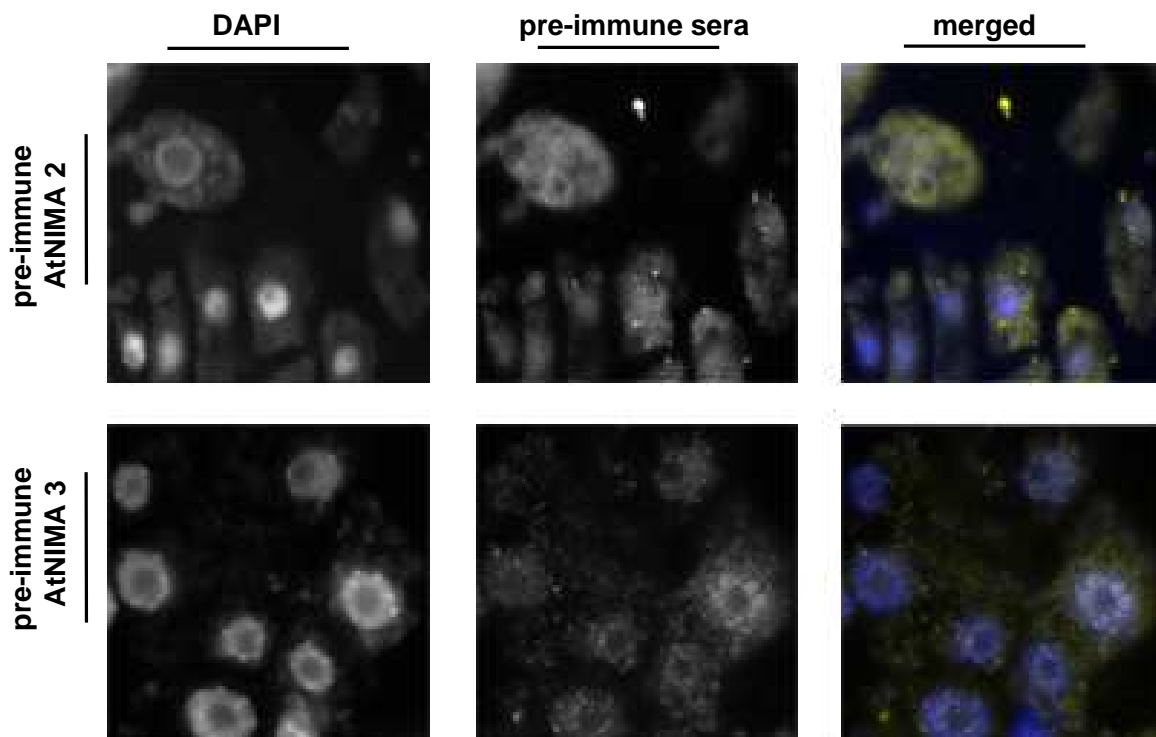


Figure 30: Immunostaining of root meristematic cells with pre immune sera of rabbits which were used to raise peptide antibodies against AtNIMA 2 and 3. Anti AtNIMA 2 pre-immune sera caused a uniform staining. Signals from anti AtNIMA 3 pre immune serum are less intense and diffused in the whole cell volume. In merged pictures blue indicates DAPI staining, yellow the fluorescence signal from Cy3-conjugated secondary antibody.

Immunostaining experiments with the putative antibodies against AtNIMA 2 and 3 were performed on meristematic cells prepared from *A. thaliana* root tips (see 3.9.2). To test for best antibody concentration, the antibodies were applied in dilutions 1:100, 1:200, 1:500 to the specimens (see 3.9.3). Immunostaining with the generated AtNIMA 2 antibodies resulted in a disperse labeling of the entire cells. However, strong signals colocalized with the position of nucleoli (Fig. 31 top). Labeling of cells prepared from RNAi plants with down regulated AtNIMA 2

activity revealed the same distribution of immunofluorescent signals. It seems that the signal pattern with AtNIMA 2 antibodies is different from that of the pre immune antibodies, in particular due to the strong staining of nucleoli. Cells immunolabelled with AtNIMA 3 antibodies were weakly stained. In contrast to anti-AtNIMA 2, nucleoli displayed almost no immunosignal (Fig. 31, bottom).

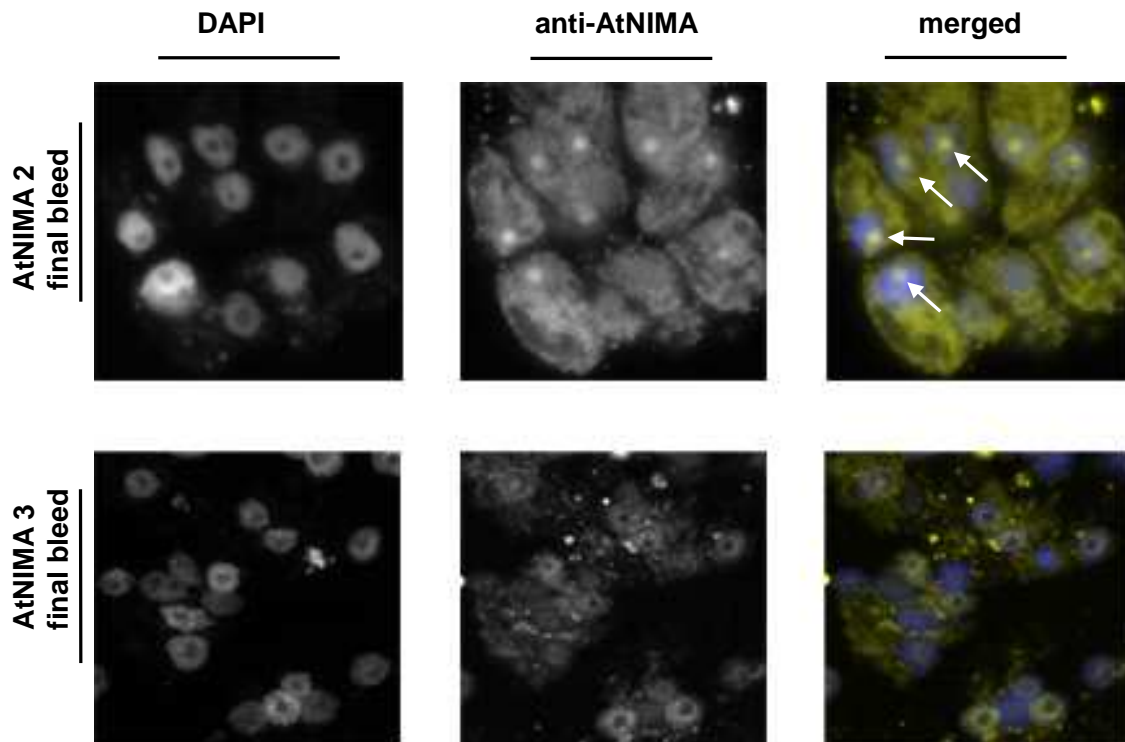


Figure 31: Immunostaining of *A. thaliana* root meristematic cells with anti AtNIMA 2 antibodies. Nucleoli (indicated by white arrowheads) display strong immunfluorescence signals. Immunostaining of *A. thaliana* root meristematic cells with anti-AtNIMA 3 antibodies. Nucleoli display very weak immunfluorescence signals. In merged pictures blue indicates DAPI staining, yellow the fluorescence signal from Cy3-conjugated secondary antibody.

To further test the specificity the putative AtNIMA antibodies immunostaining experiments were performed using a nuclei/chromosome suspension prepared from *Vicia faba* root meristems. Prometaphase chromosomes and nuclei immunolabeled with pre immune sera (Fig. 32) or with putative anti-AtNIMA 2 and 3 antibodies displayed both a weak but distinct staining of the nucleoli (Fig. 33). All together the immunostaining experiments on *V. faba* displayed a similar signal distribution, with no obvious differences between pre immune sera and the putative anti-AtNIMA antibodies.

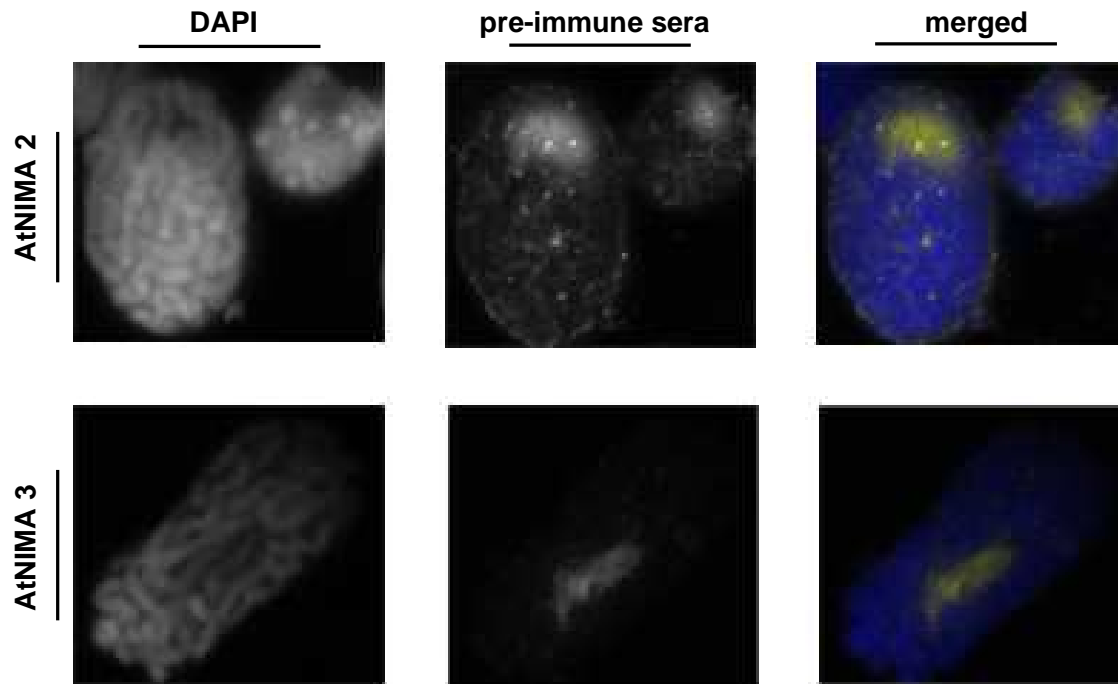


Figure 32: Immunostaining of chromosomes from *V. faba* using pre immune sera of rabbits which were used to raise peptide antibodies against AtNIMA 2 and 3. Both pre immune sera produced a weak signal in the nucleolus. In merged pictures blue indicates DAPI staining, yellow the fluorescence signal from Cy3-conjugated secondary antibody.

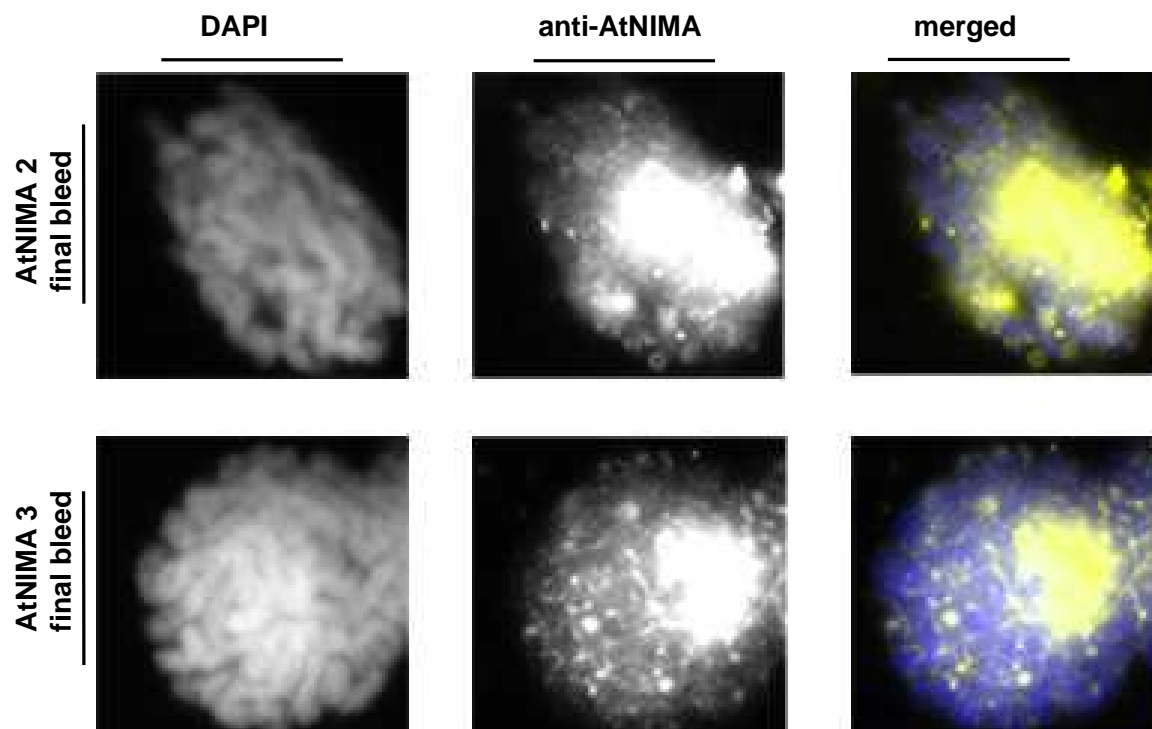


Figure 33: Immunostaining of chromosomes from *V. faba* using antibodies against AtNIMA 2 and AtNIMA 3. Nucleoli display very strong immunofluorescence signals using both antibodies. In merged pictures blue indicates DAPI staining, yellow the fluorescence signal from Cy3-conjugated secondary antibody

Whole mount immunostaining was performed on wild type seedlings of *A. thaliana* using the putative AtNIMA 2 and 3 antibodies, to determine whether the distribution of immunofluorescent signals correlates with the expression and promoter analysis data. Whole seedlings were indirectly immunolabelled with either anti-AtNIMA 2 or anti-AtNIMA 3. As negative control, the secondary Cy3-conjugated anti-rabbit antibody only, and antibodies coming from the pre-immune sera were applied. The immunostaining with anti-AtNIMA 2 and 3 revealed clear signals in the region of the root area (Fig. 34 A to C). However, the control experiments performed using the pre-immune sera (Fig. 34 D and E), or the secondary antibody only (Fig. 34 F) gave an almost identical signal distribution. Those findings suggest that the generated antibodies are not specific and therefore not suitable to visualize the distribution of AtNIMA 2 and 3 proteins by whole mount immunostaining.

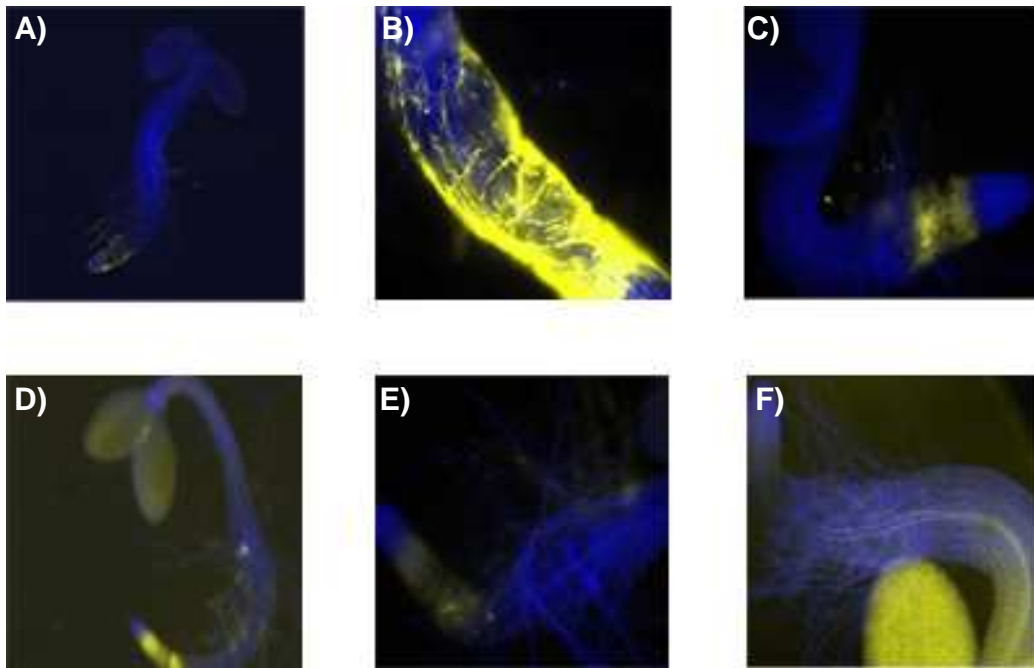


Figure 34 Whole mount immunostaining of *A. thaliana* seedlings with putative AtNIMA 2 and 3 antibodies.
(A, B) Immunofluorescent signals from the antibodies against AtNIMA 2 or AtNIMA 3 **(C)** colocalizing within the root tip and the root elongation zone. Blue indicates DAPI staining, yellow the fluorescence signal from Cy3-conjugated secondary antibody.
(D, E) Immunofluorescent signals caused by the application of the pre-immune sera
(F) Fluorescence signals resulting from the Cy3-conjugated secondary antibody alone.

Putative antibodies against AtNIMA 2 and 3 were further tested via Western blot analysis against total proteins of *A. thaliana* wild type leaves. AtNIMA 2 has an expected molecular weight of 68 kDa and AtNIMA 3 of 63 kDa, but no specific band of corresponding size was found (Fig. 35). Instead, a number of bands indicating the position of smaller proteins were recognized with the tested antibodies.

Taken together, it could be concluded that the peptide antibodies against AtNIMA 2 and 3 are not suitable to investigate the localization of AtNIMA proteins via immunostaining analysis. The absence of any specific bands corresponding to the size of AtNIMA 2 and 3 implies that the generated antibodies are also not suitable for Western blot analysis.

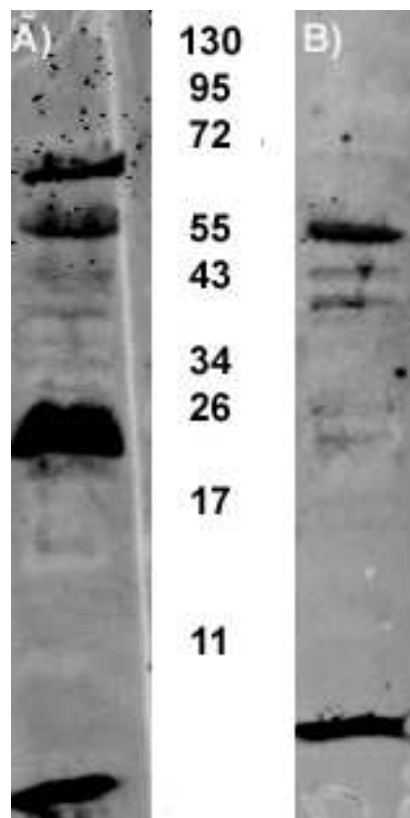


Figure 35: Western blot analysis on total protein from wild type *A. thaliana* leaves using putative anti-AtNIMA 2 (A) or anti-AtNIMA 3 (B)-specific antibodies. AtNIMA 2 has an expected site of 68 kDa, AtNIMA 3 of 63 kDa but no specific band of that size was identified.

4.8 - Analysis of *A. thaliana* plants transformed with 35S::AtNIMA 2 and 35S::YFP::AtNIMA 2

To further investigate the role of AtNIMA 2 kinase, *A. thaliana* plants were transformed with construct carrying the 35S::AtNIMA 2 cassette designed for over-express the activity of *AtNIMA 2*. In addition, Arabidopsis plants were transformed with 35S::YFP::AtNIMA 2, in order to the determine the localization of the AtNIMA 2 kinase in the plants organs by fusing it with the YFP reporter gene. For each construct approximately 30 plantlets were obtained through a selection with phosphinothricin. The candidate plantlets carrying the construct 35S::YFP::AtNIMA 2 were analyzed via fluorescence microscopy to determine if the YFP signal was expressed during early development. Later the selected plants were analyzed via genomic PCR in order to verify the presence of the sequence designed to over express *AtNIMA 2* using the combination of primers n° 4-38. However no plants carrying the expression cassette for 35S::AtNIMA 2 or 35S::YFP::AtNIMA 2 were identified through PCR and microscopy analysis. Genomic PCR performed with primers specific for BAR gene (n° 53-54), which provides resistance to phosphinothricin, demonstrated that the candidates plants contained the sequence encoding for herbicide resistance (Fig. 36) but lost the expression cassette responsible for over-expression of AtNIMA 2.

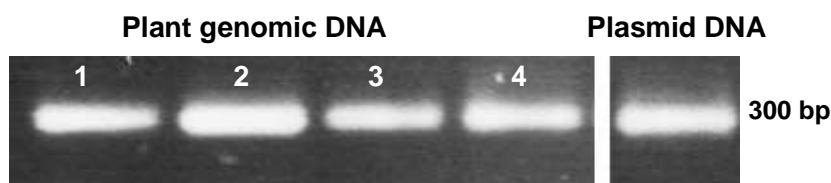


Figure 36: Genomic PCR performed to verify the presence of expression cassette for BAR gene on plants transformed with 35S::AtNIMA 2 construct, using primer n° 53 and 54 . Plasmid DNA was used as control. The presence of the BAR specific sequence was verified positively in all the analyzed plants.

All together these results suggest that the over-expression of *AtNIMA 2* has a lethal effect, thus reinforcing the hypothesis of an involvement of the gene in the regulatory pathways of plant development.

4.9 - Analysis of 35S::YFP::AtNIMA 2-specific signals in transiently transformed leaves of *N. benthamiana*

The construct 35S::YFP::AtNIMA 2 was expressed in *N. benthamiana* via transient transformation. The goal was to obtain information about the localization of AtNIMA 2 while avoiding the lethal effect caused by its over-expression in *A. thaliana*. Several leaves from *N. benthamiana* plants were injected with a suspension of *A. tumefaciens* cells containing the 35S::YFP::AtNIMA 2 construct. As control, other plants were transformed using the 35S::histone H2B::YFP and 35S::YFP constructs. After two days of incubation leaves fragments were analyzed by fluorescence microscopy and confocal laser scanning microscopy (CLSM). The fluorescence signals of 35S::YFP::AtNIMA 2 were found to decorate a filamentous network (Fig. 37a). In control leaves infiltrated with 35S::YFP the fluorescence signal was found throughout the cytoplasm and in the nucleus (Fig. 37b). While in leaves infiltrated with 35S::histone H2B::YFP the fluorescence signal was restricted to the nucleus (Fig. 37c). 3-dimensional (3D) recording of 35S::YFP::AtNIMA 2 positive cells by CLSM proved the network to be predominantly peripheral, continuous throughout the cell and not linked to any visible intracellular structures. Upon closer examination (Fig. 38, 39) the YFP decoration was found to consist of numerous distinct spots or plaques of different sizes.

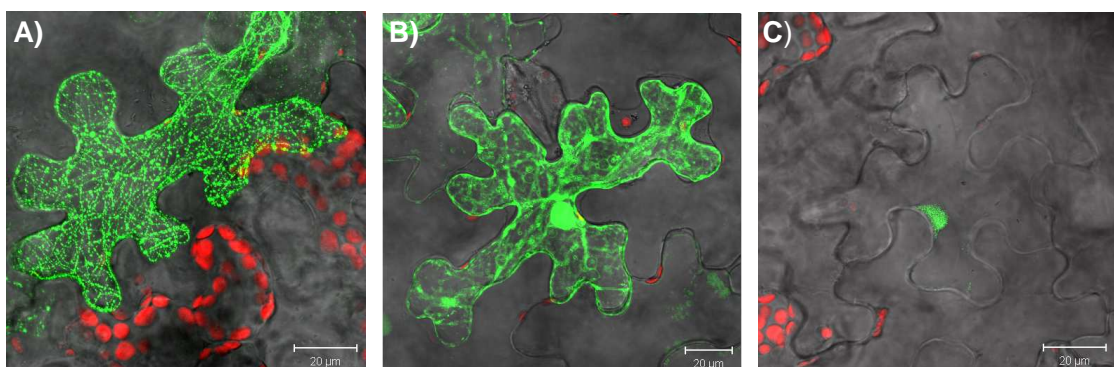


Figure 37: Transient transformation of *N. benthamiana* leaves with different constructs. (A) The fluorescent signal obtained with 35S::YFP::AtNIMA 2 is located on filamentous structures throughout the cell. On the opposite, signal coming from empty vector 35S::YFP is located in the nucleus and in the cell membranes (B), while signal obtained from 35S::histone H2B::YFP is restricted to the nucleus only (C).

Transient transformations were repeated in approximately ten plants, selecting every time three to five leaves and performing on each three-four injections. Samples of leaves transformed with 35S::YFP::AtNIMA 2 were analyzed also with confocal laser scanning microscopy to obtain a three dimensional picture and it was determined that the fibres in which the signal is localized are extended through the whole cell volume, without being limited to the surface (Fig. 36).

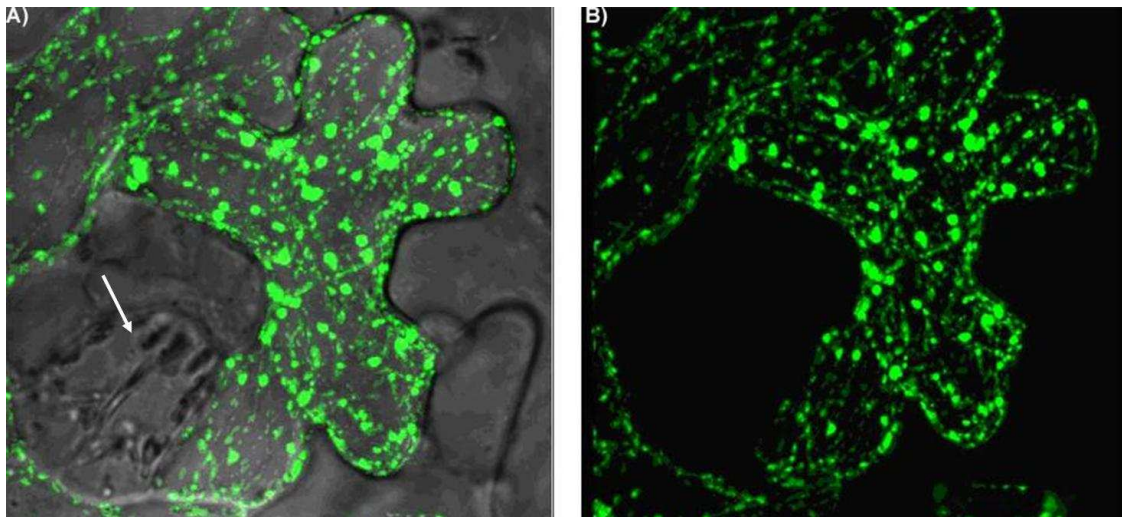


Figure 38: Confocal laser scanning microscopy analysis of leaf cells from *N. benthamiana* transformed with 35S::YFP::AtNIMA 2. **(A)** The fibres in which the fluorescence signal is located are crossing the entire cell volume. One stomata and a neighbour cell are also visible (arrowed). **(B)** Picture of the fluorescence signal alone.

The filamentous structures decorated by 35S::YFP::AtNIMA 2 obviously belong to the cytoskeleton, being either actin filaments or microtubules. The nature of the bright YFP-positive dots along these filaments was unclear. If these should represent organelles, we should be able to see translocations with time. Furthermore, since organelle movement in higher plants is exclusively over actin filaments (Staiger et al. 2009) any movement over these filaments would identify them as belonging to the actin cytoskeleton. When time lapse recordings were made by CLSM using a combination of fluorescent imaging and bright field, most YFP spots proved to be stationary stuck to the filamentous structures (Fig. 39).

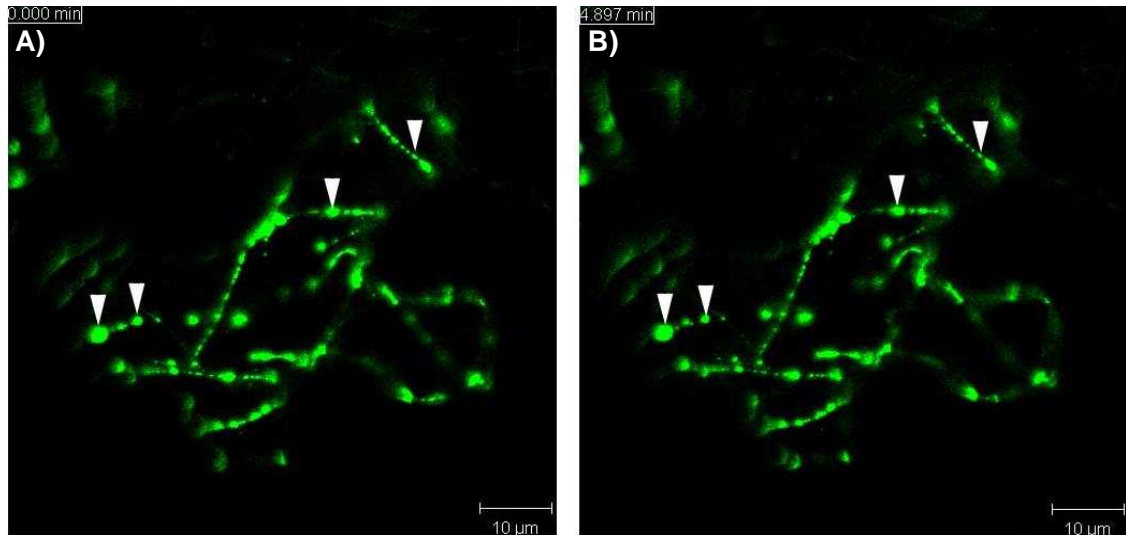


Figure 39: Time lapse analysis of 35S::YFP::AtNIMA 2 expression by CLSM. Strings of bright fluorescent dots, apparently decorating a filamentous structure, were followed for nearly 5 min without any translocation being observed (compare arrowheads in **A** and **B**).

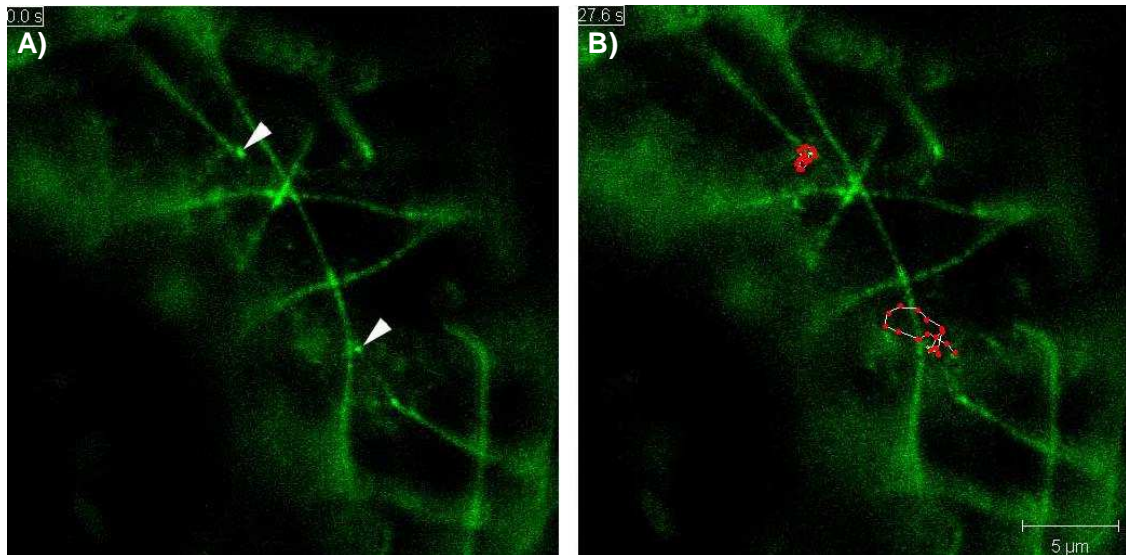


Figure 40: Time lapse recording by CLSM. Arrowheads in **A**) point to two, non-stationary, fluorescent spots. The red dots in **B**) indicate the trajectory these spots absolved over a time span of 27.6 s. The spots seem to orbit a stationary centre located on the filamentous structure.

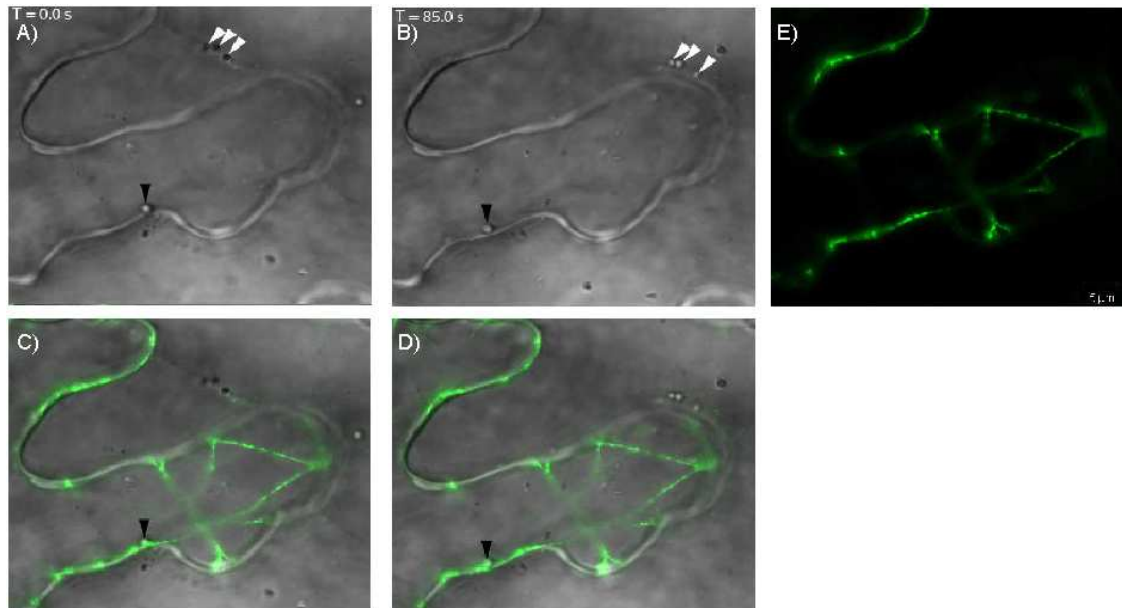


Figure 41: Time lapse recording of organelle movement. White arrowheads in (A) and (B) point at three organelles moving over a non-fluorescent structure. A further organelle, indicated by a black arrowhead, is seen to move along a fluorescent element (C-D). (E) Organization of fluorescent filamentous structures.

The few YFP-positive dots that were non-stationary displayed small nondirectional circular movements as if physically attached to a stationary structure (Fig. 40). When organelle movement was recorded, most organelles moved over non-fluorescent structures, others though seemed to move over YFP::AtNIMA 2 positive filaments (Fig. 41). From these results we can conclude that the YFP-positive dots do not represent organelles. Whether they represent true physiological structures or are the result of AtNIMA 2::YFP overexpression by the 35S-promoter can not be established here. Since most organelles moves over non-fluorescent filaments (Fig. 41), this would identify the AtNIMA 2 - decorated filaments as microtubules. This is not contradicted by the few organelles actually found moving along fluorescent strands since actin filaments also often codistribute with microtubules (Bannigan et al. 2006). So AtNIMA 2, directly or indirectly linked to the microtubular cytoskeleton, seems to cover all microtubular arrays.

4.9.1 - Disruption of the AtNIMA 2::YFP-fluorescence decorated filamentous system by oryzalin and colchicine

To test the hypothesis of AtNIMA 2 decorating the microtubular cytoskeleton, leaves transformed with 35S::YFP::AtNIMA 2 were treated with the microtubule depolymerising agents oryzalin, colchicine or the actin depolymerising agent latrunculin. In the first experiments leaf samples were incubated for up to four hours in a solution of 10 μ M colchicine or 10 μ M oryzalin in 10% DMSO. As this protocol did not produce any changes in the fluorescence distribution within the cells the strategy was changed. In the following experiments colchicines and oryzalin solutions were injected into the leaves at the same location where the AtNIMA 2 construct had been injected two days before (Fig. 42 A). Three hours after the start of the experiment clear effects were visible. In colchicine treated cells the fluorescence decorated network often had broken down in short filaments (Fig. 42 B, 43 A), while incubation with oryzalin had an even more detrimental effect leaving only dots and aggregations (Fig. 42 C, 43 B). In contrast to this, no changes in fluorescence distribution was observed when samples were incubated with 10% DMSO alone (as a control, Fig. 44 A) or with the actin depolymerising drug latrunculin (Fig. 44 B). These results support the hypothesis that AtNIMA 2 is interacting with a microtubular-based complex.

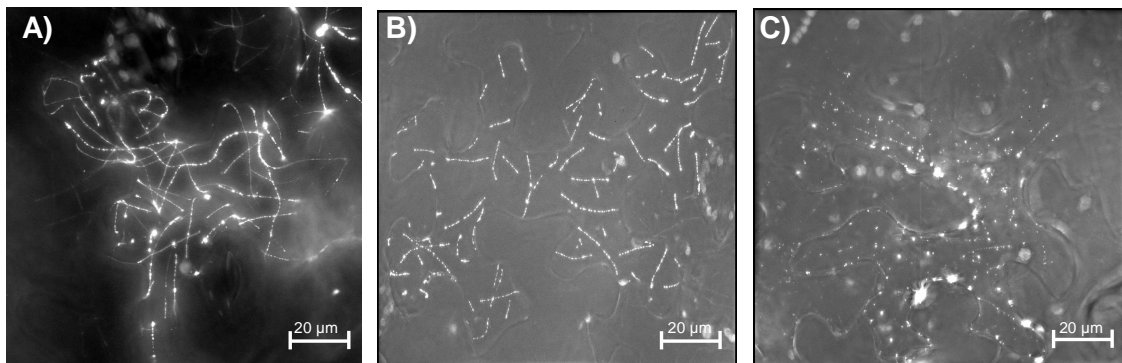


Figure 42: *N. benthamiana* leaf cells expressing 35S::YFP::AtNIMA 2. (A) Untreated cell showing fluorescence decorated filamentous network. (B) After treatment with colchicine the network is broken down into short filaments. (C) Filaments can no longer be discerned after oryzalin treatment leaving only dots of fluorescence.

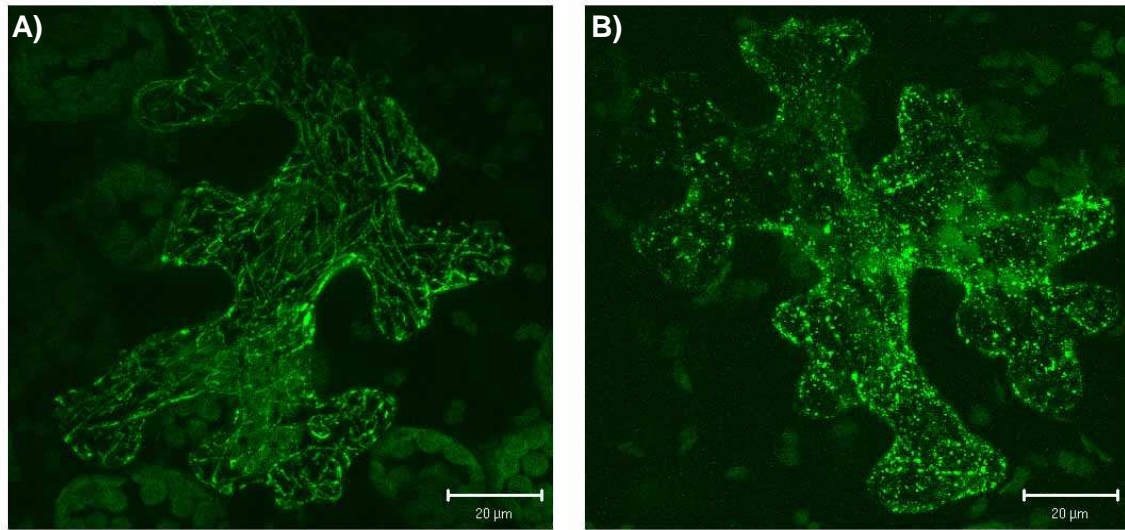


Figure 43: Confocal laser scanning microscopy on 35S::YFP::AtNIMA 2 transformed *N. benthamiana* leaf cells treated with colchicine **(A)** or oryzaline **(B)**

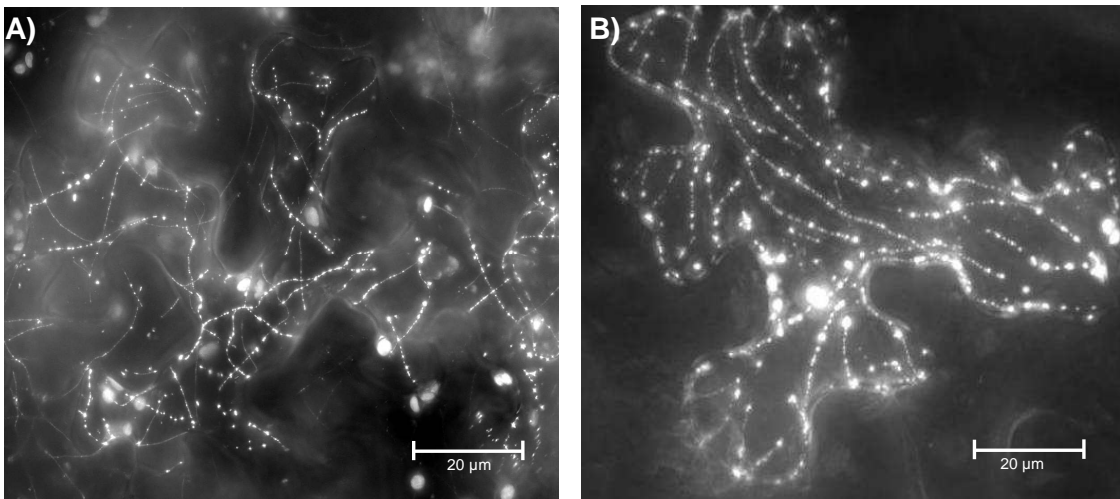


Figure 44: *N. benthamiana* leaf cells, expressing 35S::YFP::AtNIMA 2. **(A)** Treatment with 10% DMSO alone has no discernable effect on fluorescence pattern. **(B)** Incubation with the actin depolymerising drug latrunculin has no effect.

4.9.2 - Immunostaining signal from anti-tubuline antibody seems to overlap with 35S::YFP::AtNIMA 2 fluorescence

Additional confirmation of the interaction between AtNIMA 2 and microtubules was obtained by immunostaining AtNIMA 2::YFP positive cells with an antibody against α tubuline. For this experiment leaf material was used verified to express AtNIMA 2::YFP. Analysis shows that the YFP signal is partially overlapping the tubuline signal (Fig. 45), thus supporting the idea of an interaction. The experiment was also repeated using leaf material previously treated with colchicine. Unfortunately, however, the squashing procedure on leaf material already weakened by the colchicine treatment resulted in a far too low number of intact cells for a proper analysis.

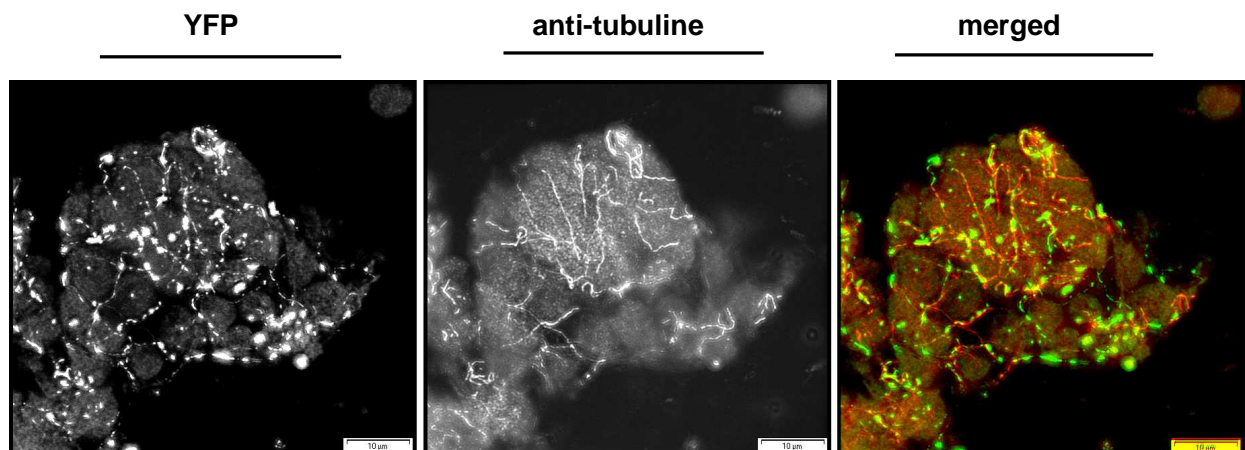


Figure 45: Immunostaining with anti-tubuline antibody of *N. benthamiana* leaf cells transiently transformed with 35S::YFP::AtNIMA 2 showing an overlap between anti tubuline and YFP signals. In the last picture the images of DAPI staining (blue), 35S::YFP::AtNIMA 2 (green) and Cy3-conjugated secondary antibody (yellow) are merged. Size bar= 10 μ M

4.10 - Determination of AtNIMA 2 promoter expression pattern using GUS histochemical staining

The tissue specific expression of AtNIMA 2 was further investigated via GUS histochemical staining. Therefore we fused a 1250 bp long genomic fragment upstream of the start codon of the AtNIMA 2 gene to the GUS reporter gene using the vector pMDC162. Wild type *A. thaliana* plants were transformed with the construct and transgenic seedlings were selected. The presence of the AtNIMA 2 promoter::GUS sequence on the transgenic plants was verified via genomic PCR (Fig. 46).

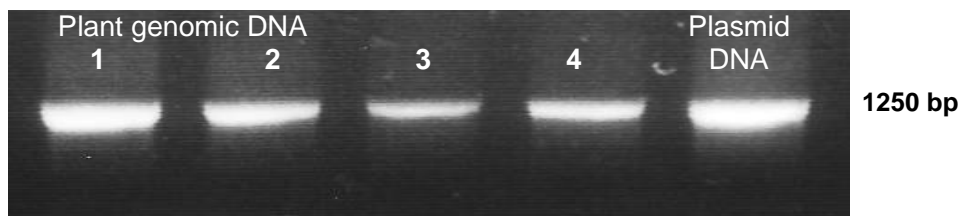


Figure 46: PCR performed on genomic DNA extracted from plants transformed with AtNIMA 2 promoter::GUS construct, using primer n° 41 and 48. Plasmid DNA was used as control. The presence of the construct was verified positively in all the analyzed plants.

After the presence of the construct was confirmed, plants were subjected to GUS staining (see 3.13). At first leaf and floral tissues in various stages of development were studied. Analysis by stereo microscopy showed strongest GUS signals in the flower buds and in the vascular bundles of young leaves (Fig. 47). The intensity of the staining differed between the various samples, most probably because the copy number of the construct varies between each transformed plant.

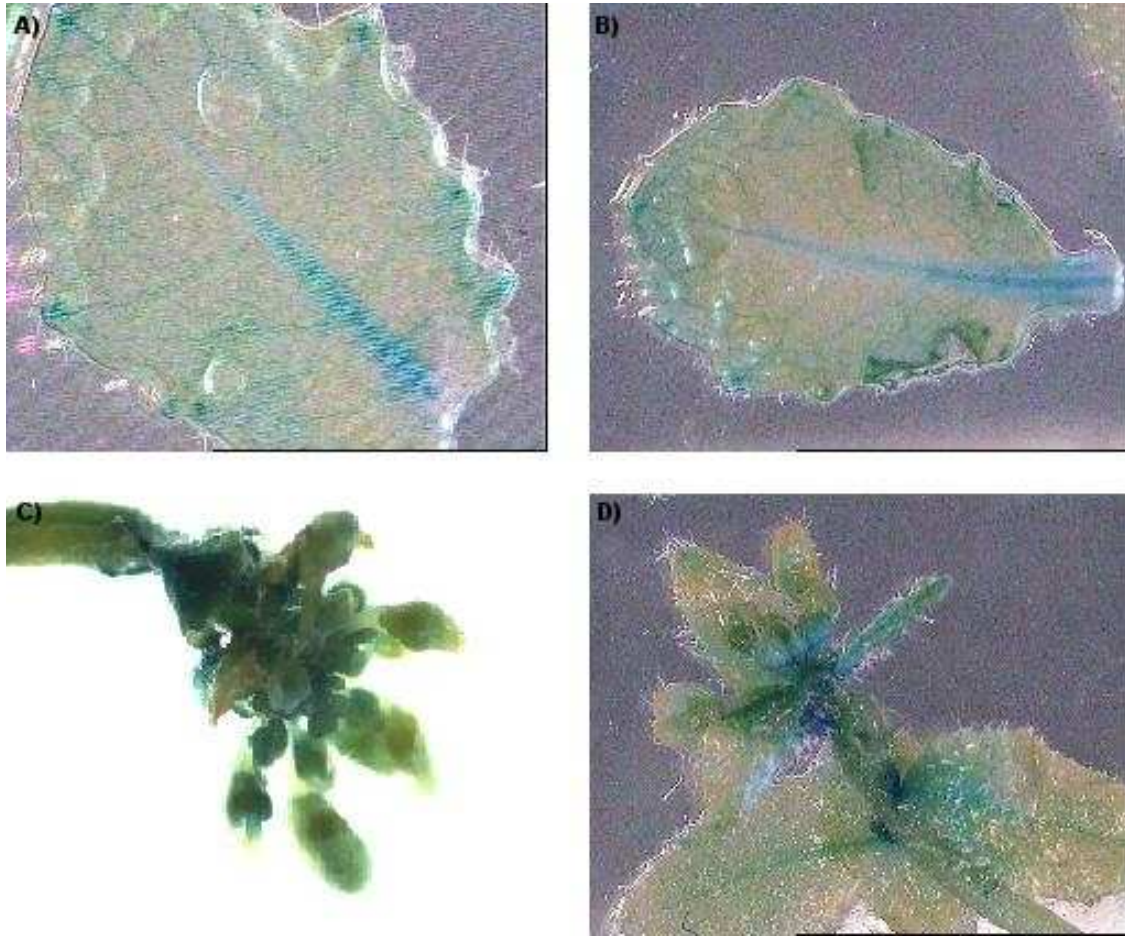


Figure 47: GUS stained organs. Promoter AtNIMA 2::GUS signal is strongly expressed in the vascular tissue of rosette leaves, particular in the primary bundle (**A** and **B**) and in the flower buds (**C** and **D**).

To improve the visual study GUS stained samples were made into permanent histological preparations using Hoyer's solution. Further analysis proved that the signal seems to concentrate preferentially in tissues that are undergoing development. After the opening of the flower the histochemical signal disappears from the stamen and concentrates mostly in the ovary (Fig 48 A-D). Once the flowering process has ended GUS signal is located inside the developing seeds (Fig 48 E).

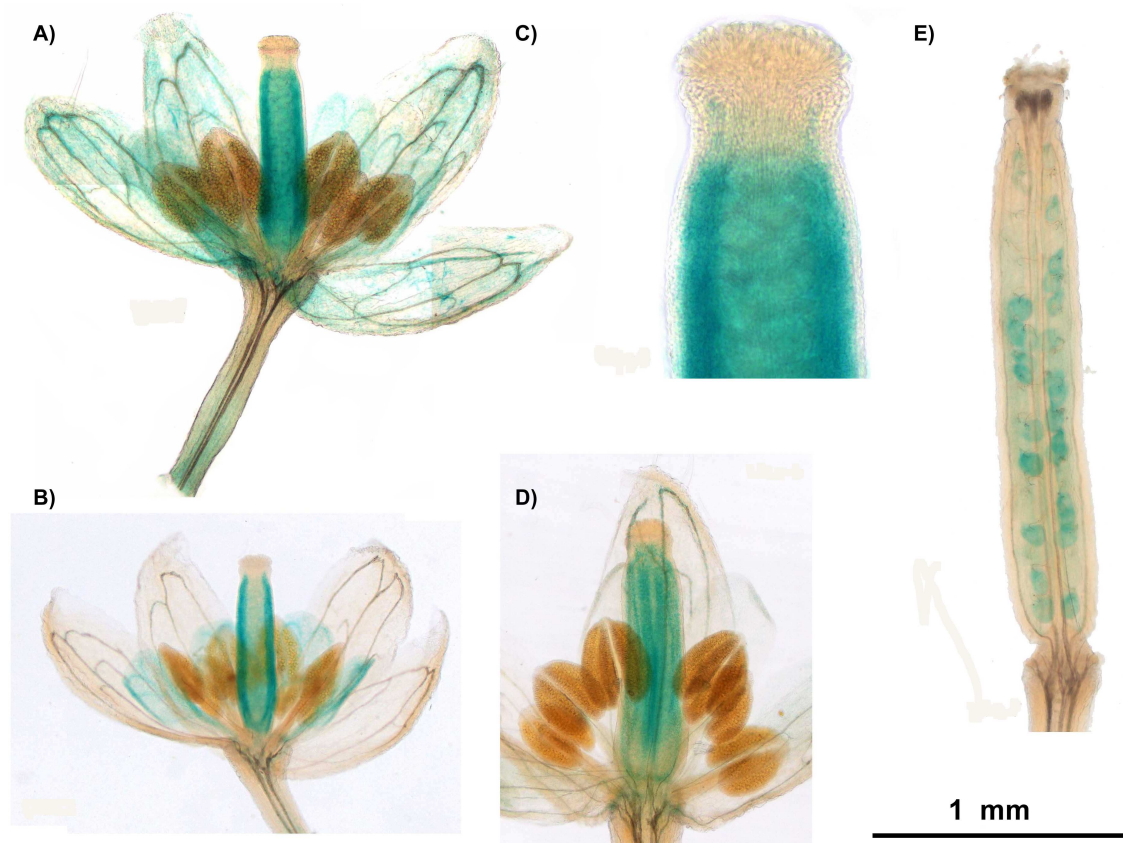


Figure 48: Embedded GUS stained floral organs.

(A) and (B) Open flowers, promoter AtNIMA 2::GUS signal is strongly expressed in the ovary and in the vascular bundles of the petals. (C) and (D) Closer view of the staining inside the ovary. (E) Young siliqua, GUS signal is located in the developing seeds.

In order to confirm the tissue-specific expression of AtNIMA 2 promoter::GUS we studied the successive generation of transgenic plants. After two weeks of culture approximately 30 plantlets were obtained and used for GUS staining. Microscopy analysis shows an intense GUS expression in the stem (Fig. 49 A), roots and, as in the previous generation, in flower buds and floral organs. Analysis of the root section shows a strong GUS expression throughout all tissues, including the vascular bundle and the epidermis (Fig. 49 B). GUS signals were also very strong in flower buds (Fig. 49 C-D-G). As flower development progresses, GUS staining becomes restricted to the vascular tissue of petals and ovary (Fig. 49 E-H). GUS signals were absent from the embryo at all stages examined.

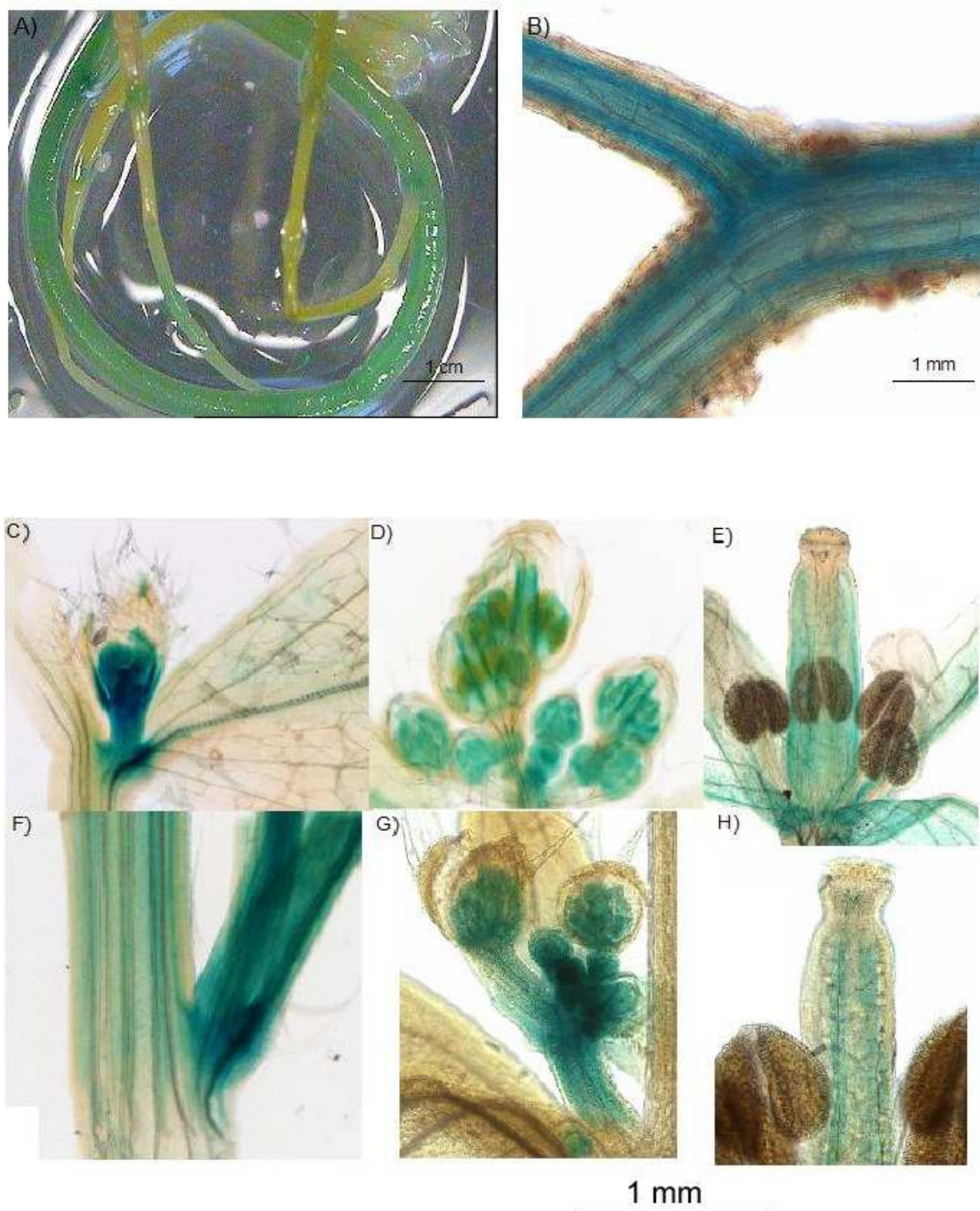


Figure 49: GUS stained organs harvested from T_1 promoter AtNIMA 2::GUS plants. Stem (A) and embedded root (B), GUS signal is expressed in the whole length of both organs. Embedded floral organs (C-H), GUS signal is located throughout the entire inflorescence during the emerging (C) and the early development of flower buds (D). Once the flower is open it remains into the ovary and the sepals. (E) Closer pictures show a strong expression also in the branches of stem (F), of the inflorescence (G) and vascular tissue of the ovary (H).

To analyse the GUS expression in young seedlings a T2 generation of AtNIMA 2 promoter::GUS plants was cultured under conditions described previously. The experiment was carried out on ten plantlets harvested three weeks after the start of culturing. GUS signal was located inside the root tips, in the transition zone between hypocotyls and root, and in the entire cotyledons (Fig. 50).

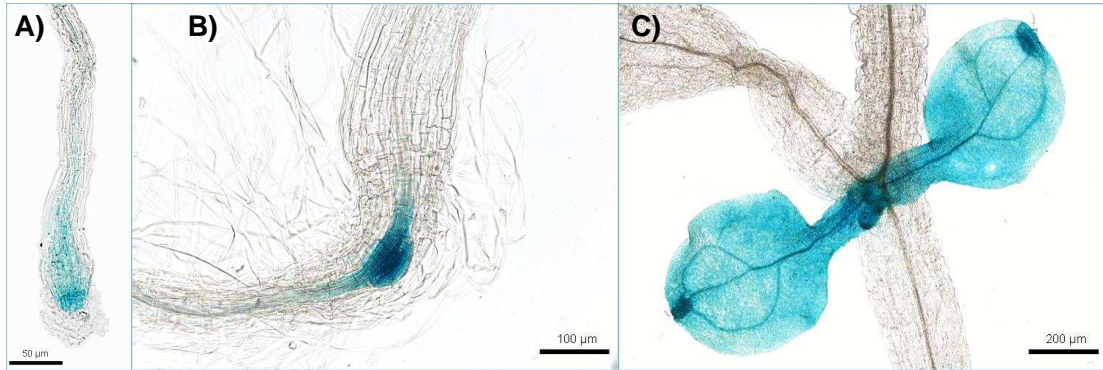


Figure 50: Promoter AtNIMA 2::GUS signal on three week old seedlings. (A) root tip (B) transition zone between hypocotyl and root (C) cotyledons with the vascular bundles.

According to the GUS results the promoter of AtNIMA 2 seems most active in young developing tissues and virtually absent from senescent tissues. Apart from this, GUS signals were also strong in the vascular bundles of all organs.

5. Discussion

5.1 - The catalytic domain of AtNIMA kinases is highly conserved

Previous studies, reviewed by Vigneault and colleagues (2007) have shown that the NIMA-like kinase family is highly conserved throughout the eukaryotic domain including plants. Despite an early discovery in the 1970's remarkably little is known about the functional role of these kinases, especially in plants. The family of NIMA-like kinases in *A. thaliana* is encoded by seven members, which are scattered throughout the whole genome of Arabidopsis. The catalytic domains of AtNIMAs are located at the N-terminal end and display a high similarity with the catalytic domain of fungal NIMA. Structural analysis proved that all the typical motifs of serine/threonine protein kinases, described by Hanks and colleagues (1995), are conserved in the AtNIMAs kinase domains. The analysis of the amino acid sequences of the catalytic domains showed that the AtNIMA kinases 2, 3 and 5 are more closely related to fungal NIMA, than to other members of the AtNIMA family. As it was reported by Cloutier and colleagues (2005), the non-catalytic C-terminal domain of the different AtNIMA kinases is variable in length, ranging from 170 residues in AtNIMA 5 to 680 residues in AtNIMA 6, with an average size of 300 residues. However, in all AtNIMA kinases the C-terminal domain always includes one or more PEST degradation sequence (Rechsteiner and Rogers 1996) and a coiled-coil motif. It should be noted that the PEST sequences and the coiled-coil domain are conserved in almost all NIMA-like kinases, implying that they are key features fulfilling a role that may be as important as that of the catalytic domain.

The remaining part of the C-terminal extension contains motifs responsible for the sub-cellular localization of the different kinases and for their interactions with other proteins. The high variability of this domain may reflect the different roles that the various AtNIMA kinases play in different pathways of the plant.

5.1.1 - The NIMA-like kinase family in plants has an early evolutionary origin

The phylogenetic analysis, performed on the Viridiplantae database using the full amino acid sequences of AtNIMA 2, 3 and 5 as baits, revealed that putative NIMA-like genes are present in all major plant groups. Interestingly, there is no separation between NIMA-like kinases from gymnosperms and angiosperms. Nevertheless, for angiosperms a division between monocots and dicots is visible inside each sub-cluster. The observation that the clustering of the various putative plants NIMA-like kinases does not reflect the division between the two groups of Spermatophyta indicates that the evolutionary origin and early diversification of the NIMA family in plants preceded the separation of the angiosperms from the gymnosperms. In the phylogenetic tree the numerous NIMA-like kinases found in plants, are clearly separated from fungal NIMA and human Nek2. This indicates that plant NIMA-like kinases have diverged to a significant degree from the ancestral NIMA during evolution, undergoing lineage specific expansion and different functional specializations (Casneuf et al. 2006). The large scale duplication event occurred in the genome of *A. thaliana* during evolution, described by Ermolaeva and colleagues (2003), could explain the existence of diverse genes encoding for AtNIMA kinases. This hypothesis is supported by the presence of at least two classes of paralogues, *AtNIMA 1-4* and *AtNIMA 2-3*, and by the conservation of the intron-exon structure between the different AtNIMA genes (Vigneault et al. 2007). Following this duplication, the members of AtNIMA family went through extensive reshuffling and divergent evolutionary processes resulting in new functions. Such processes could also explain the wide distribution of AtNIMA kinases in different sub-clusters of the phylogenetic tree. The presence of paralogues indicates either that some AtNIMA kinases have complementary roles, acting in the same molecular process in a functionally redundant manner, or that they differentiated to gain new functions during evolution.

5.1.2 - The transcription profiles of AtNIMA 2, 3 and 5 are similar in an organ specific way and are not associated with the mitotic cell cycle

Micro-array based transcription profiles available at “Genevestigator” (<https://www.genevestigator.com/gv/index.jsp>) show that *AtNIMA* 2, 3 and 5 are expressed in almost all organs of *A. thaliana*. A quantitative comparison between *AtNIMAs* transcription profiles shows that *AtNIMA* 2 and 3 display a near to identical organ dependent transcription profile. The analysis of gene expression during plant development also shows that different *AtNIMA* genes are active during the same developmental stages. Interestingly the expression of *AtNIMA* 2 and 3 is on average two fold higher than that of *AtNIMA* 5, reaching a five fold increase during the bolting stage. On the whole the expression of *AtNIMAs* is significantly lower in fully developed organs like rosettes, flowers, and mature siliques and highest in organs with active meristems (young leaves, stem, and floral organs). This might suggest a correlation between *AtNIMA* kinases activity and mitotic activity, as is the case with the fungal NIMA and the human Nek2. However, this hypothesis was rejected by reanalyzing the transcription profiles, published by Menges and coworkers (2003), of *AtNIMA* genes during cell cycle using synchronized mitotic cells from *Arabidopsis*. The mRNA levels of *AtNIMA* 2, 3 and 5 remain virtually unaltered during all stages of the cell cycle including the entry into mitosis, the time point when the expression of cyclin B dramatically increases (Ito et al. 1998).

The organ-specific expression level of mRNA from *AtNIMA* 2, 3 and 5 was also analysed by semiquantitative RT-PCR analysis. These data confirmed a high expression of *AtNIMA* 2, 3 and 5 in young leaves, stems and floral organs and an almost absent expression in older leaves and siliques. The combined results indicate that *AtNIMA* kinases 2, 3 and 5 are not associated with mitotic activity. This is clearly different from the role of fungal NIMA. However, *AtNIMA* 2, 3 and 5 may play a role in biochemical pathways related to cell proliferation and organ development. Moreover, the organ specific expressions could indicate a potential

complementary role in organ development between *AtNIMA 5* and the paralogues *AtNIMA 2* and *3* which would support the hypothesis that the *AtNIMA* kinases have acquired different specializations during the course of evolution.

5.2 - *AtNIMA 5* does not play a major role in plant development and histone H3 phosphorylation

T-DNA insertion line Salk_054652 represents a null mutant with complete inactivation of *AtNIMA 5*, as confirmed by failure to detect normal transcripts in RT-PCR experiments. The growth habitus of this *AtNIMA 5* null mutant was compared with that of wild type plants in order to identify phenotypical differences that could provide indications about the role of *AtNIMA 5*. Comparison between *AtNIMA 5* null mutants and wild type plants, performed in two different time points, shows that mutants produce a reduced number of leaves in the rosette. Although the rosettes of *AtNIMA 5* mutant plants were further expanded in the interval between the time points, the differences in leaves number between mutant and wild type remained constant. However, no other differences in the phenotype were registered while plants were able to undergo a complete life cycle. Furthermore, immunostaining experiment performed on dividing cells of *AtNIMA 5* null plants with antibodies against histone H3S10ph (Hendzel et al. 1997) revealed no difference between wild type and mutant, thus making a major role of *AtNIMA 5* in cell cycle-dependent phosphorylation of histone H3 very unlikely. Analysis of cell cycle dependant expression using synchronized mitotic cells demonstrated that the expression level of *AtNIMA 5* during cell cycle is low and the results obtained via immunostaining are in accordance with transcription data.

Although *AtNIMA 5* null mutants present a decreased number of rosette leaves, the low activity of *AtNIMA 5* during cell cycle seem to exclude that the phenotype is caused by an alteration in the processes of cell division. The observation that under normal conditions, the inactivation of *AtNIMA 5* does not dramatically affect the plant phenotype can be explained by a functional redundancy in the

NIMA gene family. A similar phenomenon was observed by Kim and colleagues (2003) for the members of the AtGRF (*Arabidopsis thaliana* GROWTH-REGULATING FACTOR) gene family. It can be concluded that either AtNIMA 5 kinase does not play a major role in the pathways of plant development or that the effects of its inactivation are mitigated by the compensatory activity of one or more members of the AtNIMA kinase family.

5.3 - AtNIMA 2 is a gene fundamental for the plant development

5.3.1 - Complete inactivation of *AtNIMA 2* has a lethal effect

T-DNA insertion line Salk_093269 proved that the gene *AtNIMA 2* is essential for the plant survival. The progeny obtained by self-fertilization of heterozygous plants comprised approximately 60% heterozygous plant, 40% wild type plants and no homozygous plants, diverging clearly from ratios of 50% heterozygous, 25% wild type and 25% homozygous plants expected according to Mendelian segregation.

The position of the insertion Salk_093269 inside the *AtNIMA 2* gene was determined by PCR amplification and sequencing of the PCR products, which univocally identified the gene specific part of the amplicons as belonging to *AtNIMA 2*. Southern blot experiments performed on DNA from heterozygous plants detected two T-DNA copies line Salk_093269. The size of the two hybridization signals, obtained after cleavage with different enzymes, suggested that the two copies of T-DNA were integrated next to each other in a tandem repeat arrangement (Jorgensen et al. 1996). This hypothesis was later confirmed through PCR experiments, meaning that the two copies of T-DNA in tandem repeat could be together responsible for the inactivation of *AtNIMA 2*.

Counting of developing seeds in immature siliques originating from self-fertilization of Salk_093269 heterozygous plants detected approximately 25% of aborted seeds. This ratio is in accordance with the expected percentage of homozygous T-DNA plants based on Mendelian segregation. The seeds abortion

data and the ratio between wild type and heterozygous plants (Brukhin et al. 2005; Johnston et al. 2007) suggest that inactivation of *AtNIMA 2* is correlated with embryo lethality, although the mechanism responsible for this phenotype is unknown.

5.3.2 - Down-regulation of *AtNIMA 2* influences the correct plant development

In contrast to complete inactivation by T-DNA insertion, down-regulation of *AtNIMA 2* by the Agrikola RNAi construct N244762 produced viable plants. RT-PCR experiments demonstrated that the RNAi construct is able to down-regulate the expression of *AtNIMA 2* mRNA without interfering with the activity of other member of the *AtNIMA* family. Analysis of transformants at T₁ and T₂ generations showed that *AtNIMA 2* down-regulated plants are typified by a retarded growth. The differences in development were already visible in within days after germination, in which *AtNIMA 2* RNAi plantlets showed a shorter primary root and a reduced number of leaves in comparison to wild type plants. During the subsequent stages of development, *AtNIMA 2* RNAi plants produced rosettes of smaller size and initiate the bolting at a later stage in comparison to wild type plants. However, eventually *AtNIMA 2* RNAi plants complete all stages of development and produce fertile seeds.

It should be noted that the phenotype of *AtNIMA 2* RNAi was not uniform, as many plants underwent a less disrupted development and present a phenotype much more similar to wild type plants. The effect of *AtNIMA 2* down-regulation on roots leaves and stem development were consistent with the data obtained *in silico* from “Genevestigator”, in particular with the high activity of *AtNIMA 2* during rosette development and bolting, suggesting a role for *AtNIMA 2* in the regulatory mechanism of plant growth (see Fig. 7A-B and Vigneault et al. 2007).

5.3.3 - *AtNIMA 2* seems to be involved in the control of cell morphogenesis

Histological analysis of leaf material from *AtNIMA 2* RNAi plants demonstrated that the altered plant development is accompanied by a distorted organization of cells. The first evidence was obtained from microscopic analysis of cross sections of leaves from RNAi plants. In comparison with wild type plants, RNAi plants were generally thinner and their mesophyll contained a reduced number of cells. In detail, the palisade layer contained fewer cells that tended to be round-shaped instead of cylindrical. The spongy tissue was composed of only one or two cell layers, instead of the three layers found in wild type leaves. Intercellular spaces also seemed to be larger in transgenic leaves.

Scanning electron microscopy recordings of leaf surfaces also confirmed that the epidermal layer of *AtNIMA 2* RNAi leaves contained fewer, though much larger, cells than wild type. Also the number of trichomes and stomata per surface area was much lower in *AtNIMA 2* RNAi leaves in comparison with wild type. The larger size of the epidermal cells and the reduced organization of the chlorenchym allowed the transgenic leaves to be of similar size as wild type leaves, despite having significantly fewer cells.

The effect of *AtNIMA 2* down-regulation on the stem was less dramatic. The stems of RNAi plants were smaller in diameter in comparison with wild type and presented also a reduced amount of parenchymal pith cells. However, the internal organization of stems of RNAi plants was virtually indistinguishable from that of the wild type. It thus seems that the retarded development of *AtNIMA 2* RNAi plants is the direct result of a lower mitotic activity leading to a reduced cell numbers. A phenomenon often related to leaf-size control is the compensation phenotype, in which a mutant that undergoes infrequent cell division produces daughter cells larger than normal. The compensation phenotype has been reported for several mutants (Tsukaya 2002; Tsukaya 2003; Kim and Kende 2004; Horiguchi et al. 2005), although its basis are largely unknown. However, it was hypothesized by Horiguchi and colleagues (2006) that compensation is

caused by a mechanism that coordinates the processes of cell proliferation and cell expansion. Interestingly, *AtNIMA 2* RNAi plants seemed to exhibit a sort of compensation phenotype. This effect is particularly obvious in leaves and most probably it could be a mechanism that ensures the production of leaves of a size suitable for plant survival. Based on the data obtained by RNAi down-regulation it can be hypothesized that *AtNIMA 2* kinase participates in the pathways that regulates cell morphogenesis. This is consistent with microarray experiments that seemed to exclude an involvement of *AtNIMA 2* in the processes of cell division (see Fig. 7 C and Menges et al., 2003).

5.3.4 - Organization of vascular bundles in cotyledons is altered by *AtNIMA 2* down-regulation

In addition to the effect on cell morphogenesis, down regulation of *AtNIMA 2* produced an altered vascular pattern. Analysis of the early vascular development was carried out in several studies, reviewed by Nelson and Dengler (1997). The vascular pattern of wild type cotyledons is composed by a primary bundle and four secondary lobes. It was observed by Nagawa and colleagues (2006) that several genes are involved in the development of vascular tissue, and mutations often results in a discontinuous formation of the primary and secondary veins. Analysis of seven-day old plantlets showed that *AtNIMA 2* RNAi mutants have an incomplete vascular network in cotyledons compared with wild type. The phenotype of *AtNIMA 2* RNAi plantlets was not uniform also regarding differences in vascularization, as many mutants showed different types of altered vascular pattern (see Fig. 27). Although the majority of mutants formed only the primary vascular bundle with two secondary lobes, few samples presented a vascular network much more similar to wild type plantlets. An involvement of a plant NIMA like gene in the vascularization processes was described also for poplar *PNek1* by Vigneault and colleagues (2007).

5.3.5 - AtNIMA 2 kinase is not involved in the process of cell cycle-dependent histone H3 phosphorylation

To determine whether down-regulation of *AtNIMA 2* affects the level of phosphorylation of histone H3, mitotic cells prepared from *AtNIMA 2* RNAi plants were immunolabeled with antibodies against histone H3 phosphorylated at serine 10. No differences in the level of phosphorylation of histone H3 between wild type and *AtNIMA 2* RNAi cells were found. Those findings were in accordance with the low activity of *AtNIMA 2* during the cell cycle as registered by microarray experiments (see Fig. 7 c). The absence of any indication for an activity related to histone phosphorylation stands in clear contrast to the role of the ancestral NIMA of *A. nidulans*. Those findings support the hypothesis, postulated also by Sakai and colleagues (2007), that during the evolution some members of the *AtNIMA* family gained functions that diverge from regulation of the cell cycle.

5.4 - Overexpression of *AtNIMA 2* has a lethal effect on plants.

Recombinant constructs designed to over-express *AtNIMA 2* were employed in order to investigate the gene activity via gain of function mutations. However, screening of T₀ transformants after selection showed that plants were only carrying the *BAR* gene, responsible for phosphinothricin resistance. There were no plants encoding for over-expressed *AtNIMA 2*. This suggests that the selected transformants were plants in which the transfer of the T-DNA was incomplete. Similarly there were also no plants identified expressing the reporter construct 35S::YFP::*AtNIMA 2*. Cloutier and colleagues (2005) already observed that overexpression of poplar NIMA *PNek1* in *Arabidopsis* severely affected plant development, particularly the morphology of floral organs. Thus while down-regulation of *AtNIMA 2* affects the correct plant development, overexpression of the same gene is lethal for the plant. It could be hypothesized that the correct temporal and spatial expression activity of *AtNIMA 2* is essential for a wild type-like plant development. Whenever the expression of *AtNIMA 2* is imbalanced, due to gain or loss-of functions mutations, the plant survival is affected although

it is unknown in which stage of development it happens. This data further define a crucial role for AtNIMA 2 in the regulation of plant development.

5.5 - AtNIMA 2 co-distributes with microtubules

5.5.1 - The fluorescence signal of 35S::YFP::AtNIMA 2

decorates filamentous structures in *N. benthamiana* cells

The intracellular distribution of AtNIMA 2 was investigated in leaves of *N. benthamiana* transiently transformed with 35S::YFP::AtNIMA 2. By this technique the lethal effect of AtNIMA 2 overexpression could be avoided. Analysis with fluorescence microscopy and CLSM showed the fluorescent signal of the 35S::YFP::AtNIMA 2 construct distributed along filamentous structures. These filaments were cortical, decorating the complete cell periphery, and not linked to any particular subcellular structure as shown by 3-dimensional recording. For controls, plants were transformed with the constructs 35S::histone H2B::YFP and 35S::YFP. The 35S::YFP signal is present throughout the cytoplasm and in the nucleus, while the signal from 35S::histone H2B::YFP is limited to the nucleus only. The filamentous distribution of the 35S::YFP::AtNIMA 2 is indicative of an interaction with cytoskeletal elements, i.e. actin filaments or microtubules. The absence of a 35S::YFP::AtNIMA 2 signal from the nucleus, supports the observation that AtNIMA 2 kinase is not involved in processes of cell cycle regulation.

A closer examination of the fluorescence signals showed that they were made up of numerous distinct spots or plaques of different sizes. The first assumption that they might represent organelles was disproved by the time-lapse observations which revealed these spots to be stationary. Furthermore, when movement of particles was recorded, the particles were unlabelled and travelled along fluorescence decorated as well as non fluorescence pathways. Since organelle transport in higher plants is over actin filaments, as discussed by Shimmen and Yokota (2004), this is a strong indication that the filaments decorated by YFP::AtNIMA 2 are microtubules. The occasional colocalization of actin filaments and microtubules (Mathur and Hulskamp 2002; Mayer and Jurgens 2002)

explains why organelles in 35S::YFP::AtNIMA 2 transformed cells move over labelled and unlabeled tracks alike. Although the fluorescence pattern can be considered a true reflection of the AtNIMA 2 distribution, the plaques most probably represent artefacts created by local accumulations due to strong protein overexpression, as observed in different works by Bhat et al. (2006) and Gehl et al. (2009).

5.5.2 - Drug treatments proofs that AtNIMA 2 is interacting with the microtubular cytoskeleton

In order to identify the cytoskeleton element with whom AtNIMA 2 is interacting, *N. benthamiana* leaves transformed with 35S::YFP::AtNIMA 2 were treated with the microtubule depolymerising drugs oryzalin (Chan et al. 1991; Bannigan et al. 2006) and colchicine (Margulis 1973; Bajer and Mole-Bajer 1986) or the actine depolymerising drug latrunculin (Coue et al. 1987; Ayscough 1998). Microscopy analysis proved that oryzalin and to a lesser degree colchicine, had a dramatic effect on the fluorescence distribution patterns within the cells. In the presence of these microtubule depolymerizing drugs the fluorescent network was reduced into short fragments (colchicine), or a collection of dots and aggregations (oryzalin). In contrast to this, no changes in the structure of the fluorescence distribution pattern was recorded after application of latrunculin.

Immunostaining of cells expressing 35S::YFP::AtNIMA 2 with antibodies against α tubuline showed that the YFP fluorescence signal overlaps with the anti-tubulin signals, giving additional proof that AtNIMA 2 co-localizes with the microtubular cytoskeleton. The interaction between members of the AtNIMA family with microtubules was already postulated for AtNIMA 6 by Motose and colleagues (2008). This interaction may give an explanation for the phenotype observed in RNAi mutants. As a microtubule-associated-protein AtNIMA 2 kinase may influence microtubule dynamics and through this cell shape and cell division (Mathur and Hulskamp 2002). It has been demonstrated that NIMA like kinases from mammals play an active role in the control of mitotic spindle assembly (Fry

2002; O'Regan and Fry 2009). A similar role for AtNIMA 2 kinase could not be proven due to the lack of dividing cells in differentiated leafs of *N. benthamiana*. However, it seems beyond doubt that AtNIMA kinases are involved in the control of cell morphogenesis and plant development through the interaction with microtubules.

6. Outlook

The effect of mis-expression of AtNIMA 2 in the organization of microtubules and cells could be further investigated using RNAi plants. To understand the biological role of AtNIMA 2 during root formation and cell morphogenesis, wild-type and AtNIMA 2-RNAi plantlets could be grown in medium containing colchicine or oryzalin in order to observe the differences in root growth and plant development. In addition, immunostaining with anti-tubulin antibodies could be performed on mitotic cells prepared from wild type and AtNIMA 2-RNAi plants to analyze differences in microtubule organization.

Inactivation and overexpression of AtNIMA 2 in *A. thaliana* produced a lethal phenotype. However, different strategies could be employed to circumvent this effect. *A. thaliana* plants heterozygous for the T-DNA insertion Salk_093269 could be transformed with a construct expressing 35S::AtNIMA 2. The aim would be to investigate whether the 35S::AtNIMA 2 overexpression cassette could complement the absence of an endogenous AtNIMA 2 kinase, thus producing a viable plant with complete inactivation of endogenous AtNIMA 2. The complementation experiment would prove the essential function of AtNIMA 2. Complementation experiments could be performed also using the construct expressing 35S::YFP::AtNIMA 2 reporter construct, in order to observe the distribution of AtNIMA 2-signals in *A. thaliana*. The effects of 35S::AtNIMA 2 transgene could be investigated also by using transactivation or chemical inducible systems (Moore et al. 2006).

To analyze the enzymatic activity of AtNIMA kinases and for the identification of putative substrate, a kinase assay could be performed. In specific, AtNIMAs full cDNA sequences could be inserted into destination vectors designed to express recombinant AtNIMA kinases tagged with polyhistidine (His-tag) or glutathione-S-transferase (GST tag). In addition, recombinant AtNIMA kinases could be used for antibody production.

The role of AtNIMA 3 and AtNIMA 5 could be further investigated by using gain of function and reporter constructs.

The close phylogenetic relationship between *AtNIMA 2* and *AtNIMA 3* allows classifying them as paralogues (Vigneault et al. 2007). Their amino-acid sequences have a high degree of similarity and they are expressed in almost the same stages of development. It could be hypothesized that *AtNIMA 3* and *AtNIMA 2* are involved in the same pathways. In order to test whether *AtNIMA 3* has functions similar to *AtNIMA 2*, a construct designed to over-express *AtNIMA 3* (35S::*AtNIMA 3*) could be used to transform T-DNA insertion line Salk_093269 heterozygous *A. thaliana* plants. If viable plants carrying a null mutation for *AtNIMA 2* are produced, then most likely *AtNIMA 3* is able to successfully complement the lack of activity from *AtNIMA 2*.

7. Summary

Using the amino acid sequence of the nimA kinase from *A. nidulans*, a BLAST research was performed on the database of the *A. thaliana* genome. As result, a family of NIMA related proteins that encodes for seven serine/threonine kinases was identified (called AtNIMAs). Alignment of the catalytic domains of the different AtNIMAs with the one belonging to the fungal nimA revealed that the structure of NIMA-like kinase domains is highly conserved. AtNIMA kinases 2, 3 and 5 are the closest homologues in Arabidopsis to the nimA from *A. nidulans*. Phylogenetic analysis performed on the Viridiplantae database, using the catalytic domain of AtNIMA 2, 3 and 5 as baits, revealed that NIMA homologues are found in all major plant groups and that their diversification has an early evolutionary origin. This evidences points to an important role for NIMA-like genes.

In silico analysis of AtNIMAs expression pattern showed that AtNIMAs are expressed in almost all organs and are active in the same developmental stages. The expression profiles of *AtNIMA* 2 and 3 were almost identical. Tissue-type specific expression analysis via semi-quantitative RT-PCR showed an abundance of AtNIMAs transcripts in young leaves, stems and floral organs. These tissues have a high level of cellular proliferation and differentiation.

The homozygous *A. thaliana* T-DNA insertion line Salk_054652 represents a null mutant with complete inactivation of *AtNIMA* 5. Comparison between *AtNIMA* 5 null mutant and wild type plants showed that the mutant produced a reduced number of leaves in rosette. However, no other differences were recorded and mutant plants were able to undergo a complete life cycle, suggesting a minor involvement of *AtNIMA* 5 in the pathways of plant development.

The T-DNA insertion of homozygous *A. thaliana* line Salk_093269, designed to inactivate *AtNIMA* 2, was lethal and overexpression of the same *AtNIMA* gene (via 35S promoter) produced also a phenotype lethal for the plant. Those evidences suggested an important and fundamental role for *AtNIMA* 2 for plant

development. Down-regulation (via RNAi) of AtNIMA 2 caused a retarded growth in plants, with defects in leaves, roots, stems and vascular tissue. Histological analysis showed that AtNIMA 2 down-regulation produced also a distorted organization of cells. The phenotype observed in AtNIMA 2 RNAi plants was similar to plants with mutations in genes involved in the regulation of cell morphogenesis.

To investigate whether the activity of the AtNIMA genes analysed affects the phosphorylation of histone H3 at position serine 10, dividing cells from *A. thaliana* plants with altered activity of AtNIMA genes (RNAi and null mutants) were immunostained with an antibody specific for phosphorylated H3Ser10. However, no obvious changes in the level of H3Ser10ph were recorded in dividing cells from AtNIMA 5 null mutants and AtNIMA 2 RNAi mutants, in comparison with wild type cells. Thus, there are no evidences of a significant involvement of AtNIMA genes in the cell-cycle dependant phosphorylation of histone H3Ser10 in plants.

Fluorescence microscopy analysis of the reporter construct 35S::YFP::AtNIMA 2 in leaves of transiently transformed *N. benthamiana* plants showed that AtNIMA 2 proteins are distributed along filamentous structures that decorate the entire cell periphery. Treatment of leaves transformed with 35S::YFP::AtNIMA 2 with microtubule depolymerising drugs oryzalin and colchicine produced dramatic effects in the fluorescence distribution pattern within the cells, while no changes were recorded using the actin depolymerising drug latunculin. Immunostaining of cells expressing 35S::YFP::AtNIMA 2 with antibodies against α tubuline showed an overlapping between YFP fluorescence signal and anti-tubuline signal. Those evidences suggest that AtNIMA 2 co-localizes and might interact with microtubule cytoskeletal elements. Therefore, misexpression of AtNIMA 2 might influence the dynamics of microtubules and cell morphogenesis. The distorted organization of cells as been observed in AtNIMA 2 RNAi mutants could be the consequence.

In conclusion, evidences show that AtNIMA kinases gained a novel role as proteins associated with the pathways of cell morphogenesis and plant development. This can explain the high degree of conservation of NIMA-like kinases in plants and the critical role of AtNIMA 2. However, the exact mechanism, of how AtNIMA kinases can affect the regulatory pathways of cell morphogenesis and plant development is still unknown.

8. Zusammenfassung

Eine aus sieben Mitgliedern bestehende NIMA-ähnliche Kinase Familie (genannt AtNIMA) mit hoher Ähnlichkeit zur nimA Kinase von *A. nidulans* wurde mit Hilfe der BLASTX Analyse im *A. thaliana* Genom identifiziert. Die Kinasedomäne von AtNIMAs und nimA zeigten einen hohen Grad an Konserviertheit. AtNIMA 2, 3 and 5 besitzen die höchste Ähnlichkeit zu nimA von *A. nidulans*. Mit Hilfe einer phylogenetischen Analyse wurden NIMA-ähnliche Kinasen in allen Pflanzengruppen identifiziert, was darauf hindeutet, dass es sich hierbei um eine Kinase mit essenzieller Funktion handelt, welche sich bereits früh in der Evolution der Eukaryoten ausbildete.

Basierend auf einer *in silico* Transkriptionsanalyse kann gefolgert werden, dass AtNIMAs in fast allen Pflanzenorganen exprimiert werden. Die Expressionsprofile von AtNIMA 2 und 3 sind ähnlich. Analyse von AtNIMA mittels semi-quantitativer RT-PCR zeigte die höchste Genaktivität dieser Kinasen in jungen Blättern, Stengeln und Blüten. Diese Gewebe sind durch hohe Zellteilung und Zelldifferenzierung gekennzeichnet.

Die homozygote AtNIMA 5 ‚knock-out‘ *A. thaliana* T-DNA Mutante (Salk_054652) ist lebensfähig, ist aber durch eine reduzierte Anzahl von Rosettenblättern gekennzeichnet. Die Inaktivierung (homozygote AtNIMA 2, *A. thaliana* T-DNA Mutante (Salk_093269)) bzw. die Überexpression (35S Promoter) von AtNIMA 2 ist letal für Arabidopsis, was darauf hindeutet, dass AtNIMA 2 essenziell für die Funktion und Entwicklung der Pflanze ist. Eine künstliche Abschwächung (via RNAi) von AtNIMA 2 resultiert in pleiotrophen Phänotypen, welche durch fehlerhafte Entwicklung der Blätter, Wurzeln und des vaskulären Systems gekennzeichnet sind. Mit Hilfe histologischer Analysen von AtNIMA 2 RNAi-Pflanzen wurden Zellorganisationsdefekte identifiziert. Dieser Phänotyp ist vergleichbar mit Mutanten mit gestörter Zelldifferenzierung.

Um eine funktionelle Verbindung zwischen der Phosphorylierung von Histon H3 an der Position Serin 10 und der Aktivität von AtNIMA zu detektieren, wurden

teilungssaktive Zellen von *A. thaliana* Pflanzen mit veränderter AtNIMA-Aktivität (RNAi und T-DNA) mit Hilfe der indirekten Immunofärbung unter Nutzung eines Histon H3Thr10-phos-spezifischen Antikörpers untersucht. Es konnten keine Unterschiede für die zellteilungsabhängige Histon H3 Phosphorylierung zwischen Wildtyp und Mutanten gewiesen. Somit gibt es keinen Hinweis, dass AtNIMA 2 oder 5 an der zellteilungsabhängigen Histon H3S10 Phosphorylierung signifikant beteiligt ist.

35S::YFP::AtNIMA 2-spezifische Signale wurden in transient transformierten Blättern von *N. benthamiana* Pflanzen in Filament-artigen Strukturen detektiert. Die Behandlung von Blättern mit den Alkaloiden Colchicin oder Oryzalin führte zur Umverteilung der AtNIMA 2-Fluoreszenzsignale. Dagegen zeigte die Behandlung mit dem Aktin-spezifischen Inhibitor Latunculin keine Auswirkung auf die zelluläre Verteilung von YFP-AtNIMA 2-Signalen. Eine Doppelfärbung mit α Tubulin-spezifischen Antikörpern zeigte eine Überlappung zwischen AtNIMA 2- and Tubulin-Signalen. Daher kann angenommen werden, dass AtNIMA 2 Proteine mit Mikrotubulifasern interagieren und eine unregelmäßige Aktivität von AtNIMA 2 die Dynamik von Mikrotubuli und der Zellmorphogenese beeinflusst. Die beobachtete veränderte Zellorganisation in AtNIMA 2 RNAi-Blättern könnte sich daraus ableiten.

Basierend auf den Beobachtungen wird postuliert, dass Mitglieder der AtNIMA Kinase Familie an der Zell- und Pflanzenentwicklung beteiligt sind, obgleich die genaue Funktion noch weitgehend unbekannt ist.

9. Literature

Adams, R. R., Carmena, M. and Earnshaw, W. C. (2001). "Chromosomal passengers and the (aurora) ABCs of mitosis." Trends Cell Biol **11**(2): 49-54.

Adams, R. R., Maiato, H., Earnshaw, W. C. and Carmena, M. (2001). "Essential roles of *Drosophila* inner centromere protein (INCENP) and aurora B in histone H3 phosphorylation, metaphase chromosome alignment, kinetochore disjunction, and chromosome segregation." J Cell Biol **153**(4): 865-80.

Ayscough, K. (1998). "Use of latrunculin-A, an actin monomer-binding drug." Methods Enzymol **298**: 18-25.

Bajer, A. S. and Mole-Bajer, J. (1986). "Drugs with colchicine-like effects that specifically disassemble plant but not animal microtubules." Ann N Y Acad Sci **466**: 767-84.

Bannigan, A., Wiedemeier, A. M., Williamson, R. E., Overall, R. L. and Baskin, T. I. (2006). "Cortical microtubule arrays lose uniform alignment between cells and are oryzalin resistant in the *Arabidopsis* mutant, radially swollen 6." Plant Cell Physiol **47**(7): 949-58.

Becher, M., Talke, I. N., Krall, L. and Kramer, U. (2004). "Cross-species microarray transcript profiling reveals high constitutive expression of metal homeostasis genes in shoots of the zinc hyperaccumulator *Arabidopsis halleri*." Plant J **37**(2): 251-68.

Bhat, R. A., Lahaye, T. and Panstruga, R. (2006). "The visible touch: in planta visualization of protein-protein interactions by fluorophore-based methods." Plant Methods **2**: 12.

Bischoff, J. R., Anderson, L., Zhu, Y., Mossie, K., Ng, L., Souza, B., Schryver, B., Flanagan, P., Clairvoyant, F., Ginther, C., Chan, C. S., Novotny, M., Slamon, D. J. and Plowman, G. D. (1998). "A homologue of *Drosophila* aurora kinase is oncogenic and amplified in human colorectal cancers." Embo J **17**(11): 3052-65.

Boisnard-Lorig, C., Colon-Carmona, A., Bauch, W., Hodge, S., Doerner, P., Bancharel, E., Dumas, C., Haseloff, J. and Berger, F. (2001). "Dynamic analyses of the expression of the HISTONE :: YFP fusion protein in *arabidopsis* show that syncytial endosperm is divided in mitotic domains." Plant Cell **13**(3): 495-509.

Brand L, H. M., Nüesch E, Vassalli S, Barrell P, Yang W, Jefferson RA, Grossniklaus U, Curtis MD (2006). "A versatile and reliable two-component system for tissue-specific gene induction in *Arabidopsis*." Plant Physiology **141**: 1194-1204.

Brukhin, V., Curtis, M. D. and Grossniklaus, U. (2005). "The angiosperm female gametophyte: No longer the forgotten generation." CURRENT SCIENCE **89**: 1844-1852.

Casneuf, T., De Bodt, S., Raes, J., Maere, S. and Van de Peer, Y. (2006). "Nonrandom divergence of gene expression following gene and genome duplications in the flowering plant *Arabidopsis thaliana*." Genome Biol **7**(2): R13.

Chadee, D. N., Hendzel, M. J., Tylipski, C. P., Allis, C. D., Bazett-Jones, D. P., Wright, J. A. and Davie, J. R. (1999). "Increased Ser-10 phosphorylation of histone H3 in mitogen-stimulated and oncogene-transformed mouse fibroblasts." J Biol Chem **274**(35): 24914-20.

Chan, M. M., Triemer, R. E. and Fong, D. (1991). "Effect of the anti-microtubule drug oryzalin on growth and differentiation of the parasitic protozoan *Leishmania mexicana*." Differentiation **46**(1): 15-21.

Chomczynski P, S. N. (1987). "Signal-Step Method of RNA Isolation by Acid Guanidinium Thiocyanate –Phenol –Chloroform Extraction." Analytical Biochemistry **162**(1): 156-159

Clough S.J., B. A. F. (1998). "Floral dip: a simplified method for *Agrobacterium*-mediated transformation of *Arabidopsis thaliana*." The Plant Journal **16**(6): 735-743.

Cloutier, M., Vigneault, F., Lachance, D. and Seguin, A. (2005). "Characterization of a poplar NIMA-related kinase PNek1 and its potential role in meristematic activity." FEBS Lett **579**(21): 4659-65.

Coue, M., Brenner, S. L., Spector, I. and Korn, E. D. (1987). "Inhibition of actin polymerization by latrunculin A." FEBS Lett **213**(2): 316-8.

Crosio, C., Fimia, G. M., Lorry, R., Kimura, M., Okano, Y., Zhou, H., Sen, S., Allis, C. D. and Sassone-Corsi, P. (2002). "Mitotic phosphorylation of histone H3: spatio-temporal regulation by mammalian Aurora kinases." Mol Cell Biol **22**(3): 874-85.

Dai, J., Sultan, S., Taylor, S. S. and Higgins, J. M. (2005). "The kinase haspin is required for mitotic histone H3 Thr 3 phosphorylation and normal metaphase chromosome alignment." Genes Dev **19**(4): 472-88.

De Souza, C. P., Horn, K. P., Masker, K. and Osmani, S. A. (2003). "The SONB(NUP98) nucleoporin interacts with the NIMA kinase in *Aspergillus nidulans*." Genetics **165**(3): 1071-81.

De Souza, C. P., Osmani, A. H., Wu, L. P., Spotts, J. L. and Osmani, S. A. (2000). "Mitotic histone H3 phosphorylation by the NIMA kinase in *Aspergillus nidulans*." Cell **102**(3): 293-302.

Demidov, D., Van Damme, D., Geelen, D., Blattner, F. R. and Houben, A. (2005). "Identification and dynamics of two classes of aurora-like kinases in *Arabidopsis* and other plants." Plant Cell **17**(3): 836-48.

Dolezel, J., Binarová, P. and Lucretti, S. (1989). "Analysis of nuclear DNA content in plant cells by flow cytometry." Biol Plant **31**: 113-120.

Earley K.W., H. J. R., Pontes O., Oppen K., Juehne T., Song K. and Pikaard C. S. (2006). "Gateway-compatible vectors for plant functional genomics and proteomics." The Plant Journal **45**: 616-629.

Ermolaeva, M. D., Wu, M., Eisen, J. A. and Salzberg, S. L. (2003). "The age of the *Arabidopsis thaliana* genome duplication." Plant Mol Biol **51**(6): 859-66.

Feige, E., Shalom, O., Tsurie, S., Yissachar, N. and Motro, B. (2006). "Nek1 shares structural and functional similarities with NIMA kinase." Biochim Biophys Acta **1763**(3): 272-81.

Fry, A. M. (2002). "The Nek2 protein kinase: a novel regulator of centrosome structure." Oncogene **21**(40): 6184-94.

Fry, A. M. and Nigg, E. A. (1995). "Cell cycle. The NIMA kinase joins forces with Cdc2." Curr Biol **5**(10): 1122-5.

Fu, H., Subramanian, R. R. and Masters, S. C. (2000). "14-3-3 proteins: structure, function, and regulation." Annu Rev Pharmacol Toxicol **40**: 617-47.

Gehl, C., Waadt, R., Kudla, J., Mendel, R. R. and Hansch, R. (2009). "New GATEWAY vectors for High Throughput Analyses of Protein-Protein Interactions by Bimolecular Fluorescence Complementation." Mol Plant **2**(5): 1051-8.

Gernand, D., Demidov, D. and Houben, A. (2003). "The temporal and spatial pattern of histone H3 phosphorylation at serine 28 and serine 10 is similar in plants but differs between mono- and polycentric chromosomes." Cytogenet Genome Res **101**(2): 172-6.

Giet, R. and Glover, D. M. (2001). "Drosophila aurora B kinase is required for histone H3 phosphorylation and condensin recruitment during chromosome condensation and to organize the central spindle during cytokinesis." J Cell Biol **152**(4): 669-82.

Giet, R., McLean, D., Descamps, S., Lee, M. J., Raff, J. W., Prigent, C. and Glover, D. M. (2002). "Drosophila Aurora A kinase is required to localize D-TACC to centrosomes and to regulate astral microtubules." J Cell Biol **156**(3): 437-51.

Glover, D. M., Leibowitz, M. H., McLean, D. A. and Parry, H. (1995). "Mutations in aurora prevent centrosome separation leading to the formation of monopolar spindles." Cell **81**(1): 95-105.

Goto, H., Tomono, Y., Ajiro, K., Kosako, H., Fujita, M., Sakurai, M., Okawa, K., Iwamatsu, A., Okigaki, T., Takahashi, T. and Inagaki, M. (1999). "Identification of a novel phosphorylation site on histone H3 coupled with mitotic chromosome condensation." J Biol Chem **274**(36): 25543-9.

Goto, H., Yasui, Y., Nigg, E. A. and Inagaki, M. (2002). "Aurora-B phosphorylates Histone H3 at serine28 with regard to the mitotic chromosome condensation." Genes Cells **7**(1): 11-7.

Grallert, A. and Hagan, I. M. (2002). "Schizosaccharomyces pombe NIMA-related kinase, Fin1, regulates spindle formation and an affinity of Polo for the SPB." Embo J **21**(12): 3096-107.

Gurley, L. R., Walters, R. A. and Tobey, R. A. (1975). "Sequential phosphorylation of histone subfractions in the Chinese hamster cell cycle." J Biol Chem **250**(10): 3936-44.

Hanks, S. K. and Hunter, T. (1995). "Protein kinases 6. The eukaryotic protein kinase superfamily: kinase (catalytic) domain structure and classification." Faseb J **9**(8): 576-96.

Hashimoto, Y., Akita, H., Hibino, M., Kohri, K. and Nakanishi, M. (2002). "Identification and characterization of Nek6 protein kinase, a potential human homolog of NIMA histone H3 kinase." Biochem Biophys Res Commun **293**(2): 753-8.

Hendzel, M. J., Wei, Y., Mancini, M. A., Van Hooser, A., Ranalli, T., Brinkley, B. R., Bazett-Jones, D. P. and Allis, C. D. (1997). "Mitosis-specific phosphorylation of histone H3 initiates primarily within pericentromeric heterochromatin during G2 and spreads in an ordered fashion coincident with mitotic chromosome condensation." Chromosoma **106**(6): 348-60.

Hohmann, P., Tobey, R. A. and Gurley, L. R. (1976). "Phosphorylation of distinct regions of f1 histone. Relationship to the cell cycle." J Biol Chem **251**(12): 3685-92.

Horiguchi, G., Ferjani, A., Fujikura, U. and Tsukaya, H. (2006). "Coordination of cell proliferation and cell expansion in the control of leaf size in *Arabidopsis thaliana*." J Plant Res **119**(1): 37-42.

Horiguchi, G., Kim, G. T. and Tsukaya, H. (2005). "The transcription factor AtGRF5 and the transcription coactivator AN3 regulate cell proliferation in leaf primordia of *Arabidopsis thaliana*." Plant J **43**(1): 68-78.

Houben, A., Demidov, D., Caperta, A. D., Karimi, R., Agueci, F. and Vlasenko, L. (2007). "Phosphorylation of histone H3 in plants--a dynamic affair." Biochim Biophys Acta **1769**(5-6): 308-15.

Houben, A., Demidov, D., Rutten, T. and Scheidtmann, K. H. (2005). "Novel phosphorylation of histone H3 at threonine 11 that temporally correlates with condensation of mitotic and meiotic chromosomes in plant cells." Cytogenet Genome Res **109**(1-3): 148-55.

Houben, A., Wako, T., Furushima-Shimogawara, R., Presting, G., Kunzel, G., Schubert, I. I. and Fukui, K. (1999). "Short communication: the cell cycle dependent phosphorylation of histone H3 is correlated with the condensation of plant mitotic chromosomes." Plant J **18**(6): 675-9.

Hsu, J. Y., Sun, Z. W., Li, X., Reuben, M., Tatchell, K., Bishop, D. K., Grushcow, J. M., Brame, C. J., Caldwell, J. A., Hunt, D. F., Lin, R., Smith, M. M. and Allis, C. D. (2000). "Mitotic phosphorylation of histone H3 is governed by Ipl1/aurora kinase and Glc7/PP1 phosphatase in budding yeast and nematodes." Cell **102**(3): 279-91.

Ito, M., Iwase, M., Kodama, H., Lavis, P., Komamine, A., Nishihama, R., Machida, Y. and Watanabe, A. (1998). "A novel cis-acting element in promoters of plant B-type cyclin genes activates M phase-specific transcription." Plant Cell **10**(3): 331-41.

Ito, T. (2007). "Role of histone modification in chromatin dynamics." J Biochem **141**(5): 609-14.

Johansen, K. M. and Johansen, J. (2006). "Regulation of chromatin structure by histone H3S10 phosphorylation." Chromosome Res **14**(4): 393-404.

Johnston, A. J., Meier, P., Gheyselinck, J., Wuest, S. E., Federer, M., Schlagenhauf, E., Becker, J. D. and Grossniklaus, U. (2007). "Genetic subtraction profiling identifies genes essential for *Arabidopsis* reproduction and reveals interaction between the female gametophyte and the maternal sporophyte." Genome Biol **8**(10): R204.

Jorgensen, R. A., Cluster, P. D., English, J., Que, Q. D. and Napoli, C. A. (1996). "Chalcone synthase cosuppression phenotypes in petunia flowers: Comparison of sense vs antisense constructs and single-copy vs complex T-DNA sequences." Plant Molecular Biology **31**(5): 957-973.

Kaitna, S., Pasierbek, P., Jantsch, M., Loidl, J. and Glotzer, M. (2002). "The aurora B kinase AIR-2 regulates kinetochores during mitosis and is required for separation of homologous Chromosomes during meiosis." Curr Biol **12**(10): 798-812.

Kandli, M., Feige, E., Chen, A., Kilfin, G. and Motro, B. (2000). "Isolation and characterization of two evolutionarily conserved murine kinases (Nek6 and nek7) related to the fungal mitotic regulator, NIMA." Genomics **68**(2): 187-96.

Kim, J. H., Choi, D. and Kende, H. (2003). "The AtGRF family of putative transcription factors is involved in leaf and cotyledon growth in Arabidopsis." Plant J **36**(1): 94-104.

Kim, J. H. and Kende, H. (2004). "A transcriptional coactivator, AtGIF1, is involved in regulating leaf growth and morphology in Arabidopsis." Proc Natl Acad Sci U S A **101**(36): 13374-9.

Kim, M. K., Choi, J. W., Jeon, J. H., Franceschi, V. R., Davin, L. B. and Lewis, N. G. (2002). "Specimen block counter-staining for localization of GUS expression in transgenic arabidopsis and tobacco." Plant Cell Rep **21**(1): 35-9.

Kouzarides, T. (2007). "Chromatin modifications and their function." Cell **128**(4): 693-705.

Krien, M. J., Bugg, S. J., Palatsides, M., Asouline, G., Morimyo, M. and O'Connell, M. J. (1998). "A NIMA homologue promotes chromatin condensation in fission yeast." J Cell Sci **111** (Pt 7): 967-76.

Krien, M. J., West, R. R., John, U. P., Koniaras, K., McIntosh, J. R. and O'Connell, M. J. (2002). "The fission yeast NIMA kinase Fin1p is required for spindle function and nuclear envelope integrity." Embo J **21**(7): 1713-22.

Lu, K. P. and Hunter, T. (1995). "Evidence for a NIMA-like mitotic pathway in vertebrate cells." Cell **81**(3): 413-24.

Lu, K. P. and Means, A. R. (1994). "Expression of the noncatalytic domain of the NIMA kinase causes a G2 arrest in *Aspergillus nidulans*." Embo J **13**(9): 2103-13.

Mahadevan, L. C., Willis, A. C. and Barratt, M. J. (1991). "Rapid histone H3 phosphorylation in response to growth factors, phorbol esters, okadaic acid, and protein synthesis inhibitors." Cell **65**(5): 775-83.

Manzanero, S., Arana, P., Puertas, M. J. and Houben, A. (2000). "The chromosomal distribution of phosphorylated histone H3 differs between plants and animals at meiosis." Chromosoma **109**(5): 308-17.

Margulis, L. (1973). "Colchicine-sensitive microtubules." Int Rev Cytol **34**: 333-61.

Markaki, Y., Christogianni, A., Politou, A. S. and Georgatos, S. D. (2009). "Phosphorylation of histone H3 at Thr3 is part of a combinatorial pattern that marks and configures mitotic chromatin." J Cell Sci **122**(Pt 16): 2809-19.

Mathur, J. and Hulskamp, M. (2002). "Microtubules and microfilaments in cell morphogenesis in higher plants." Curr Biol **12**(19): R669-76.

Mayer, U. and Jurgens, G. (2002). "Microtubule cytoskeleton: a track record." Curr Opin Plant Biol **5**(6): 494-501.

Menges, M., de Jager, S. M., Gruissem, W. and Murray, J. A. (2005). "Global analysis of the core cell cycle regulators of Arabidopsis identifies novel genes, reveals multiple and highly specific profiles of expression and provides a coherent model for plant cell cycle control." Plant J **41**(4): 546-66.

Menges, M., Hennig, L., Gruissem, W. and Murray, J. A. (2003). "Genome-wide gene expression in an Arabidopsis cell suspension." Plant Mol Biol **53**(4): 423-42.

Meraldi, P., Honda, R. and Nigg, E. A. (2002). "Aurora-A overexpression reveals tetraploidization as a major route to centrosome amplification in p53^{-/-} cells." Embo J **21**(4): 483-92.

Meraldi, P., Honda, R. and Nigg, E. A. (2004). "Aurora kinases link chromosome segregation and cell division to cancer susceptibility." Curr Opin Genet Dev **14**(1): 29-36.

Moore, I., Samalova, M. and Kurup, S. (2006). "Transactivated and chemically inducible gene expression in plants." Plant J **45**(4): 651-83.

Motose, H., Tominaga, R., Wada, T., Sugiyama, M. and Watanabe, Y. (2008). "A NIMA-related protein kinase suppresses ectopic outgrowth of epidermal cells through its kinase activity and the association with microtubules." Plant J **54**(5): 829-44.

Murata-Hori, M., Tatsuka, M. and Wang, Y. L. (2002). "Probing the dynamics and functions of aurora B kinase in living cells during mitosis and cytokinesis." Mol Biol Cell **13**(4): 1099-108.

Murata-Hori, M. and Wang, Y. L. (2002). "The kinase activity of aurora B is required for kinetochore-microtubule interactions during mitosis." Curr Biol **12**(11): 894-9.

Nagawa, S., Sawa, S., Sato, S., Kato, T., Tabata, S. and Fukuda, H. (2006). "Gene trapping in Arabidopsis reveals genes involved in vascular development." Plant Cell Physiol **47**(10): 1394-405.

Nelson, T. and Dengler, N. (1997). "Leaf Vascular Pattern Formation." Plant Cell **9**(7): 1121-1135.

Nowak, S. J. and Corces, V. G. (2004). "Phosphorylation of histone H3: a balancing act between chromosome condensation and transcriptional activation." Trends Genet **20**(4): 214-20.

O'Connell, M. J., Krien, M. J. and Hunter, T. (2003). "Never say never. The NIMA-related protein kinases in mitotic control." Trends Cell Biol **13**(5): 221-8.

O'Connell, M. J., Norbury, C. and Nurse, P. (1994). "Premature chromatin condensation upon accumulation of NIMA." Embo J **13**(20): 4926-37.

O'Regan, L., Blot, J. and Fry, A. M. (2007). "Mitotic regulation by NIMA-related kinases." Cell Div **2**: 25.

O'Regan, L. and Fry, A. M. (2009). "The Nek6 and Nek7 protein kinases are required for robust mitotic spindle formation and cytokinesis." Mol Cell Biol **29**(14): 3975-90.

Osmani, A. H., McGuire, S. L. and Osmani, S. A. (1991). "Parallel activation of the NIMA and p34cdc2 cell cycle-regulated protein kinases is required to initiate mitosis in *A. nidulans*." Cell **67**(2): 283-91.

Osmani, S. A., May, G. S. and Morris, N. R. (1987). "Regulation of the mRNA levels of nimA, a gene required for the G2-M transition in *Aspergillus nidulans*." J Cell Biol **104**(6): 1495-504.

Osmani, S. A., Pu, R. T. and Morris, N. R. (1988). "Mitotic induction and maintenance by overexpression of a G2-specific gene that encodes a potential protein kinase." Cell **53**(2): 237-44.

Paulson, J. R. and Taylor, S. S. (1982). "Phosphorylation of histones 1 and 3 and nonhistone high mobility group 14 by an endogenous kinase in HeLa metaphase chromosomes." J Biol Chem **257**(11): 6064-72.

Pnueli, L., Gutfinger, T., Hareven, D., Ben-Naim, O., Ron, N., Adir, N. and Lifschitz, E. (2001). "Tomato SP-interacting proteins define a conserved signaling system that regulates shoot architecture and flowering." Plant Cell **13**(12): 2687-702.

Polioudaki, H., Markaki, Y., Kourmouli, N., Dialynas, G., Theodoropoulos, P. A., Singh, P. B. and Georgatos, S. D. (2004). "Mitotic phosphorylation of histone H3 at threonine 3." FEBS Lett **560**(1-3): 39-44.

Preuss, U., Landsberg, G. and Scheidtmann, K. H. (2003). "Novel mitosis-specific phosphorylation of histone H3 at Thr11 mediated by Dlk/ZIP kinase." Nucleic Acids Res **31**(3): 878-85.

Rechsteiner, M. and Rogers, S. W. (1996). "PEST sequences and regulation by proteolysis." Trends Biochem Sci **21**(7): 267-71.

Sakai, T., Honing, H., Nishioka, M., Uehara, Y., Takahashi, M., Fujisawa, N., Saji, K., Seki, M., Shinozaki, K., Jones, M. A., Smirnov, N., Okada, K. and Wasteneys, G. O. (2007). "Armadillo repeat-containing kinesins and a NIMA-related kinase are required for epidermal-cell morphogenesis in Arabidopsis." Plant J **53**(1): 157-71.

Sambrook, J. R. D., Fritsch, E. F. and Maniatis, T., Eds. (1989). Molecular cloning: a laboratory manual.

Schagger, H. and von Jagow, G. (1987). "Tricine-sodium dodecyl sulfate-polyacrylamide gel electrophoresis for the separation of proteins in the range from 1 to 100 kDa." Anal Biochem **166**(2): 368-79.

Schubert, I., Dolezel, J., Houben, A., Scherthan, H. and Wanner, G. (1993). "Refined examination of plant metaphase chromosome structure at different levels made feasible by new isolation methods." Chromosoma **102**: 96-101.

Schultz, S. J., Fry, A. M., Sutterlin, C., Ried, T. and Nigg, E. A. (1994). "Cell cycle-dependent expression of Nek2, a novel human protein kinase related to the NIMA mitotic regulator of *Aspergillus nidulans*." Cell Growth Differ **5**(6): 625-35.

Shimmen, T. and Yokota, E. (2004). "Cytoplasmic streaming in plants." Curr Opin Cell Biol **16**(1): 68-72.

Simon, V. R. and Pon, L. A. (1996). "Actin-based organelle movement." Experientia **52**(12): 1117-22.

Soloaga, A., Thomson, S., Wiggin, G. R., Rampersaud, N., Dyson, M. H., Hazzalin, C. A., Mahadevan, L. C. and Arthur, J. S. (2003). "MSK2 and MSK1 mediate the mitogen- and stress-induced phosphorylation of histone H3 and HMG-14." Embo J **22**(11): 2788-97.

Staiger, C. J., Sheahan, M. B., Khurana, P., Wang, X., McCurdy, D. W. and Blanchoin, L. (2009). "Actin filament dynamics are dominated by rapid growth and severing activity in the Arabidopsis cortical array." J Cell Biol **184**(2): 269-80.

Stenoiien, D. L., Sen, S., Mancini, M. A. and Brinkley, B. R. (2003). "Dynamic association of a tumor amplified kinase, Aurora-A, with the centrosome and mitotic spindle." Cell Motil Cytoskeleton **55**(2): 134-46.

Strelkov, I. S. and Davie, J. R. (2002). "Ser-10 phosphorylation of histone H3 and immediate early gene expression in oncogene-transformed mouse fibroblasts." Cancer Res **62**(1): 75-8.

Sugiyama, K., Sugiura, K., Hara, T., Sugimoto, K., Shima, H., Honda, K., Furukawa, K., Yamashita, S. and Urano, T. (2002). "Aurora-B associated protein phosphatases as negative regulators of kinase activation." Oncogene **21**(20): 3103-11.

Thomson, S., Clayton, A. L., Hazzalin, C. A., Rose, S., Barratt, M. J. and Mahadevan, L. C. (1999). "The nucleosomal response associated with immediate-early gene induction is mediated via alternative MAP kinase cascades: MSK1 as a potential histone H3/HMG-14 kinase." Embo J **18**(17): 4779-93.

Tsukaya, H. (2002). "Interpretation of mutants in leaf morphology: genetic evidence for a compensatory system in leaf morphogenesis that provides a new link between cell and organismal theories." Int Rev Cytol **217**: 1-39.

Tsukaya, H. (2003). "Organ shape and size: a lesson from studies of leaf morphogenesis." Curr Opin Plant Biol **6**(1): 57-62.

Vermeulen, L., Berghe, W. V., Beck, I. M., De Bosscher, K. and Haegeman, G. (2009). "The versatile role of MSKs in transcriptional regulation." Trends Biochem Sci **34**(6): 311-8.

Vigneault, F., Lachance, D., Cloutier, M., Pelletier, G., Levasseur, C. and Seguin, A. (2007). "Members of the plant NIMA-related kinases are involved in organ development and vascularization in poplar, Arabidopsis and rice." Plant J **51**(4): 575-88.

Wei, Y., Mizzen, C. A., Cook, R. G., Gorovsky, M. A. and Allis, C. D. (1998). "Phosphorylation of histone H3 at serine 10 is correlated with chromosome condensation during mitosis and meiosis in Tetrahymena." Proc Natl Acad Sci U S A **95**(13): 7480-4.

Wei, Y., Yu, L., Bowen, J., Gorovsky, M. A. and Allis, C. D. (1999). "Phosphorylation of histone H3 is required for proper chromosome condensation and segregation." Cell **97**(1): 99-109.

Wu, L., Osmani, S. A. and Mirabito, P. M. (1998). "A role for NIMA in the nuclear localization of cyclin B in Aspergillus nidulans." J Cell Biol **141**(7): 1575-87.

Yaffe, M. B., Rittinger, K., Volinia, S., Caron, P. R., Aitken, A., Leffers, H., Gamblin, S. J., Smerdon, S. J. and Cantley, L. C. (1997). "The structural basis for 14-3-3:phosphopeptide binding specificity." Cell **91**(7): 961-71.

Ye, X. S., Xu, G., Pu, R. T., Fincher, R. R., McGuire, S. L., Osmani, A. H. and Osmani, S. A. (1995). "The NIMA protein kinase is hyperphosphorylated and activated downstream of p34cdc2/cyclin B: coordination of two mitosis promoting kinases." Embo J **14**(5): 986-94.

Zeitlin, S. G., Shelby, R. D. and Sullivan, K. F. (2001). "CENP-A is phosphorylated by Aurora B kinase and plays an unexpected role in completion of cytokinesis." J Cell Biol **155**(7): 1147-57.

Zhang, H., Scofield, G., Fobert, P. and Doonan, J. H. (1996). "A nimA-like protein kinase transcript is highly expressed in meristems of Antirrhinum majus." J Microsc **181**(Pt 2): 186-94.

Zhou, H., Kuang, J., Zhong, L., Kuo, W. L., Gray, J. W., Sahin, A., Brinkley, B. R. and Sen, S. (1998). "Tumour amplified kinase STK15/BTAK induces centrosome amplification, aneuploidy and transformation." Nat Genet **20**(2): 189-93.

Zimmermann, P., Hennig, L. and Gruissem, W. (2005). "Gene-expression analysis and network discovery using Genevestigator." Trends Plant Sci **10**(9): 407-9.

Publications in connection with the submitted dissertation

Houben, A., Demidov, D., Caperta, A.D., Karimi, R., Agueci, F., and Vlasenko, L. (2007). Phosphorylation of histone H3 in plants-A dynamic affair. *Biochim Biophys Acta*.

Conference contributions in connection with the submitted dissertation

Agueci, F., and Houben, A. (2006) Characterization of NIMA-like kinases in *Arabidopsis thaliana*. 2nd IPK student conference (ISC), Gatersleben, 30.05-01.06.2006 (poster)

Demidov, D., Karimi, R., Vlasenko, L., Agueci, F., Houben, A. (2006) Histone H3 phosphorylation and characterisation of candidate H3-kinases. DFG Meeting Chromatin mediated biological decisions, 5.-7.10.2006, Marburg/Germany (poster)

Agueci, F., Karimi, R., and Houben, A., (2007) Characterisation of NIMA and Haspin-like kinases in *Arabidopsis thaliana*. 16th International Chromosome Conference, Amsterdam, The Netherlands, 25.- 29. August 2007 (poster)

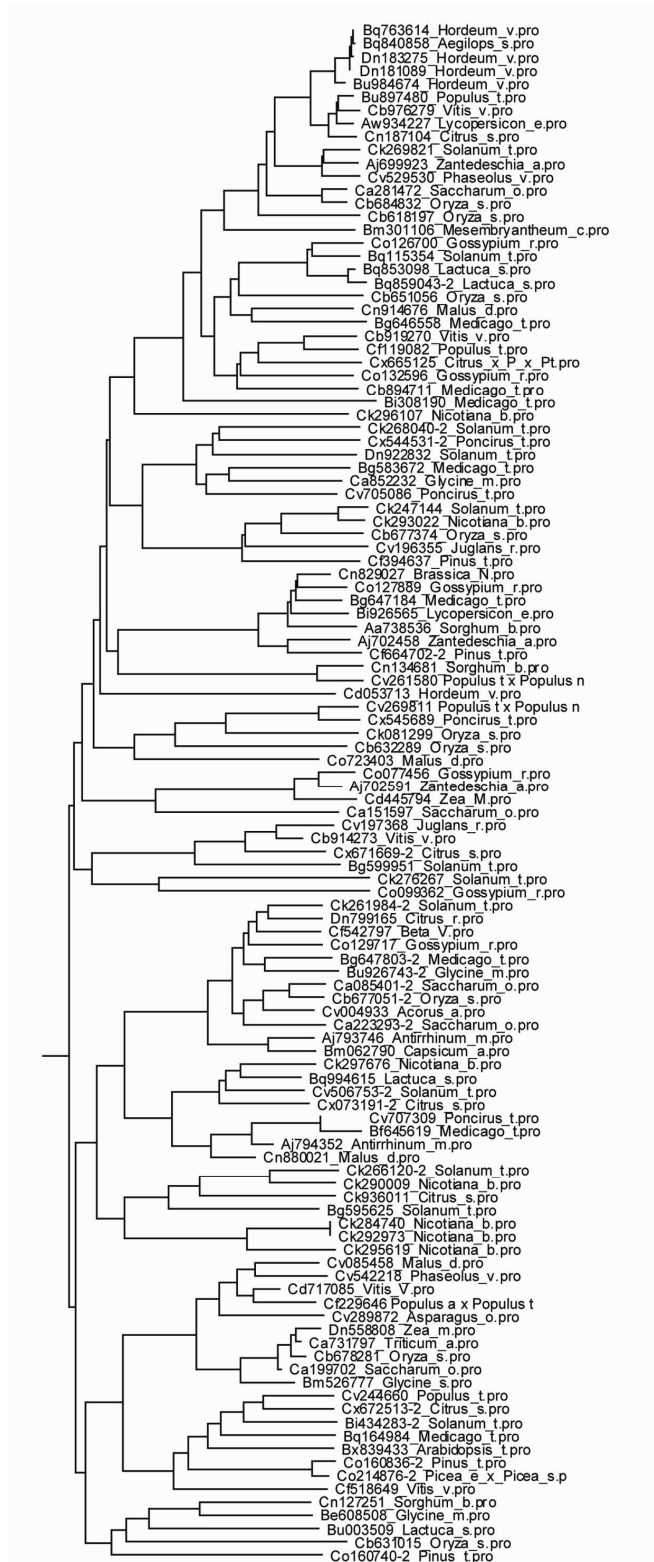
Demidov, D., Karimi, R., Agueci, F., Vlasenko, L. and Houben, A. (2007) Histone H3 phosphorylation and characterisation of candidate H3-kinases in plants. Institutstag IPK, 22.10.2007, Gatersleben (poster)

Agueci, F., Rutten, T., Houben, A., Title: Characterization of NIMA-like kinases in *Arabidopsis thaliana*, 3rd Plant science student conference (PSSC 2007) June 5th – 8th, 2007 at Institute of Plant Biochemistry (IPB) Halle (Saale)

Agueci, F., Rutten, T., Houben, A., Title: Characterization of NIMA-like kinases in *Arabidopsis thaliana*, 4th Plant science student conference (PSSC 2008) July 1st - 4th, 2008 at IPK, Gatersleben

Demidov, D., Karimi, R., Agueci, F., Vlasenko, L. Houben, A. Title: Characterization of putative histone H3-related kinases. Institute day, 29.09 – 30.09.2008 , IPK, Gatersleben

Supplemental Material



Supplementary figure 1: Branch of the neighbour joining tree indicated as **C)** in figure 6. This cluster does not contain any NIMA like kinases from *A. thaliana*.

Eidesstattliche Erklärung

Hiermit erkläre ich, dass diese Arbeit von mir bisher weder der Naturwissenschaftlichen Fakultät III der Martin-Luther-Universität Halle-Wittenberg noch einer anderen wissenschaftlichen Einrichtung zum Zweck der Promotion eingereicht wurde.

Ich erkläre ferner, dass ich diese Arbeit selbstständig und nur unter Zuhilfenahme der angegebenen Hilfsmittel und Literatur angefertigt habe.

Gatersleben, den

Francesco Agueci

CURRICULUM VITAE

Personal informations

Name Francesco Agueci
Address Amselweg 6 – 06466 Gatersleben
Tel +4915777/7809758 - +49(0)39482/5477
E-mail agueci@ipk-gatersleben.de
Nationality Italian
Date of Birth 07/03/1979

Education

October 1997-February 2005: Attended the Biology course at the University of Roma Tre, with the specialization in Molecular Biology

September 2001-September 2002: attended the **Albert-Ludwigs-Universität Freiburg** in Germany, thanks to the Erasmus program.

Relevant Courses: practical course in Microbiology, practical course in Biochemistry, Advanced Laboratory course in Molecular Biology

February 2005: Graduation in Biology at the University of Roma Tre, with an experimental thesis in Biochemistry (Internal Relator Prof.ssa Laura Fiorucci, External Relator Dott. Fabio Polticelli) titled: *“Conformational changes of yeast cytochrome iso-1 induced by lipids: nucleotides effects and implications in the apoptotic process”*

Mark 105/110.

Employment history

March 2005: research activity in Biochemistry in the laboratories of the Department of Experimental Medicine of the University of Roma Tor Vergata

Since January 2006: PhD student at IPK-Gatersleben in the research group “Chromosome structure and function”

Well known experimental techniques

- Site specific mutagenesis
- Heterologous expression of proteins in *E.coli*
- Transformation of *E.coli* and *A.tumefaciens* and plasmid extractions
- Purification and spectroscopic characterization of proteins (spectrofluorimetry, spectrophotometry, circular dichroism)
- Techniques of enzymatic kinetic
- Techniques of Molecular biology (PCR, RT-PCR, extraction of RNA and DNA, enzymatic digestion)
- Cloning and recombination procedures
- Stable transformation of *A.thaliana*, transient transformation of *N. benthamiana*
- Analysis via reporter constructs (GFP, GUS)

Publications

Agueci F, Polticelli F, Sinibaldi F, Piro MC, Santucci R, Fiorucci L. (2007)
"Probing the effect of mutations on cytochrome C stability." Protein Pept Lett.
14(4): 335-9

References

Name and position: Dr Andreas Houben, leader of Research group
"Chromosome structure and function"

Institution: IPK-Gatersleben

Email: houben@ipk-gatersleben.de

Name and position: Laura Fiorucci, Associated Prof. In Biochemistry

Institution: University of Rome "Tor Vergata"

Email: fiorucci@uniroma2.it

Name and position: Fabio Polticelli, Ph D., Research Scientist

Institution: University of Roma Tre

Email: polticel@uniroma3.it